

# Thermoluminescence Dating of Hawaiian Basalt

---

GEOLOGICAL SURVEY PROFESSIONAL PAPER 1095



# Thermoluminescence Dating of Hawaiian Basalt

*By* RODD J. MAY

---

GEOLOGICAL SURVEY PROFESSIONAL PAPER 1095



---

UNITED STATES GOVERNMENT PRINTING OFFICE, WASHINGTON : 1979

**UNITED STATES DEPARTMENT OF THE INTERIOR**

**CECIL D. ANDRUS, *Secretary***

**GEOLOGICAL SURVEY**

**H. William Menard, *Director***

May, Rodd J.  
Thermoluminescence dating of Hawaiian basalt.  
(Geological Survey Professional Paper 1095)  
Bibliography: p. 41-43.  
1. Thermoluminescence dating. 2. Basalt—Hawaii. I. Title. II. Series: United States. Geological Survey.  
Professional Paper 1095.  
QE508.M36 551.7'01 78-26826

---

For sale by the Superintendent of Documents, U.S. Government Printing Office

Washington, D.C. 20402

Stock Number 024-001-03142-6

## CONTENTS

---

	<i>Page</i>		<i>Page</i>
<b>Abstract</b>	1	<b>Radioactive element contents of the alkalic and tholeiitic ba-</b>	25
<b>Introduction</b>	1	salts and dose-rate calculations	25
Previous work	2	Radioactive element contents of the basalts	25
Purpose and goals	4	Calculation of radioactive decay energies	27
<b>Basic physical properties of thermoluminescence</b>	4	Dose rate calculations	28
Ionization and electron trapping	4	Discussion	28
Trap depth	5	Summary	29
Stability of trapped electrons	6	<b>Natural TL</b>	29
Nonthermal drainage	6	Alkalic basalt natural TL	30
Thermoluminescent emission	6	Tholeiitic basalt natural TL	31
Radiation damage in dosimeter crystals	9	<b>Artificial TL</b>	33
<b>Experimental equipment and technique</b>	10	Alkalic basalt artificial TL	33
Sample collection	10	Tholeiitic basalt artificial TL	34
Sample preparation	12	<b>TL dating and analysis of errors</b>	36
Major-element plagioclase compositions	13	TL dating of the alkalic basalts	36
TL measuring and recording equipment	14	TL saturation and the age limits of the method	38
Procedure	16	TL dating of the tholeiitic basalts	39
<b>Analysis of the plagioclase emission spectrum</b>	18	Summary of the TL-dating procedures and predictions for	
Procedure and results	18	future applications	40
Discussion	18	<b>References cited</b>	41
Summary	20	<b>Supplemental information</b>	44
<b>Linearity of TL acquisition, saturation effects, and</b>		Sample location and age data	44
sensitization	20	Alkalic basalts	44
Linearity of TL acquisition and saturation	20	Tholeiitic basalts	45
Sensitization effects	22	<b>Derivation of equations for the error in the TL ratios and</b>	
<b>Fading of artificially induced TL</b>	23	TL ages	46
		Error equations for the TL age ratio	46
		Equation for the error in the TL ages	47

## ILLUSTRATIONS

---

	<i>Page</i>
<b>FIGURE 1.</b> Generalized TL glow curve	2
2. Schematic representation of the distribution of energy levels in an insulator mineral	7
3. Simplified geologic index map of the Island of Hawaii showing sample localities	11
4. Ternary diagram of plagioclase composition of alkalic and tholeiitic basalt	13
5. Schematic diagram of the thermoluminescence reader	14
6. Spectral response curves for the PM tube and filter CS5-60	15
7. An approximate segregation of an artificial TL glow curve into its four constituent peaks	17
8. Transmission curves for the interference filters used for spectrum analysis	18
9. Spectral composition of the 300°C artificial TL emission from selected alkalic and tholeiitic basalt plagioclase separates	19
10. Rate of TL accumulation with increasing radiation exposure in both the alkalic and tholeiitic basalts	21
11. Artificial TL decay during a 40-day storage of irradiated samples	24
12. Curves of average percentage of 300°C peak TL remaining in alkalic and tholeiitic basalt samples after each decay interval	24
13. Natural and artificial TL glow curves for selected alkalic and tholeiitic basalts	30
14. Alkalic basalt natural TL relative to sample age	31
15. Tholeiitic basalt natural TL relative to sample age	32
16. Alkalic basalt 300°C artificial TL relative to sample age	34
17. Tholeiitic basalt 300°C artificial TL relative to sample age	35
18. 300°C artificial TL peak-height averages for historic tholeiitic basalts	36
19. Alkalic basalt TL ratios relative to sample age	37
20. Tholeiitic basalt natural TL peak-height averages for the carbon-14-dated prehistoric basalts relative to sample age	39
21. Tholeiitic basalt $NE_a/AE_n$ ratios plotted relative to sample age	40

## TABLES

	Page
TABLE 1. Major-element chemical compositions of selected plagioclase separates	13
2. Percentage of total TL in the 4,000-Å to 5,000-Å bandwidth for the 300°C alkalic basalt plagioclase artificial TL peak	20
3. Percentage of TL remaining in the 300°C peak of both the alkalic and tholeiitic basalts at the end of each decay interval	23
4. Radioactive element contents of the alkalic basalts	26
5. Radioactive element contents of the tholeiitic basalts	27
6. Abbreviated radioactive decay series and decay energies for the radioactive isotopes of uranium, thorium, and potassium	27
7. Natural abundances and half-lives of the isotopes	28
8. Energy constants in rads per parts per million per year adjusted for natural isotopic abundances	28
9. Annual dose rates for the alkalic and tholeiitic basalts	28
10. Alkalic basalt natural TL peak-height averages for crushing stages 1 and 2	31
11. Individual and cumulative errors in the energy-normalized peak-height average for the alkalic basalts	31
12. Tholeiitic basalt natural TL peak-height averages for crushing stages 1 and 2	32
13. Individual and cumulative errors in the energy-normalized peak-height average for the tholeiitic basalts	33
14. Alkalic basalt 300°C artificial TL peak-height averages for crushing stages 1 and 2 measured with and without filter CS5-60	34
15. Tholeiitic basalt 300°C artificial TL peak-height averages for crushing stages 1 and 2 measured with and without filter CS5-60	35
16. Alkalic basalt TL ratios, TL ages, and calculated errors	37

# THERMOLUMINESCENCE DATING OF HAWAIIAN BASALT

By RODD J. MAY

## ABSTRACT

The thermoluminescence (TL) properties of plagioclase separates from 11 independently dated alkalic basalts 4,500 years to 3.3 million years old and 17 tholeiitic basalts 16 years to 450,000 years old from the Hawaiian Islands were investigated for the purpose of developing a TL dating method for young volcanic rocks. Ratios of natural to artificial TL intensity, when normalized for natural radiation dose rates, were used to quantify the thermoluminescence response of individual samples for age-determination purposes. The TL ratios for the alkalic basalt plagioclase were found to increase with age at a predictable exponential rate that permits the use of the equation for the best-fit line through a plot of the TL ratios relative to known age as a TL age equation. The equation is applicable to rocks ranging in composition from basaltic andesite to trachyte over the age range from about 2,000 to at least 250,000 years before present (B.P.). The TL ages for samples older than 50,000 years have a calculated precision of less than  $\pm 10$  percent and a potential estimated accuracy relative to potassium-argon ages of approximately  $\pm 10$  percent. An attempt to develop a similar dating curve for the tholeiitic basalts was not as successful, primarily because the dose rates are on the average lower than those for the alkalic basalts by a factor of 6, resulting in lower TL intensities in the tholeiitic basalts for samples of equivalent age, and also because the age distribution of dated material is inadequate. The basic TL properties of the plagioclase from the two rock types are similar, however, and TL dating of tholeiitic basalts should eventually be feasible over the age range 10,000 to at least 200,000 years B.P.

The average composition of the plagioclase separates from the alkalic basalts ranges from oligoclase to andesine; compositional variations within this range have no apparent effect on the TL ratios. The average composition of the plagioclase from the tholeiitic basalts is labradorite.

The natural radiogenic dose rates for the alkalic basalts calculated on the basis of assumed secular equilibrium range from 0.228 to 0.462 rad per year and average 0.335 rad per year exclusive of the cosmic-ray energy dose and with the alpha-particle component equal to one-tenth of the total alpha decay energy. The TL measurements were made using material of a 37- to 44-micrometer size range; the crushing required during sample preparation was found to have a negligible effect on natural TL.

Both natural and artificial TL were filtered to the bandwidth 3,500 Å to 5,000 Å to restrict the light detected to that from the plagioclase emission peak centered at about 4,500 Å and associated with structural defects. Within this bandwidth, the natural TL from both the alkalic and tholeiitic basalt plagioclase consists of a single peak with a maximum amplitude at about 350°C; the artificial TL glow curves produced by an exposure of the drained samples to a standard dose of X-radiation consist of four broad,

variably overlapping peaks with maxima at about 110°C, 150°C, 225°C, and 300°C. The maximum amplitude of the 350°C natural and 300°C artificial TL peaks, both produced by the same general activation energy distribution of trapping centers, were used for TL dating. The high-temperature artificial TL peak occurs at a lower temperature than the corresponding natural TL peak owing to the presence of a large number of electrons retained in traps near the lower end of the trap-depth energy range in samples whose TL is measured a short time after intense artificial irradiation. These traps remain essentially empty in the natural environment owing to spontaneous decay and do not produce measurable low-temperature natural TL peaks. With prolonged storage after irradiation, the 300°C artificial TL peak migrates to higher temperatures and decreases in amplitude.

## INTRODUCTION

Thermoluminescence (TL) is the transient emission of light in or near the visible spectrum that accompanies the heating of certain semiconductor and insulator minerals to temperatures below that of incandescence. The phenomenon is incompletely understood but originates in the ionization of lattice atoms of the dosimeter crystals by decay particles from radioactive elements incorporated in the rock or mineral. If enough energy is transferred to the excited electrons during ionization, they will be elevated to the conduction band, where a proportion will become trapped in electrically charged defect structures in the crystal lattice. These trapped electrons lose energy in the form of light (TL) as they return to the valence band during heating.

TL is distinguished from the other two principal types of luminescence, fluorescence and phosphorescence, by the existence of a significant delay time between excitation and the emission of stored energy and by the temperature-dependent nature of the emission process. In general, all types of luminescence are distinguished from incandescent glow by their occurrence in the spectral region where the mineral or other crystal is nonabsorbing (optically transparent), whereas incandescent emissivity by Kirchoff's Law is strong only in the spectral region where the crystal is strongly absorbing.

The phenomenon of TL was first reported more than 300 years ago by Boyle (1663) and has been studied in various contexts since that time. Only in the past two decades, however, following a discussion of the potential of TL for a variety of applications, including dating (Daniels and others, 1953), has a concentrated effort been made to understand the TL phenomenon and to employ it in solving such diverse problems as radiation dosimetry, stratigraphic correlation, and the dating of various archeologic and geologic materials.

The use of TL for dating is based on the cumulative retention of a representative proportion of the electrons excited to the conduction band by radioactive decay and their detectable release during laboratory heating. With increasing temperature, thermal stimulation provides sufficient kinetic energy to free electrons from progressively deeper (higher activation energy) traps. The untrapped electrons then return to the valence energy band at defect or impurity "recombination centers," emitting the energy differential between the excited and ground states as light. The low levels of light emitted are typically measured with a photomultiplier tube, and concurrently the voltage produced is plotted in relation to temperature using an X-Y plotter to obtain what are referred to as glow curves.

A generalized glow curve, figure 1, shows a curve representing TL emission and one representing the combined electronic noise and blackbody (incandescent) radiation background, which is measured during a second heating of the sample. The magnitude of the natural or artificial (laboratory induced) TL emission can be quantified either as the area between the two curves within specified temperature boundaries or in terms of peak heights by the vertical distance between the two curves at the point of maximum amplitude of the particular TL peak being studied.

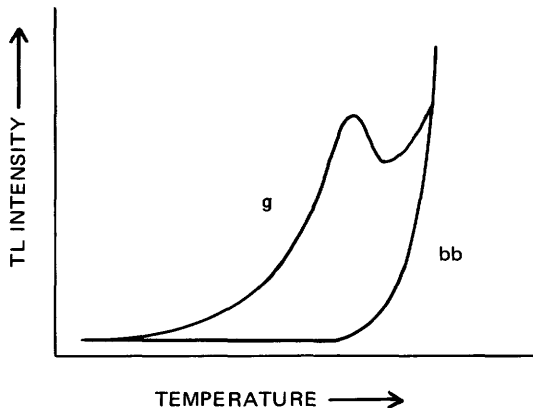


FIGURE 1.—Generalized TL glow curve. g, TL emission; bb, blackbody radiation (incandescence) background.

Absolute TL ages can be calculated directly from the natural TL data if the natural radiation dose rate, the sensitivity (trap density) of the samples, and the ionization efficiency of the different components of natural radiation are known. Ideally, dividing the magnitude of the laboratory (artificial) radiation dose required to reinstate an artificial TL peak equivalent to the natural peak by the natural annual dose rate should yield the age of the sample. Unfortunately, this direct approach, in which quartz is used as the TL dosimeter, has not been generally successful for samples older than about 30,000 years, mainly because of spontaneous natural TL decay. The derivation of an empirical TL-dating method of more widespread applicability is the principal goal of this investigation.

#### PREVIOUS WORK

After what was probably the first recorded description of the TL phenomenon by Boyle in 1663, relatively little research was done until the 1950's. Significant early papers include the classic study of both phosphorescence and thermoluminescence by Randall and Wilkins (1945) and the general review of TL research by Daniels and others (1953), which includes one of the earliest proposals for using TL in dating.

More recently TL has been a subject of increasing interest and investigation, with applications in a number of fields. One of the more important of these outside the general field of dating archeologic and geologic materials has been the use of TL in radiation dosimetry and personnel monitoring. In this application, synthetic dosimeter crystals, of which lithium fluoride is the most widely used, are employed to monitor a wide range of radiation energies and total doses in industrial and laboratory situations.

Numerous attempts have been made in recent years to develop TL-dating procedures for a variety of materials and a wide range of geologic ages, but most have encountered difficulty. The greatest degree of success has been achieved with the dating of young archeologic artifacts using several different materials and techniques. These methods exemplify the "absolute" dating approach in that sample ages are calculated directly from measurements of TL, trap density (sensitivity), and natural radiation dose rate. They are distinct from "relative" dating, which requires a comparison of individual TL values with an age curve based on independently dated samples of similar composition for an assignment of geologic age.

Aitken, Zimmerman, and Fleming (1968) have developed a TL-dating method using crushed and sized, but mineralogically unseparated, potsherds, for which they have obtained ages from 640 to 3,500 years B.P.

(before present) with a precision of  $\pm 10$  percent relative to carbon-14 ages. The same basic experimental procedure has been used in authenticity testing of more recent artifacts for which apparent ages are known but for which questions of origin (that is, authenticity) exist (Fleming, 1970; Fleming and others, 1970). Refinement of this method has led to the development of a "fine-grain" technique that promises a routine precision of less than  $\pm 10$  percent (Aitken, 1970; Zimmerman, 1971). This technique, which now largely supersedes the earlier technique, involves the separation of a 2- to 8- $\mu\text{m}$  (micrometer) "whole-sherd" (mineralogically unseparated) fraction from carefully crushed sherds. The grain-size constraint is imposed by the very short range in a crystalline matrix of the decay particles that are critical in both defect formation and ionization. At the same laboratory at Oxford University, a "quartz-inclusion" method has also been developed for application to the same types of artifacts to which the "fine-grain" method is applied. This method, which involves the preparation, from gently crushed sherds, of a pure quartz separate composed of grains 95 to 105  $\mu$  in diameter, has been shown to yield ages near 1,500 to 2,000 years B.P. with an average deviation of the TL ages from the archeologic ages of only 5.4 percent (Fleming, 1970). The theoretical considerations and analytical techniques for the two methods are essentially identical.

Another TL method, based on the use of thin slices from pyrolyzed chert fragments recovered from archeologic sites as the TL dosimeter, yields ages in the range 12,000 to 50,000 years B.P. with an accuracy of better than  $\pm 15$  percent relative to cultural ages as reported by Goksu and others (1974). These workers predict the eventual extension of their method, which is similar to that developed for pottery, to possibly 200,000 years.

Relatively little work has been done to develop a TL-dating method for geologic materials, and most attempts have been unsuccessful, partly because much work has been attempted with samples older than the probable saturation limit of TL accumulation and partly because of the limitations of the materials and procedures used. Although the development of a reliable dating method has proved difficult, most investigations have identified a general tendency for natural TL to increase with age in a variety of materials.

The potential of using calcium carbonate (principally limestone) for dating has been investigated by several workers, among them Zeller and others (1957), Johnson (1963), and Zeller (1968). Hutchinson (1968) attempted to date tectonic and magmatic events using limestone, with generally poor results. An investiga-

tion of the TL of foraminifers collected from independently dated pelagic sediment cores by Bothner and Johnson (1969) identified a systematic increase in the natural TL of the calcium carbonate tests to an age of approximately  $10^5$  to  $10^6$  years. This predictable increase could conceivably provide the basis for a reliable dating procedure. In general, however, the TL properties of calcium carbonate are complex and are frequently subject to interference from spurious TL emission. The mineral is at the present time of uncertain value for age determinations, although research is continuing.

Studies of the age of deposition of fluorite using that mineral as the TL dosimeter by Blanchard (1966) and Kaufhold and Herr (1968) have been generally unsuccessful. The alkali halide minerals do not appear at this time to provide a reliable basis for age determination. Attempts to determine the age and thermal history of meteorites (Houtermans and Liener, 1966) and tektites by TL (Durrani and Christodoulides, 1969; Durrani and others, 1970) have yielded similarly discouraging results. A moderate degree of success was reported by Vaz and Senftle (1971) in the correlation of radiometric and TL ages obtained for a collection of zircon crystals from Ceylon (now Sri Lanka) that range in age from about  $1 \times 10^9$  to  $3 \times 10^9$  years. Their method, however, is more an evaluation of the extent of radiation damage in the crystals of high radioactive element content than of simple TL accumulation.

Slightly more attention has been devoted to the minerals of intrusive igneous rocks, particularly quartz and feldspar, two of the most sensitive and widely occurring natural TL dosimeters. One attempt to date vein quartz of approximate Precambrian age (Hwang, 1972) failed, apparently because saturation effects produced lower than expected TL values. Panov and others (1970) identified progressively increasing TL intensities for both quartz and feldspar from four intrusive complexes in Transbaykalia that range in age from about 83 to 227 million years old; however, they did not attempt to use the data to calculate TL ages, and the suitability of the data for such calculations was not evaluated.

Mineral separates and whole-rock fractions from young volcanic rocks used in several TL studies appear to offer the most promise for the successful derivation of a TL age method. Sabels (1963) performed one of the earliest and most definitive TL studies using crushed whole-rock fractions from a number of dated basalt flows as old as 15 m.y. He was not successful in assigning reliable TL ages to most of the rocks but did establish the potential viability of TL dating for rocks younger than 1 m.y. and identified

many of the problems inherent in TL dating. Several subsequent dating attempts have employed mineral separates from volcanic flows as the basis for age determination. Hwang (1970), in dating orthoclase separated from an 1,800-year-old flow from Mount Vesuvius, reported a good correlation of the TL and archeologic ages. Two younger flows studied as part of the same investigation did not possess any measurable natural TL. Aitken, Fleming, Doell, and Tanguy (1968) used feldspar separates to study the TL from flows of known age from several volcanoes but were unable to derive realistic TL ages from their data. A more recent attempt by Aitken and Fleming (1971) to date volcanic products including lava, tephra, and pumice by the fine-grain technique gave an approximately correct age for the lava but unsatisfactory ages for the tephra and pumice owing to suspected spurious TL interference from an unidentified mineral. Wintle (1973) attempted to date several flows ranging in age from 5,000 to 50,000 years B.P. by using the TL from feldspar separates but was unable to obtain accurate dates owing to lower-than-expected natural TL values, which were attributed to "anomalous fading"—nonthermal drainage of trapped electrons during geologic time.

A preliminary investigation by Berry (1973) of the TL properties of plagioclase separates from a suite of six samples of tholeiitic and alkalic basalt from the island of Hawaii ranging in age from approximately 225 to 17,000 years led to the identification of a progressive increase in the TL of the samples with increasing age. No attempt was made on the basis of the preliminary results to develop a dating method for these rocks, but the data display the same basic TL relative to age relation identified by other workers for prehistoric pottery.

#### PURPOSE AND GOALS

The investigation by Berry (1973) prompted May to initiate a more detailed and comprehensive study of the potential of using TL to date Hawaiian basalts. The principal impetus for the research was the possibility of using TL dating to bridge the significant age gap that exists between the limits of the two principal methods for dating young rocks, radiocarbon and potassium-argon. The age range of specific interest was that from about 35,000 years, the approximate upper limit of the carbon-14 method, to about 100,000 years, the approximate lower limit for the potassium-argon method for most kinds of rocks.

The rocks selected for use in this investigation included samples of both alkalic and tholeiitic basalt from flows of independently determined young age

from the Hawaiian Islands. These rocks were chosen because (1) a reasonably large selection of well-dated material was available; (2) some of the flows had already been studied on a preliminary basis; (3) the Hawaiian rocks are of considerable geologic interest; and (4) except for those few flows that have associated carbon, young Hawaiian lavas have proved difficult to date by other methods.

The experimental procedure will begin with the investigation of critical aspects of the TL process followed by a presentation and discussion of the TL measurements and an analysis of the feasibility of using the data in the development of a TL-dating technique.

#### BASIC PHYSICAL PROPERTIES OF THERMOLUMINESCENCE

Thermoluminescence, as defined briefly in the introduction, is the energy in excess of thermal radiation emitted as light during the heating of an activated dosimeter mineral. The phenomenon can be depicted spatially by a three-dimensional array of orthogonal axes representing light intensity, activating temperature, and spectral composition.

Details of the TL process are still only partially understood, even though a number of empirical and theoretical investigations have been made over the past 30 years. Nonetheless, understanding of the phenomenon is sufficient to permit a qualitative discussion of specific aspects of the TL process.

#### IONIZATION AND ELECTRON TRAPPING

Thermoluminescent emission is observed only (1) in semiconductor and insulator minerals having a forbidden energy band-gap of at least several, but probably not more than 10, electronvolts between the valence and conduction band and (2) to varying degrees in different minerals exhibiting this basic property. Igneous minerals that possess a significant innate thermoluminescent capability include quartz, feldspar, apatite, and zircon.

During the process of spontaneous decay of the isotopes  $^{238}\text{U}$ ,  $^{235}\text{U}$ ,  $^{232}\text{Th}$ , and  $^{40}\text{K}$ , which occur in varying amounts in rocks and minerals, high-energy alpha, beta, and gamma radiations are emitted. This internal radiation is supplemented in rocks near the Earth's surface by the more penetrating component of cosmic radiation. In the event these high-energy radiations intercept dosimeter minerals, such as quartz or feldspar in a rock or pottery sherd, they can produce ionization of constituent atoms of the crystals. If only a small amount of energy is transferred to an electron of

a struck atom during the coulomb interaction of a decay particle with the electronic field of the atom, the ionization event will result in "pair" formation. In this case, the electron and positively charged "hole" in the valence band of the atom remain spatially associated by mutual charge attraction and recombine with the transfer of excess energy to the lattice as heat. If, however, sufficient energy is imparted to an electron during ionization, it will be excited to the conduction band of the crystal. Dislocation of atoms from normal lattice sites can also occur, as discussed in a later section.

Once in the conduction band, an electron wanders through the lattice until it either becomes trapped or encounters a recombination center, which can serve to degrade it back to the valence band with the emission of the energy differential as a photon of light.

The properties of traps and their influence on TL are complex. In general, a trap is a localized condition of inhomogeneity in the electronic field of the crystal. It may be associated with any of a number of physical defects including vacancies, interstitial ions, impurity ions, or dislocation defects and may have either a net positive or negative charge. Both electrons and positively charged holes can become trapped in these locations of unbalanced charge for periods of time that are both temperature and time (probability) dependent.

The probable lifetime ( $\tau$ ) of an electron in a trap of depth ( $E$ ) has been described by Randall and Wilkins (1945) as

$$\tau = s e^{-E/kT}$$

where  $s$  is the "attempt to escape" frequency,  $T$  the absolute temperature, and  $k$  the Boltzmann constant. From this relation, it is apparent that electrons in deep traps ( $E$  large) would be more stable than those in shallow traps ( $E$  small). For an isothermal situation, the decay rate for an initial population ( $n$ ) of electrons in traps of a single activation energy (depth) according to the Randall-Wilkins equations is

$$\frac{dn}{dt} = -n s e^{-E/kT}$$

This model assumes first-order (monomolecular) kinetics and does not provide for nonthermal drainage by quantum mechanical "tunneling" or other possible decay processes that do not require that trapped electrons return to the conduction band before combining with an impurity or defect center or for retrapping of thermally released charge carriers. An investigation of the effect of retrapping by Garlick and Gibson (1948) led to the conclusion that it was negligible. More recently, Durrani and others (1973) demonstrated that there was no detectable retrapping of electrons re-

leased from deep traps by shallower (lower temperature peak) traps.

The Randall-Wilkins model has since been found to be incomplete but still represents the best available approximation to the TL process. The basic equation has served as the basis for a number of more recent derivations, including those by Christodoulides and Ettinger (1971), Braunlich (1968), and Land (1969b). More complex models based on second-order kinetics have been derived (see for example, Curie, 1963; Medlin, 1968) but do not provide substantially better explanations of the TL process in compositionally complex natural minerals such as feldspar.

#### TRAP DEPTH

Electron trap "depths" are measured in units of electronvolts whose calculated values represent the activation energy required to release an electron from a trap of specified depth. Trap depths have been determined both from theoretical considerations and by measurement of actual TL properties (for a comprehensive compilation of trap depth determinative methods, see Braunlich, 1968). Physical methods include "isothermal annealing" experiments in which the rate of decay of artificially induced TL is measured over a specified time interval for samples stored at constant temperature and "initial rise" techniques that derive pertinent information directly from the morphology of the rising portion of the TL glow curve and from, in at least one instance (Land, 1969a), inflection points and peak maxima of the glow curves. The two basic physical methods have been used essentially interchangeably by many workers in terms of the accuracy and reliability of the data obtained. Recently, however, they have been shown by Wintle (1975) to yield significantly different results when carefully applied to the same material, in the particular example cited, quartz.

The trap depth calculations typically are made by using artificial radiation to fill traps in samples from which the natural TL has been drained; the results are then extrapolated to the natural TL situation.

Trap depths calculated for two of the prominent peaks of quartz by the isothermal annealing technique by Hwang and Goksu (1971) gave values of  $0.97 \pm 0.1$  eV (electronvolts) for the  $110^\circ\text{C}$  peak and  $1.1 \pm 0.1$  eV for the  $370^\circ\text{C}$  peak. Using the same basic isothermal annealing approach, Wintle (1975) obtained a value of  $1.7 \pm 0.1$  eV for the  $325^\circ\text{C}$  peak of quartz. The difference in trap depth and peak maximum temperature obtained during these two experiments for what is probably the same high-temperature peak (trap type and depth) is probably a result of differences in equip-

ment and in sample handling and irradiation techniques.

#### STABILITY OF TRAPPED ELECTRONS

The probable lifetime of electrons in traps of a single depth or narrow range of depths is critical because the TL peak selected for dating use must be sufficiently stable that the traps that produce it retain a representative proportion of the charge trapped over the time period of dating interest. Peak stability is usually defined in terms of half-lives ( $t_{1/2}$ ) expressed with the equation

$$t_{1/2} = \frac{\ln 2}{s} e E/kT$$

based on the Randall-Wilkins model for electron retention, where, as before,  $k$  represents the Boltzmann constant. Differences in the assigned values for the trap depth ( $E$ ), storage temperature ( $T$ ), and frequency factor ( $s$ ), for which estimated values in the literature range from  $10^7$  to  $10^{12}$  sec $^{-1}$ , commonly produce differences in the half-lives calculated for the same TL peak by different workers. For example, the half-life of a hypothetical peak produced by an electron population stored in traps with an arbitrary depth of 1.1 eV and a frequency factor of  $5 \times 10^8$  sec $^{-1}$ , as calculated with the equation listed above, is  $3.7 \times 10^2$  years. Increasing the trap depth by 0.1 eV, the limit of precision reported by many workers for trap depth calculations, to 1.2 eV increases the calculated half-life by a factor of approximately 51 to  $1.9 \times 10^4$  years. This large difference in calculated half-lives produced by a difference in trap depth, equal in many cases to the limit of resolution of the determinative methods, severely limits the usefulness of such calculations for detailed peak stability evaluation. The reliability of the calculations is further reduced by the fact that the TL peaks are probably produced by a narrow continuum of trap depths rather than a single discrete depth and that nonthermal drainage of electrons from traps may be significant. Neither of these factors is adequately accounted for by existing models. Moreover, as there are large differences in the dose rate between natural and artificial radiation, the use of artificially induced TL to model detailed properties of natural TL is probably not strictly valid.

There is at this time no definitive method for accurately determining natural TL peak half-lives that incorporates an assessment of all the variables mentioned above. In general, natural TL peaks that occur at 300°C or more are probably sufficiently stable to be of use in TL-dating experiments.

#### NONTHERMAL DRAINAGE

The spontaneous decay of artificially induced TL in samples stored in the dark after irradiation in excess of that caused by thermally related processes as predicted by existing theory has been termed anomalous fading by Wintle (1973). This anomalous fading is probably in fact nonthermal drainage, the spontaneous escape of electrons from traps by tunneling or other processes that do not require that the trapped electrons reenter the conduction band before being degraded to the valence band. The existence of this phenomenon has been studied recently in connection with the TL properties of both terrestrial and lunar plagioclase, with apparently conflicting results. Anomalous fading of TL in artificially irradiated samples of terrestrial feldspar from several volcanic regions, and significantly lower than expected natural TL values in the same samples, were attributed by Wintle (1973) to nonthermal drainage. A more recent investigation has shown the process to be essentially nonluminescent within limits of detection (Wintle, written commun., 1975). Garlick and Robinson (1972) reported significant nonthermal drainage over a wide range of trap depths in both terrestrial and lunar plagioclase, as manifest by similar isothermal TL decay rates for artificial TL peaks with a wide range of activation temperatures. Blair and others (1972) stored artificially irradiated samples at -196°C and noted some TL decay, which they attributed to nonthermal leakage. Durrani and others (1973) restudied the problem, and although they could not detect significant nonthermal drainage, they could not rule out its possible existence or significance. The preponderance of the evidence seems to support the existence of nonthermal drainage; the general significance of the phenomenon for dating applications of TL has been discussed by Garlick (1973). This is an example of the type of complexity that makes the calculation of reliable values for such parameters as peak half-lives extremely difficult.

#### THERMOLUMINESCENT EMISSION

Luminescent emission during thermal stimulation is a complex phenomenon that has been extensively studied, but like many aspects of TL, is only partially understood. The process has been qualitatively modeled and can perhaps be most easily visualized in terms of a band-theory representation of the distribution of energy levels in a hypothetical crystal, as shown in figure 2.

Electrons elevated to the conduction band by the ionization of any of the atoms of a dosimeter crystal

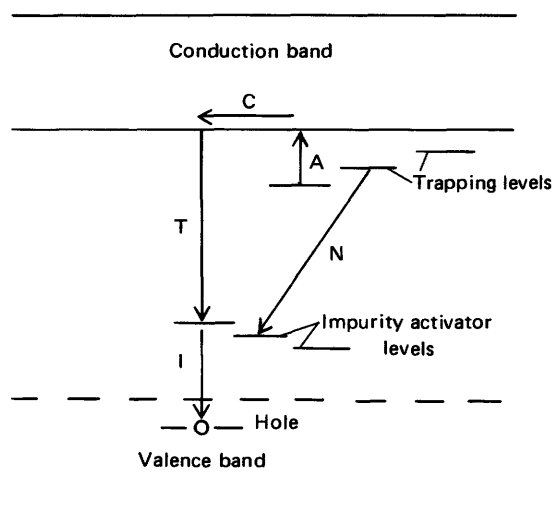


FIGURE 2.—Schematic representation of the distribution of energy levels in an insulator mineral. A, activation of a trapped electron; C, mobility of a free electron in the conduction band; T, recombination of a conduction band electron with an impurity or defect center, with thermoluminescent emission characteristic of the center; I, ionization of an impurity by a hole in the valence band; N, nonthermal untrapping of an electron and recombination with an impurity center.

may return to the valence band only through recombination centers consisting of certain impurity atoms and some types of structural defects. According to Mott and Gurney (1964), activator impurities are effective as recombination centers because they contribute a valence level above the upper energy limit for the valence band of the pure crystal, as shown schematically (fig. 2). When a hole produced by an ionization event moves through the valence band and encounters a suitable activator impurity, an electron from the impurity atom theoretically combines with the hole (process I in fig. 2), eliminating the state of positive charge. The result is exactly the same as if the impurity had been ionized initially; owing to energy differentials, this vacant level is not mobile.

During heating, electrons released from traps to the conduction band (A in fig. 2) move about until they encounter an ionized impurity or suitable defect, then combine with it, emitting radiation characteristic of the particular recombination center (T in fig. 2). Once combination has occurred, the center is capable of repeating the process anew.

In natural minerals, the number of impurity recombination centers is essentially a constant fixed at the time of crystallization, whereas the defect center population can increase with prolonged exposure to defect-producing natural radiation.

The emission spectrum that results from the recombination process consists of broad peaks on a wave-

length relative to intensity plot whose maxima occur within restricted wavelength bands. The spectral position of the peaks are characteristic both of the host mineral and the activating defect or impurity. In plagioclase the luminescence spectrum measured at or near room temperature consists of three broad peaks in the blue, green, and red-near infrared portions of the spectrum. The peaks have maxima at about 4,500 Å, 5,600 Å, and between 7,000 and 7,800 Å, respectively (Geake and others, 1973). This spectral distribution has been found to remain essentially unchanged with respect to peak position at temperatures to 400°C, although there may be some change in relative intensities. The 4,500-Å peak remains prominent in the plagioclase spectrum to at least 400°C (Durrani and Hwang, 1974).

The transition metals, particularly iron and manganese, have been shown to be the principal impurity activators in natural plagioclase, although in some synthetically grown feldspars, relatively high concentrations of several rare-earth elements have been shown to be capable of stimulating characteristic luminescent emission.

Variations in the overall emission spectrum of plagioclase have been shown by Smith and Stenstrom (1965) and Sippel and Spencer (1970) to have no systematic correlation with plagioclase mineralogic type. This is perhaps to be expected because emission is determined by the content of minor- and trace-element impurities rather than the major-element constituents. The position of the emission peaks has been shown by luminescence studies by Leverenz (1968), Garlick and others (1971), and Geake and others (1972) to be independent of the type of artificial exciting radiation, whether X-rays, electrons, or protons.

The plagioclase emission spectrum is not unique in wavelength distribution properties. It has been shown in general that the peak positions and associated activators are common to all feldspars and to other natural silicate minerals, including quartz and sodalite. Some spectral components have been observed in synthetic silicate minerals. The emission peak at approximately 4,500 Å has been found to occur widely in natural silicate minerals, including, in addition to feldspar, quartz (Smith and Stenstrom, 1965; Sippel and Spencer, 1970), sodalite (Van Doorn and Schipper, 1971), and forsterite and iron-free enstatite (Geake and Walker, 1966). It has been identified in synthetic  $\text{SiO}_2$  (Leverenz, 1968) and in some nonsilicate minerals, including pure ZnS (Mott and Gurney, 1964). The origin of the 4,500-Å emission peak in feldspar has been attributed by Geake and others (1972) to a specific but as yet unidentified type of lattice defect on the basis of both deductive reasoning and theo-

retical calculations using crystal field theory. The peak was postulated by Leverenz (1968) to originate in the anion radicals (for example,  $\text{SiO}_4$  tetrahedra) of framework silicate minerals such as quartz and feldspar.

Structural damage produced by impact shock has been reported by Sippel and Spencer (1970) to cause broadening and shifts in the relative proportions of the emission peaks of both terrestrial and lunar feldspar and to result in enhanced emission in the blue band for some shocked plagioclase crystals.

The rare-earth elements cerium and europium have been found to stimulate emission peaks in the ultraviolet and blue portions of the spectrum when incorporated in synthetically grown  $\text{CaAl}_2\text{Si}_2\text{O}_8$  (anorthite) in quantities to 1 percent (Laud and others, 1971; Isaacs, 1971). The correlation of blue emission with europium content in plagioclase was noted by Drake (1972).

The effect of these elements on the luminescence spectra of natural minerals in the blue band is probably small relative to structural defects. Cerium is present in basaltic plagioclase in quantities that average only about 2 to 5 ppm (parts per million) and is almost always less than 10 ppm. Europium, although it has a high partition coefficient for plagioclase relative to the melt and most other mineral phases, occurs only in basaltic plagioclase in amounts that average 0.3 to 0.5 ppm and is almost always less than 1 ppm (Smith, 1974).

Geake and his coworkers (1971, 1973) have recently shown by theoretical calculations and doping experiments with both natural and synthetically grown plagioclase that the broad plagioclase emission peak at approximately 5,600 Å is caused by manganese, probably substituting in calcium lattice sites. Doping of a natural plagioclase with manganese by heating the sample with  $\text{MnSO}_4$  (Geake and others, 1971) resulted in a 16-fold increase in the amplitude of the green peak accompanied by a halving of the amplitude of the blue and infrared emission peaks. An attempt by these workers to develop a detailed correlation between the magnitude of the green peak and manganese content failed, probably because analytical measurements of total manganese content are not necessarily equivalent to the number of  $\text{Mn}^{2+}$  ions in  $\text{Ca}^{2+}$  sites, the presumed critical relation for emission. The substitutional manganese is inferred to be in the  $\text{Mn}^{2+}$  oxidation state to preserve electrical neutrality in the crystals.

The 5,600-Å peak has been observed by a number of workers (Nash and Greer, 1970; Sippel and Spencer, 1970; Geake and others, 1971, 1973; Durrani and others, 1973) to occur in nearly all terrestrial and lunar

plagioclase examined. The common occurrence of the peak can probably be attributed to the relative abundance of manganese in igneous rocks. It occurs in basaltic plagioclase in quantities that typically range from 50 to 100 ppm (Smith, 1974). The peak and its manganese origin have been observed in other silicate minerals, including sodalite (Van Doorn and Schipper, 1971) and  $\text{ZnSiO}_4:\text{Mn}$  (Leverenz, 1968).

The position of the peak maximum has been found by Geake and others (1971) to occur consistently in the interval between 5,550 Å and 5,650 Å independent of feldspar composition. Sippel and Spencer (1970) found the amplitude of the peak to be prominent in samples for which the anorthite molecule exceeds 11 mole percent and to be low or missing in the spectra of alkali feldspar, including albite, presumably owing to low concentrations of manganese.

The third prominent peak in the plagioclase emission spectrum is that occurring in the red-near infrared between 7,000 Å and 7,800 Å. Theoretical calculations and doping experiments similar to those used to identify the origin of the 5,600-Å peak have demonstrated that the red peak is produced by  $\text{Fe}^{3+}$ , probably substituting in tetrahedral  $\text{Al}^{3+}$  sites (Geake and others, 1973; Telfer and Walker, 1975), although it could possibly be substituting in  $\text{Ca}^{2+}$  sites (Geake and others, 1972b, 1973).

The red peak has been shown by Sippel and Spencer (1970) to have a mean position at 7,300 Å and a range of 400 Å over which peak position correlates roughly with mole percent albite. In general, they found the red peak of alkali feldspar to be less intense than that of plagioclase. The position of the red peak was found by Geake and others (1973) to vary over about a 500-Å interval and to correlate with composition, emission from albites tending to be at longer wavelength than that from anorthites.

Comparisons of the emission spectra from lunar and terrestrial plagioclase have shown that the red peak is typically prominent in terrestrial feldspar but small or absent in lunar plagioclase. This difference has been attributed by Geake and others (1972) to a low oxidation potential in the lunar environment during the period of formation of the rocks that would have the effect of inhibiting the oxidation of iron, resulting in a high  $\text{Fe}^{2+}:\text{Fe}^{3+}$  ratio in lunar plagioclase. In terrestrial feldspars, the amplitude of the red peak is almost always greater than that of the blue peak and for most is equal or greater than the green peak. The prominence of the red peak probably derives from the fact that iron is the second most abundant minor element in natural feldspar. In basaltic plagioclase, it usually occurs in amounts that range from 0.2 to 0.5 weight percent, the higher concentrations being in samples with

a higher anorthite content (Smith, 1974). The average value for plagioclase from basaltic rocks is about 0.5 weight percent iron.

Other transition metals such as titanium and vanadium (Geake and others, 1972) and chromium (Geake and others, 1973) are probably capable of producing luminescence in the red band but, owing to their proportionally minor abundance in natural feldspar, have an effect on luminescence that is subordinate to that of iron and is probably not detectable in most samples. The rare-earth element samarium has been identified as causing luminescent emission in the red band (Drake, 1972) but is present in basaltic plagioclase in amounts of 1 ppm or less (Smith, 1974) and should not have a noticeable effect on the observed spectra.

Certain elements, among them iron, cobalt, and nickel, have been proposed by some workers to act as inhibitors to suppress TL emission. These elements are apparently effective in promoting radiationless transitions from the conduction to the valence band at the expense of radiative transitions (Leverenz, 1968). There is some specific evidence to indicate that  $\text{Fe}^{2+}$  acts as a TL suppressant, whereas  $\text{Fe}^{3+}$  is an activator (Geake and others, 1971), as described.

#### RADIATION DAMAGE IN DOSIMETER CRYSTALS

Radioactive decay particles of sufficient energy, in addition to producing ionization, are capable of displacing atoms from normal lattice positions. Few studies have been made of the extent of naturally produced radiation damage in TL dosimeters and the effects of such damage on luminescence spectra and TL efficiency. Most studies have used high-intensity doses of artificial radiation to create defects; the production rates and effects are then extrapolated to the natural situation. For example, bombardment of a lunar fines sample with  $\sim 10^{10}$  fission fragments from a  $^{252}\text{Cf}$  source was found to produce no significant alteration in the TL response of the sample to a standard dose of beta radiation (Hoyt and others, 1972). A calculation of the number of new traps theoretically produced in a mineral by natural radioactive decay over a period of  $10^4$  years by Tite (1968) showed the effect to be negligible. As a consequence, in most archeologic dating schemes, the trap population is assumed constant over the geologically short time span for which these methods are used (Aitken, 1970). There is considerable evidence, however, to indicate that the defect density of minerals is increased by prolonged exposure to natural radiation and that this increase has an augmentive effect on TL response.

Alpha particles and recoil nuclei from both uranium and thorium atoms are particularly efficient in terms

of the number of defects produced per unit of radiation dose. They are relatively inefficient in producing ionization, as the ionization efficiency of alpha particles has been found to be about an order of magnitude less than that of an equivalent dose of beta or gamma radiation (Aitken, Zimmerman, and Fleming, 1968).

Alpha particles from uranium and thorium decays range in energy from about 4 to 7 MeV (million electronvolts) and, for particles to 5 MeV, produce an average 30 to 100 stable dislocations per decay event in a material of  $Z \leq 30$  (Levy, 1968). Recoil nuclei from alpha decays produce many more dislocations along a very short ( $\sim 500$  Å), highly disturbed path through the crystal lattice that can be revealed for study by etching; such paths are referred to as "tracks" (Walker, 1973). Only about 2 percent of the total alpha decay energy is partitioned to the recoil nucleus.

The effectiveness of alpha particles in producing defects is severely limited by the fact that they have an average range of only about  $25 \mu\text{m}$  in a crystalline matrix (Fleming, 1972). Since most of the uranium and thorium in rocks and pottery is located in the groundmass and clay matrix, respectively, of these two important materials, this restricted range limits both the number of alpha particles that are likely to reach TL dosimeter grains and the effect in large grains of the few that do. This constraint was the principal reason for developing the fine-grain dating technique for pottery, where the fraction used has a dimension range of 2 to  $8 \mu\text{m}$  (Aitken, Zimmerman, and Fleming, 1968). For grains much larger than  $10 \mu\text{m}$ , alpha particles probably penetrate only the periphery. This limit can theoretically result in a discrepancy between the anticipated TL intensity based on the calculated natural dose rate and the actual measured TL.

Beta particles and gamma rays are capable of displacing atoms from lattice positions if an appropriate collision occurs before the particles have been degraded below the necessary energy threshold by ionization events, the principal form of energy dissipation. In the case of gamma rays, displacement events are rare and require as an intermediate step the formation of a Compton electron, which is then indistinguishable from other high-energy electrons (beta particles).

Travel distances for beta particles and gamma rays in a crystalline matrix vary widely in accordance with the broad range of particle energies but in general average a few millimeters for beta particles and a few centimeters for gamma rays. Even parent nuclides located in the matrix can emit radiation that has an essentially unattenuated effect on enclosed dosimeter grains. In plagioclase, the beta radiation from  $^{40}\text{K}$ ,

much of which is located in the crystals, supplies about 75 percent of the total beta and gamma radiation energy released during the decay of all the nuclides in a rock or other material and about 50 percent of the total dose rate adjusted for diminished alpha-particle efficiency.

According to Hwang and Goksu (1971), the minimum amount of energy that must be transferred to the struck atom in a displacement event is about 30 eV (electronvolts). Levy (1968) estimated the critical displacement energy to be about 25 eV and further stated that the minimum beta-particle energies required to displace oxygen and silicon atoms are  $1.6 \times 10^5$  eV and  $2.6 \times 10^5$  eV, respectively. These threshold energies indicate that a significant proportion of the beta and gamma radiation emitted during radioactive decay has sufficient energy to cause displacements, even though the probabilities of such events are rather low, being only  $10^{-2}$  to  $10^{-1}$  per beta decay event for particles from 0–5 MeV in energy and  $10^{-3}$  per gamma-ray emission for gamma rays of 0–3 MeV (Levy, 1968). Although the potential of these radiations for creating displacements is small, in view of their penetrating power relative to alpha particles, they could produce enough defects to add significantly to the total defect population.

### EXPERIMENTAL EQUIPMENT<sup>1</sup> AND TECHNIQUE

The experimental dating technique developed at the U.S. Geological Survey is technically similar to methods used in other laboratories but differs significantly in the philosophy of the approach. In an attempt to overcome the principal problem encountered with existing "absolute" dating methods—the apparent limitation of the range of the methods to probably the past few tens of thousands of years, principally because of anomalous fading and other factors—this investigation was undertaken with the specific goal of developing a "relative" dating procedure based on rocks of known age against which other samples of similar composition but unknown age could be compared. The concept embodied by this approach requires that natural TL accumulate in a predictable and monotonic manner but does not require that the storage of trapped charge be 100 percent cumulative with time. It also requires that the measurements of TL parameters be reproducible and representative but minimizes the need for the determination of absolute magnitudes.

### SAMPLE COLLECTION

The alkalic and tholeiitic basalts analyzed during this investigation, with the exception of three samples (5X340, Klpa 10a, Mol 1e), were collected from the Island of Hawaii at locations shown on the index map (fig. 3). A detailed description of sample locations is given in the list of sample locations and age data at the end of this report.

Most of the samples were collected in or near roadcuts mainly for convenience and the availability of fresh material, but also because that is where the original samples of flows dated by the potassium-argon method were obtained. Sample-collection criteria stressed collection of the freshest material available. Thin sections prepared during later laboratory processing revealed no alteration of the plagioclase laths in any of the samples collected. The samples were obtained as far beneath the exposed surface as possible to minimize the heating effect of isolation, which can be significant in black basalt at 20° N. lat. In roadcut sampling, an effort was made to avoid collecting near fractures produced by blasting operations, since the possible effects of shock on TL had not been evaluated. Where contacts were visible, samples were collected at least 1 m below the tops of flows to avoid any possibility of thermal TL drainage by overlying younger flows.

The alkalic basalt samples are from the Hawi Volcanic Series of the Kohala Volcano, Hawaii, with four exceptions: The youngest sample (023) is from Mauna Kea Volcano, Hawaii; the three oldest are from the islands of Molokai (Klpa 10a and Mol 1e) and Oahu (5X340).

The Hawi flows presented critical sampling problems, as all are prehistoric and are not identified on existing maps as discrete dated units. A few samples obtained from Donald Swanson (U.S. Geological Survey), including H71-3 and H71-10, represent extra material from earlier potassium-argon dating studies (McDougall and Swanson, 1972). The others (033, 035, 036, 041, and 042) were collected in the field on the basis of published distance measurements from recognizable landmarks. The obvious potential for error in sample collection under these conditions was minimized by comparing whole-rock K<sub>2</sub>O contents for the samples collected with those published with the potassium-argon data for the samples they were supposed to duplicate. Concordance to within less than  $\pm 2$  percent, or an average of about 0.025 weight percent K<sub>2</sub>O, was stipulated as the acceptable maximum limit of variation outside which samples were discarded as unreliable. This test should be reliable because most adjacent alkalic basalt flows from the Hawi Volcanic Series differ in whole-rock K<sub>2</sub>O content

<sup>1</sup>Any use of trade names and trademarks in this publication is for descriptive purposes only and does not constitute endorsement by the U.S. Geological Survey.

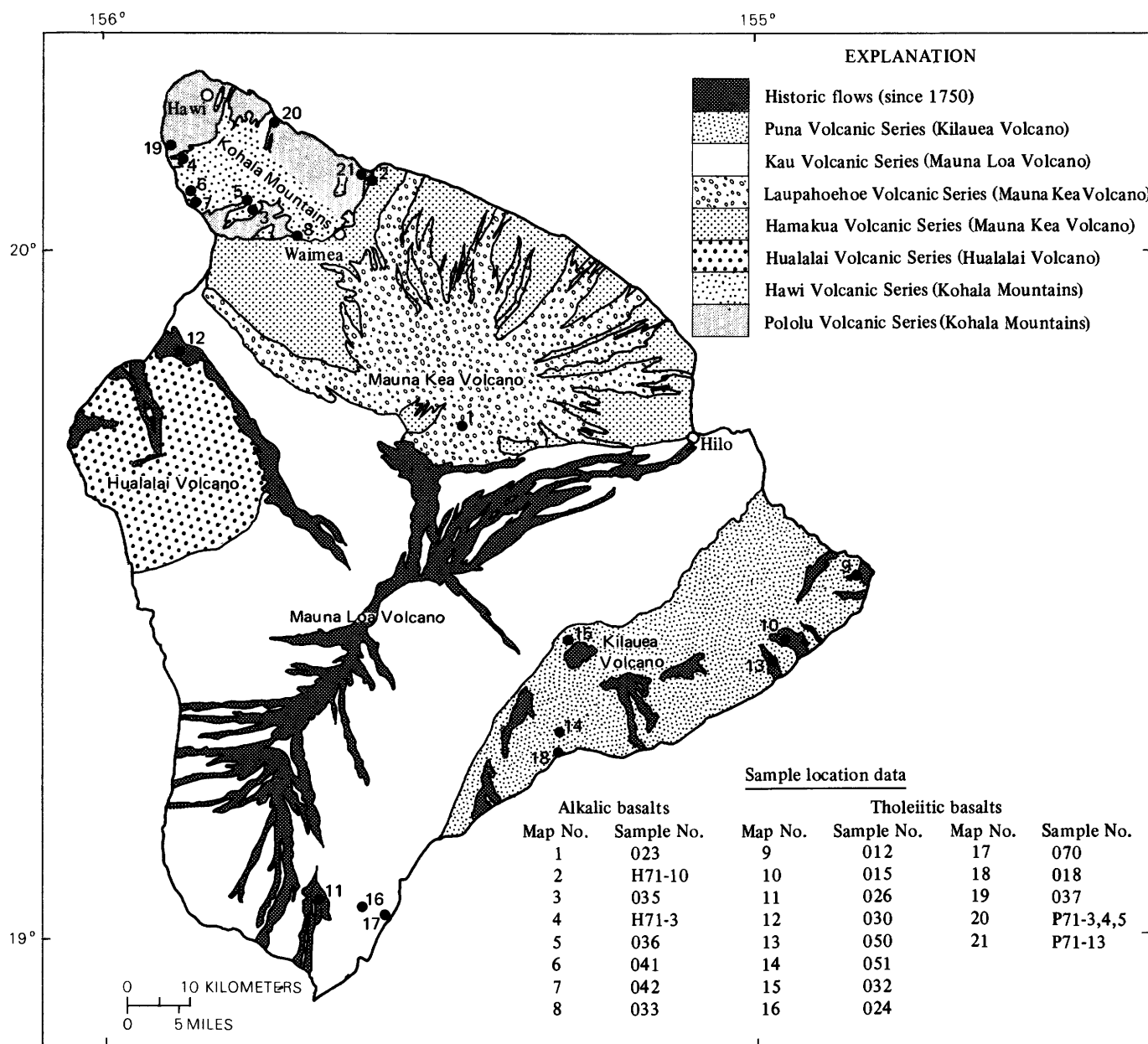


FIGURE 3.—Simplified geologic map of the Island of Hawaii showing sample localities. Samples are listed in order of increasing age for each rock type, as given under sample locations and age data. Geology generalized from G. A. Macdonald, *Atlas of Hawaii*, 1973 (R. W. Armstrong, ed.).

by at least 10 percent, commonly by as much as 30 percent. The test requires, though, that both  $K_2O$  analyses used in the comparison, if made by different laboratories, be highly accurate.

Sample 023 was collected from a young flow on the flank of Mauna Kea Volcano using location data supplied by Stephen C. Porter (Univ. of Washington). Samples Klpa 10a and Mol 1e from Molokai were supplied by M. H. Beeson (U.S.G.S.). Sample 5X340, from the Waianae Volcanic Series on the island of Oahu, was obtained from short drill cores (Doell and

Dalrymple, 1973).

The historic tholeiitic basalts were collected from roadcuts and flow surfaces on the basis of flow locations and eruption dates shown on U.S. Geological Survey topographic series 7½' quadrangle maps and on the geologic map of Hawaii by Stearns and Macdonald (1946). Samples dated by the carbon-14 method were recollected on the basis of careful sample location data compiled by G. B. Dalrymple (U.S.G.S.) during his initial collection of these flows for TL dating in 1966 and 1970.

Samples from the older tholeiitic flows from the Pololu Volcanic Series of Kohala Volcano whose identification numbers are prefaced by the letter "P" represent, like alkalic basalts H71-3 and H71-10, extra material from samples dated by I. McDougall (Australian National Univ.). They were provided for TL study by D. A. Swanson (U.S.G.S.). Sample 037 was collected in a roadcut identified by road mileage measurements. Its validity is suspect because its K<sub>2</sub>O content differs by 0.04 weight percent from the sample it was supposed to duplicate. It was tentatively accepted as valid.

#### SAMPLE PREPARATION

Measurements of thermoluminescent intensity were made on both alkalic and tholeiitic basalts using pure plagioclase separates of a carefully restricted size range as the TL dosimeter. The sample-preparation procedure involved crushing, separation of a precisely sized whole-rock fraction by sieving, and the final segregation of plagioclase with heavy liquids.

Crushing during sample preparation has been found by several workers to alter the natural TL of several materials and minerals. The effect involves either enhancement of the natural TL signal by a stress-related process involving the ionization of constituent atoms (tribothermoluminescence), or by TL drainage. Tribothermoluminescence produced during crushing was found to contribute significantly to the natural TL signal of calcite (Zeller and others, 1955) and tektites (Durrani and others, 1970) but to produce less than a 2-percent change in the measured TL from crushed meteorite samples (Houtermans and Liner, 1966). No detectable effects were found in crushing experiments with fossil shells unless the <88-μm fraction was used (Johnson and Blanchard, 1967), nor were such effects as the filling of existing empty traps or the draining of filled traps found during crushing experiments with pottery (Tite, 1966). Negligible tribothermoluminescence effects were found by Hoyt and others (1970) in an experiment in which they vigorously shook samples of lunar fines for periods of half an hour. Drainage of natural TL during crushing has been observed and was found by Aitken, Zimmerman, and Fleming (1968) to result in an average of 30 percent more natural TL in pottery fragments crushed gently in the jaws of a vise than in the same size range of material from the same shards crushed with a mortar and pestle. A preliminary crushing experiment performed as part of this investigation involved the crushing of a piece of tholeiite basalt (018) in a press by several applications of moderate stress of approximately 2 seconds duration each. Nearly all measurea-

ble natural TL was found to be drained by the crushing process.

The wide disparity in apparent crushing effects is probably a function of the wide variety of materials studied, some being more susceptible to modification by crushing than others. The duration and (or) intensity of the crushing process and the size range of the material used for TL measurement are critical parameters. In order to investigate the effects of crushing on plagioclase in more detail, a careful crushing experiment was conducted as part of this investigation. The results of the crushing experiment are discussed in the section entitled "Natural TL."

The crushing experiment consisted of two successive crushings of each sample at different applied stress intensities. All sample handling from this stage on was under indirect or subdued light conditions to avoid any possible modification of natural TL properties by either artificial or natural ambient light.

The first, or stage one, crushing consisted of putting fist-size and smaller pieces of basalt, obtained by reducing larger blocks with a minimum number of blows from a 1-kg rock hammer, through a chipmunk (jaw) crusher whose minimum discharge opening was about 1.5 cm. Two to 3 kg of basalt was usually required to be certain of an adequate plagioclase yield during subsequent separation procedures. The fraction greater than 74 μm from the stage-one crushing was separated by sieving with metal screens and a Tyler sieve shaker. A preliminary separation of the ≈37- to 44-μm (<325, >400 mesh) fraction used in the TL-dating studies was conducted simultaneously at a lower position in the sieve stack. The coarse fraction (>74 μm) was subsequently run through a roller crusher with the rollers set 0.16 cm apart. This constituted crushing stage two, the fines from which were sized to 37 to 44 μm by a preliminary sieving identical to that described for stage one.

Final sizing consisted of a precision separation of the 37- to 44- μm whole-rock fraction using an Allen-Bradley sonic sifter. This instrument consists of a sonically driven vibrating air column incorporating screens of desired size. Cycles of 10 minutes' duration produced separates that were both dimensionally uniform and free of all adhering finer material.

A restricted range in grain size is a critical requirement in TL work because variations in grain size have been shown to produce significant differences in TL response from the same material. The effect is probably produced by differences in sample surface area per unit weight involving a lesser probability of self absorption for TL photons emitted from within smaller grains. Sabels (1963) showed that TL emission from the <37-μm fraction was nearly 100 percent

greater than emission for the 105- to 177- $\mu\text{m}$  fraction in crushed whole-rock basalt.

A size range of 37 to 44  $\mu\text{m}$  was selected for use in this research because it generally yielded monomineritic plagioclase separates with a minimum of binary grain contamination.

Plagioclase was separated from the whole-rock material with a centrifuge using bromoform adjusted to the desired densities with water-free ethanol. The procedure used for all samples was successive separations at carefully controlled densities of 2.80 and 2.65. For most samples, the separates obtained had a purity of better than 90 percent. The few percent of contaminants consisted mainly of binary grain attachments of nonthermoluminescent silicate minerals (pyroxene and olivine) and oxides (principally magnetite).

#### MAJOR-ELEMENT PLAGIOLASE COMPOSITIONS

In an attempt to determine the range in average feldspar composition represented by the plagioclase separates from the samples of each rock suite and to provide a basis for an evaluation of the effect that differences in major-element composition have on TL response, analyses of the plagioclase separates for the elements calcium, sodium, and potassium were obtained for those alkalic and tholeiitic basalt samples for which adequate material remained after completion of the TL measurements. The analyses, made in U.S. Geological Survey Analytical Laboratories Branch, are reported in terms of the oxides of the elements (table 1). CaO was determined by atomic absorption; Na<sub>2</sub>O and K<sub>2</sub>O by flame photometry. Minor and trace elements were not determined because adequate material for such detailed measurements was not available.

The CaO, Na<sub>2</sub>O, and K<sub>2</sub>O contents of each separate when recalculated to 100 percent and plotted on a CaO-Na<sub>2</sub>O-K<sub>2</sub>O ternary diagram (fig. 4) were used to estimate an average plagioclase composition for each sample. The assignment of approximate mineralogic type was made by association of the plotted points with the plagioclase compositional line calibrated on the basis of the stoichiometric proportions of CaO and Na<sub>2</sub>O in each of the members of the plagioclase solid-solution series, as tabulated in Winchell and Winchell (1951).

The chemical composition of the plagioclase separates from the tholeiitic basalts all fall in a tight group within the labradorite field (fig. 4). The average composition for the group as estimated from the graph is about An<sub>60-65</sub>. This plagioclase composition is typical for tholeiitic basalts and compares favorably with a

TABLE 1.—Major-element chemical compositions of selected plagioclase separates, in weight percent

[Elements are reported as weight percent of the oxides. Analysts: CaO, Fred Simon; Na<sub>2</sub>O and K<sub>2</sub>O, Lois Schlocker]

Sample No.	CaO	Na <sub>2</sub> O	K <sub>2</sub> O
<b>Alkalic basalts</b>			
023	7.11	5.90	2.02
H71-10	4.09	6.14	2.87
035	2.32	7.53	3.25
H71-3		Insufficient material	
036	5.14	6.78	2.32
041		Insufficient material	
042	4.68	6.77	2.40
033	7.80	6.66	2.18
<b>Tholeiitic basalts</b>			
032	11.0	3.84	0.398
024	11.5	3.66	.364
070	12.8	3.61	.215
074	11.9	3.61	.322
018		Insufficient material	
019	11.0	3.22	.490
P71-13	11.1	3.29	.136
037	10.5	4.54	.720
P71-4		Insufficient material	
P71-3		Insufficient material	
P71-5	11.5	3.64	.182

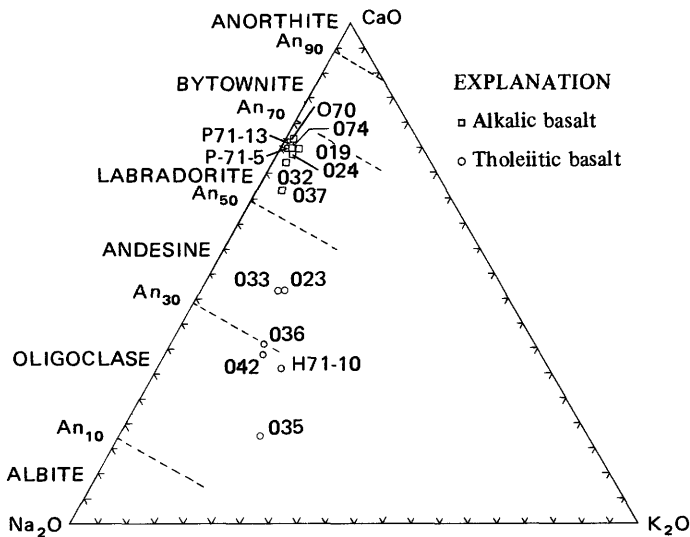


FIGURE 4.—Ternary diagram of alkalic and tholeiitic basalt plagioclase compositions expressed in terms of CaO, Na<sub>2</sub>O, and K<sub>2</sub>O. Plotted points represent analyses for the three oxides in weight percent recalculated to 100 percent. The dashed lines represent the mineralogical increments into which the plagioclase solid-solution series is divided, expressed in terms of CaO and Na<sub>2</sub>O.

petrographically determined compositional range of An<sub>59-70</sub>.

The plagioclase separates from the alkalic basalts have a considerably wider range in major-element chemistry. The compositional averages vary from about An<sub>20</sub> to An<sub>40</sub>, or from oligoclase to andesine, in a manner that reflects reasonably closely the bulk composition of the parent basalts in terms of position in

the magma-differentiation series. The alkalic basalts range in composition from hawaiite (036) through mugearite (042 and H71-10) to trachyte (035). The effects of this range in feldspar compositions on the TL properties of the samples are discussed in later sections.

#### TL MEASURING AND RECORDING EQUIPMENT

The TL measurement apparatus used in this investigation, shown schematically in figure 5, is a modification of the instrument described by Dalrymple and Doell (1970a). It consists of a black anodized aluminum sample chamber whose main function is to exclude external light and provide a sealed environment in which the composition of the atmosphere can be adjusted to exclude oxygen. The chamber incorporates fused silica (quartz) windows at both top and bottom; the upper window also serves as a thermal barrier to minimize heat conduction to the photomultiplier (PM) tube. The construction of the chamber permits installation of one or two optical filters in the TL light path to remove undesired portions of the emitted spectrum. Immediately above the sample is a screen designed to limit the emission detected to that from the sample alone.

The sample planchets used in the TL measurements consist of circular discs, 4.7 cm in diameter and 0.015 cm thick, pressed from fine (99.99+ percent pure) silver sheet. Silver was selected as the planchet material because it has one of the lowest emissivities of all the metals and one of the highest thermal conductivities, which minimizes thermal gradients during heating. The planchets have a central circular depression 1.2 cm in diameter and 0.04 cm deep for sample

placement. The backs of the planchets were coated with a thin layer of graphite (Aerodag G) to reduce the reflectivity of the silver and enhance absorption from the infrared heat source. The planchets were installed in the sample chamber in the position shown in figure 5 and sealed with silicone rubber O-rings above and below the periphery of the disc to prevent light from the heat source from reaching the PM tube.

The heating system consists of three symmetrically arranged quartz-iodide lamps whose radiation is focused on the bottom of the planchets with mangin mirrors, as shown in the diagram. Voltage to the lamps is increased linearly with a variable autotransformer driven by a variable speed DC motor.

Temperature during heating was monitored with a chromel-alumel thermocouple (T.C. in fig. 5) welded to each planchet with a 0.0076-cm-thick disc of pure nickel as an intermediary to overcome problems arising from spot-welding directly together two materials of widely differing resistivities, thermocouple wire, and silver. The nickel disc and attached wires were welded to each planchet immediately adjacent to the sample depression to insure accurate temperature measurement. Connection of the wires from each planchet to the rest of the thermocouple system was made with a simple overlapping compression joint at the edge of the sample chamber. The thermocouple output was connected to the X-Y recorder abscissa through a thermocouple reference junction, which provided electronically a room-temperature-compensated 0°C reference voltage. Temperature measurement reproducibility was estimated to be about  $\pm 3$  percent.

The TL was detected with an EMI 6255S "Q" quartz-window photomultiplier tube with a Cs<sub>3</sub>Sb cathode and an extended range in the near ultraviolet, mounted in an Electro Optics Associates (type PM-103) housing. The tube has a gain of about  $3 \times 10^7$  and a spectral response from 1,700 Å to about 6,500 Å with a maximum sensitivity near 3,900 Å (fig. 6). It was operated at an experimentally determined optimum potential of 1,100 volts. As the dark current at room temperature was found to be negligible, the tube was not cooled.

The pulsed signal from the PM tube was measured with an SSR model 1105/1120 photon counter/amplifier-discriminator, which has a deadtime of 25 nanoseconds and counts pulses of electrons at the anode of less than 10 nanoseconds duration as discrete events. All measurements were made with an instrumental statistical counting precision of  $\pm 2$  percent. The output of the photon-counting system was used to drive the ordinate of the X-Y recorder. The high-voltage power supply, photon counter, X-Y recorder, and

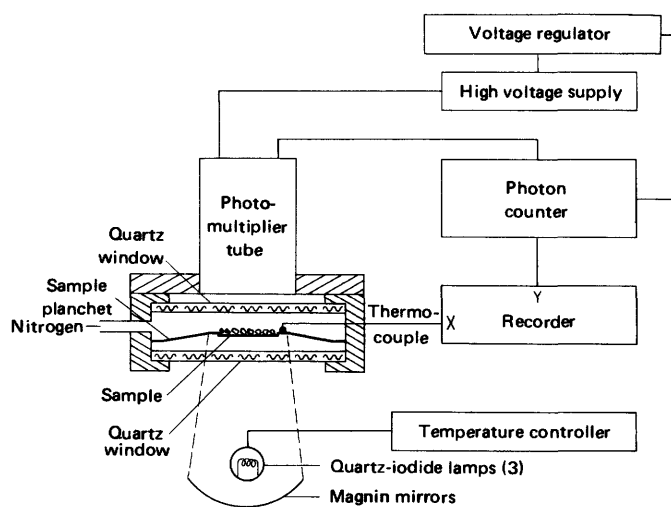


FIGURE 5.—Schematic diagram of the thermoluminescence reader.

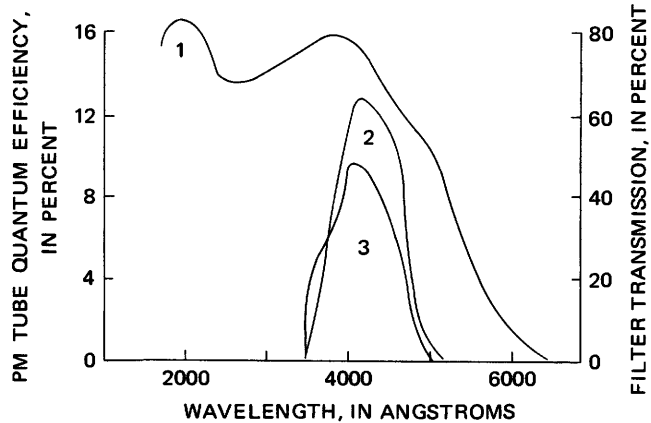


FIGURE 6.—Spectral response curves for the photomultiplier (PM) tube and filter CS5-60. Curve 1, response for PM tube 6255S "Q" in percent quantum efficiency, reproduced from manufacturer's calibration curve; 2, transmission curve for Corning filter CS5-60 in percent transmittance, reproduced from manufacturer's data; 3, schematic representation of the relative intensity and spectral distribution of the TL measured by this combination of filter and PM tube.

heating system were all powered through an isolation transformer and a voltage regulator to remove irregularities in the line current.

In all natural and artificial TL measurements made during this investigation that were used for age calculation, a Corning long-wavelength-absorbing blue filter (CS5-60) was used to inhibit the transmission of blackbody radiation. The filter, inserted in the light path above the upper silica window of the sample chamber, effectively delayed the onset of blackbody radiation interference to about 350°C. The wavelength detection range of the PM tube-filter combination is limited to the bandwidth from 3,500 Å to approximately 5,000 Å, with a maximum sensitivity at about 3,900 Å (fig. 6). This restricted bandwidth limits the TL detected to that from the 4,500-Å plagioclase emission peak.

Calibration of the TL detection system was performed at frequent intervals with a carbon-14-activated standard light source of known luminous flux to determine the extent of equipment drift, which was found never to exceed 5 percent from day to day or over an 8-hour series of experiments. Unfortunately, the light source has a markedly greater luminous intensity than any of the TL emissions observed in this investigation; in order to calibrate the detection system at the same level of light intensity as the TL observed, it was necessary to filter the output of the light source. Since the extent of filter attenuation of the intensity of the light source is not precisely known, it was not possible to use the light source to calibrate the TL signal in standard light units.

Radiation sources available at the laboratory for the production of artificial TL consist of both an X-ray and a beta source. The beta source is a plane-surface 45-millicurie  $^{90}\text{Sr}$ - $^{90}\text{Y}$  irradiator; the beta particles have an essentially bimodal energy distribution with maximum intensities from the two isotopes of about 0.2 and 0.9 MeV, respectively. This beta source has a flux of about  $100 \text{ rad min}^{-1}$  (air-equivalent). The X-ray source consists of a CA8S tungsten tube with beryllium windows that is mounted horizontally in a lead-lined aluminum irradiation chamber. The tube is equipped with a solenoid shutter and powered by a General Electric XRD-5 generator. The tube is operated at a power setting of 50 kilovolts and 25 milliamperes; the unfiltered radiation has a measured effective average energy of 14 keV at a tube-to-sample distance of 29 cm. Radiation output is approximately  $525 \text{ rad min}^{-1}$  (air-equivalent).

Samples were centered in the X-ray beam path by means of a fixed sample holder on a sliding tray, the guides and stops for which were carefully set to insure that the positioning was reproducible. An air-equivalent ionization chamber probe (Victoreen model 555-100 ma) was installed immediately adjacent to the sample depression of each planchet but was located such that it did not shadow any part of the sample depression during irradiation. The probe was used with a Victoreen model 555 Radocon II integrating radiation detection system to measure total radiation dose and control exposures. Radiation exposures could be automatically terminated by a circuit in the integrating system that tripped the shutter on the X-ray tube at a preselected total dose.

Calibration of the X-ray source was performed periodically using premeasured 30-mg batches of lithium fluoride TLD-100 thermoluminescent dosimeter. Each 30-mg sample was used only once owing to serious annealing effects produced in lithium fluoride by the heating required during TL determinations. The energy calibration measurements were made in the same experimental fashion as those for geologic samples. Comparison of peak heights provided the means of checking for uniformity of energy output, which was estimated to be constant over the duration of the investigation to within  $\pm 1$  percent.

An experiment designed to determine the relative efficiency of the two radiation sources in producing TL showed that to within measurable limits the TL produced by comparable total exposures (in air-equivalent rads) of beta and X-radiation were identical. In all irradiations made during this investigation, the X-ray source was used because of a higher radiation intensity, which reduced exposure times, and the convenience of the automatic exposure-termination system.

### PROCEDURE

Samples were isolated from direct laboratory light as much as possible during processing in order to minimize the detrimental effects that light has on TL. Ultraviolet light of sufficiently high intensity has a well-documented capability for draining TL from all trapping levels in most materials. It has been used to drain natural TL in studies where such drainage was desired, but an initial heating for that purpose was found to alter the response of the sample to subsequent doses of artificial radiation. Ultraviolet illumination has been found to be capable of inducing TL in many of the same materials, preferentially in traps contributing to low temperature peaks. Ultraviolet light from fluorescent bulbs was found to fill low-temperature traps in separates from pottery while draining high-temperature traps (Tite, 1966) and similarly to induce TL in the 150°C peak of lunar fines while draining the TL in the 200°–250°C peak of the same samples (Hoyt and others, 1972). A detailed study by Durrani and others (1973), using lunar fines and a relatively intense ultraviolet source, found that ultraviolet radiation will induce TL in all trapping levels but will do so preferentially in shallower traps if the sample is drained of preexisting TL. It will drain some of the TL from all trapping levels in irradiated samples.

An experiment performed as part of this investigation showed that exposure of drained plagioclase samples to a 150-watt frosted incandescent bulb at a distance of 60 cm for a period of 18 hours produced only a moderate low-temperature TL peak and no measurable TL in the high-temperature peak that is used for TL-dating studies. A 96-hour exposure of the same samples to the same light source did not produce any additional TL in the low-temperature peak but did produce a level of TL in the high-temperature (300°C) peak range that had an amplitude of about 15 to 20 percent of the previously measured natural TL. In general, these experiments indicate that to avoid possible modification of TL properties, sample handling should be under subdued light conditions, avoiding light sources with a large ultraviolet component such as fluorescent bulbs. If samples are stored in the dark between experiments and exposure to laboratory lighting is minimized during sample handling, incandescent lighting should not produce measurable adverse effects on the TL of plagioclase.

Preparation of samples for TL measurement consisted of spreading 4- to 7-mg aliquants of plagioclase as uniformly as possible over the sample depression of each planchet. The depressions were coated with a thin film of nonluminescent silicone fluid (Duxé Products) before sample placement to increase thermal contact and inhibit sample movement during subse-

quent handling. Seven aliquants (from each crushing stage) were measured for all samples for which adequate material was available, because this number of measurements was found to maximize the statistical benefits of multiple determinations within the limits of practicality.

The amount of plagioclase used in each TL measurement is critical. Differences in the intensity of light emitted by each of the several aliquants measured for a given sample are largely the result of variations in the amount of emitter present. In order to compensate for these variations in emission, the amount of material must be known. Unfortunately, although TL intensity increases with sample weight, above a certain optimum weight equivalent to a uniform layer one grain thick over the bottom of the sample depression, the increase in TL with further increase in sample weight is not linear. This is the result of the fact that the addition of material in excess of the optimum amount produces multiple grain layering, which reduces the emission effectiveness for those grains below the surface layer.

The most effective of the several empirical methods tried during this investigation for compensating for differences in TL response due to differences in sample weight is based on the observation that about 4.5 mg of material is required to uniformly cover the bottom of the sample depression; more material produces multiple grain layering. The method devised for calculating an effective sample weight, and used in all subsequent TL calculations, is based on an equation that assigns an effectiveness of 0.5 to the portion of the sample weight in excess of 4.5 mg:

$$W_a = 4.5 \text{ mg} + \frac{W_t - 4.5 \text{ mg}}{2}$$

where  $W_a$  is the adjusted sample weight and  $W_t$  is the total or measured weight.

After each planchet had been loaded with sample, it was placed in the sample chamber, the chamber sealed, and the PM tube placed in position directly over the sample depression. The chamber was then flushed with dry nitrogen containing less than 5 ppm oxygen at a rate of about 50 L hr<sup>-1</sup> for 7 minutes prior to heating, and continuously during the heating process, to strip oxygen in the chamber and any adhering to the sample grains. This procedure is necessary because many materials give a spurious emission when heated in the presence of oxygen (Johnson and Blanchard, 1967; Aitken, 1968), possibly a phenomenon caused by oxidation reactions on the surfaces of the dosimeter grains (Johnson and Daniels, 1961) or ignition of organic material. Radiative oxidation processes in general have been referred to by several

workers as chemiluminescence. The effect can obscure the natural TL in some low TL materials and may be partly responsible for the failure of several early TL-dating attempts. The levels of oxygen that have been observed to cause spurious TL are small; nitrogen containing about 30 ppm oxygen was found to produce a substantially greater spurious component in the TL of pottery than nitrogen with less than 5 ppm oxygen (Aitken, Fleming, Reid, and Tite, 1968). The use of dry nitrogen was found by Johnson and Blanchard (1967) to substantially reduce, or eliminate entirely, the spurious emission observed in TL measurements on fossil shells.

For the present study, samples were heated at a rate of  $20^\circ \pm 0.5^\circ \text{C sec}^{-1}$  from room temperature to a maximum of  $450^\circ \text{C}$ . This heating rate was selected primarily because it provides an optimum compromise between slower rates, which maximize peak resolution at a cost of reduced amplitude and faster rates, which produce maximum TL amplitudes with somewhat poorer peak resolution. Heating was terminated at a maximum temperature of  $450^\circ \text{C}$  because, even with filter CS5-60, blackbody radiation caused saturation of the TL detection equipment in the range 400– $450^\circ \text{C}$ .

Following an initial heating during which the natural TL was measured and drained, the samples were allowed to cool to a maximum of  $50^\circ \text{C}$ , then heated again to obtain the blackbody radiation background (see fig. 1). Upon cooling, the samples were removed from the chamber and exposed to a standard dose of X-radiation. The purpose of the irradiation was to refill the traps that had originally stored the natural TL-producing electron population. Radiation doses were measured electronically in roentgens (air ionization) and converted to rads, the unit of absorbed dose typically used in dosimetry. The conversion coefficient for air from ionization (roentgens) to absorbed dose (rads) is approximately 0.87. This factor was used in this investigation to approximate the dose absorbed by the feldspar because a specific conversion coefficient for compositionally complex feldspar has not yet been determined.

For age-determination purposes, the alkalic basalts were exposed to an 870-rad dose of X-rays and the tholeiitic basalts, which had a markedly lower sensitivity, to 1,740 rads. Both of these dose levels are low relative to those used by many other workers for a similar purpose but were found to be adequate since in this investigation the only requirement of a specific artificial radiation dose is that it produce a measurable peak that constitutes a reliable relative measure of the trap density in individual samples. Samples were sequenced such that none was irradiated within

1 hour of the last heating.

Following irradiation, the samples were replaced immediately in the sample chamber and allowed to equilibrate in the dark for 7 minutes (with the nitrogen flowing) to permit spontaneous decay of the most unstably trapped electrons. The samples were then re-heated in the same manner as that used during natural TL measurement to measure the artificial TL and blackbody radiation background. The artificial TL was used during age calculations to normalize differences in natural TL due to differences in trap density.

TL magnitudes were quantified in terms of peak heights measured vertically from the blackbody curve to the glow curve at the point of maximum amplitude on the TL curve of the particular peak being studied. Peak heights were used instead of peak areas because measurement of peak heights minimized the interference from overlapping tails of adjacent lower temperature peaks. Low-temperature peak interference was not a problem in measuring the high-temperature natural TL peak that occurs between  $340^\circ$  and  $365^\circ \text{C}$ , because spontaneous decay over geologic time eliminates the electrons in shallow traps. In the measurement of artificial TL, where as many as four peaks with maxima at about  $110^\circ$ ,  $150^\circ$ ,  $225^\circ$ , and  $300^\circ \text{C}$  were observed in most samples, as shown in figure 7, the high-temperature tail of the  $225^\circ \text{C}$  peak occasionally interfered with the measurement of the  $300^\circ \text{C}$  peak. The interference, when present, did not usually add more than a few percent to the amplitude of the  $300^\circ \text{C}$  peak maximum.

The effectiveness of peak heights for quantitative TL measurement was tested by comparing peak height and area data using samples for which interference from the adjacent low-temperature peak was minimal. The peak heights were found to be as reliable a relative measure of intensity as the corresponding areas.

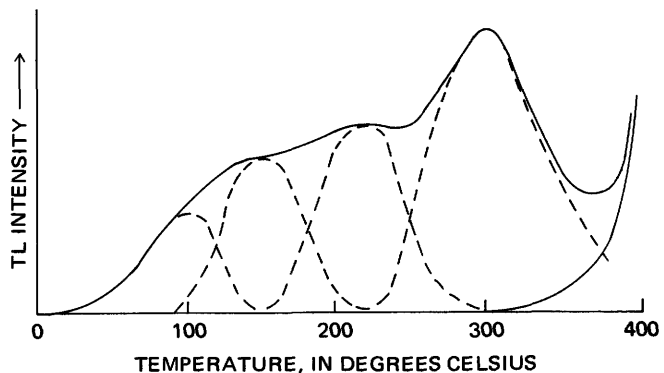


FIGURE 7.—An approximate schematic segregation of a plagioclase artificial TL glow curve into the four peaks identified as the principal constituents of artificial TL emission.

### ANALYSIS OF THE PLAGIOCLASE EMISSION SPECTRUM

The TL spectra of plagioclase from several of the alkalic and tholeiitic basalts were analyzed for the purpose of identifying the extent to which variations in the emission spectra influence the peak heights recorded during TL measurement and the possible effect of such variations on calculated TL ages. The data would also provide an opportunity to evaluate possible correlations between basic TL properties and major feldspar composition.

#### PROCEDURE AND RESULTS

Interference filters (Spectracote Varipass Filters manufactured by Optics Technology) were used to segregate the portion of the emission spectrum of the 300°C artificial TL peak between 4,000 Å and 5,000 Å into 500-Å bandwidths. The transmission characteristics of the filters, shown in figure 8, were designed for use with normally incident light. Their use to resolve uncollimated TL introduces a systematic error in the results because the effective cut-off limit of each filter migrates to progressively shorter wavelengths as the angle of incidence of the TL deviates increasingly from the normal. In view of this limitation, the data presented must be considered to be approximate.

The experiment was performed by exposing two aliquants of each sample to a standard dose of X-radiation followed by TL measurement. The natural TL emission spectrum of these samples was not analyzed, because material available was insufficient for the multiple determinations required.

Alternate irradiations of each aliquant were measured without an interference filter to provide a check on possible changes in TL sensitivity resulting from the repeated irradiation-heating cycles. In practice, the two unfiltered measurements preceding and following each filtered measurement were averaged to provide an accurate unfiltered peak height against which the filtered measurement could be compared. The percentage of TL in the 4,000–5,000-Å and 4,500–5,000-Å bandwidths as well as that in the bandwidths 1,700–4,000 Å and 5,000–6,000 Å were obtained by calculating the difference between the amplitude of the 300°C peak transmitted by each of the filters and the unfiltered average peak height described above.

The results of the spectrum analysis for both the alkalic and tholeiitic basalts are shown by a histogram (fig. 9) representing the average of the data for the two aliquants from the sample. The data have been corrected for both the approximate attenuation of the interference filters in the bandwidth transmitted and the bias imposed on the measurements by the spectral response of the PM tube.

The individual bandwidth values for the two aliquants from each sample were surprisingly similar, differing in most cases by less than 5 percent. With all sources of error taken into account, the individual spectral bandwidth values are probably accurate to within an estimated  $\pm 20$  percent.

#### DISCUSSION

The natural TL emission spectra at 300°C of these samples, though not studied, are expected to be simi-

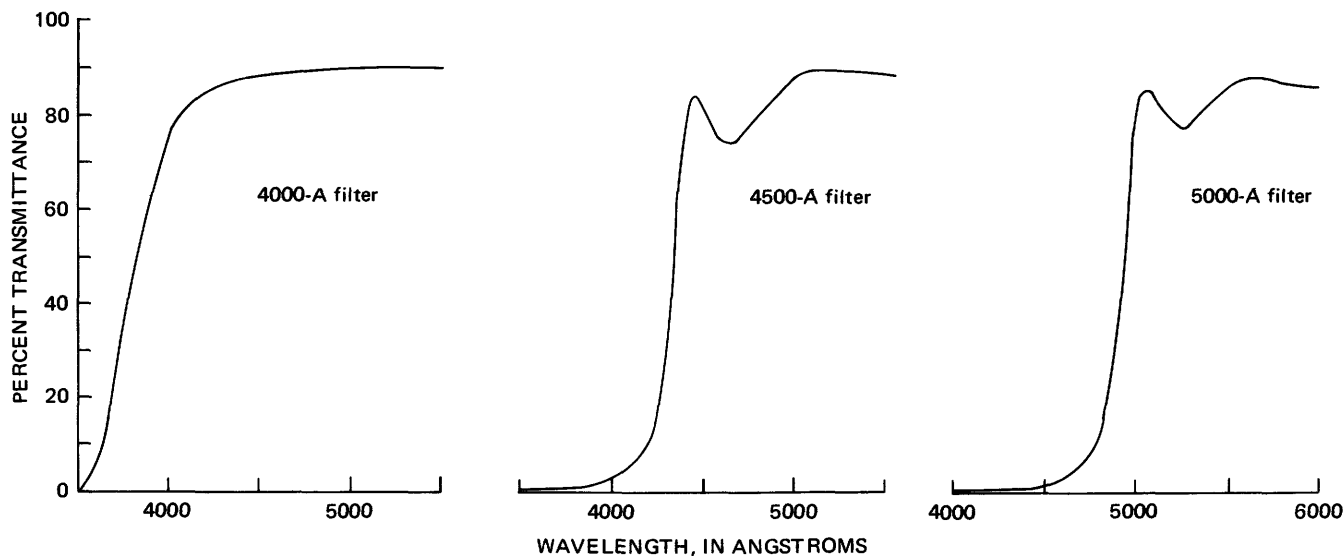


FIGURE 8.—Transmission curves for the interference filters used for spectrum analysis. Curves reproduced from manufacturer's data.

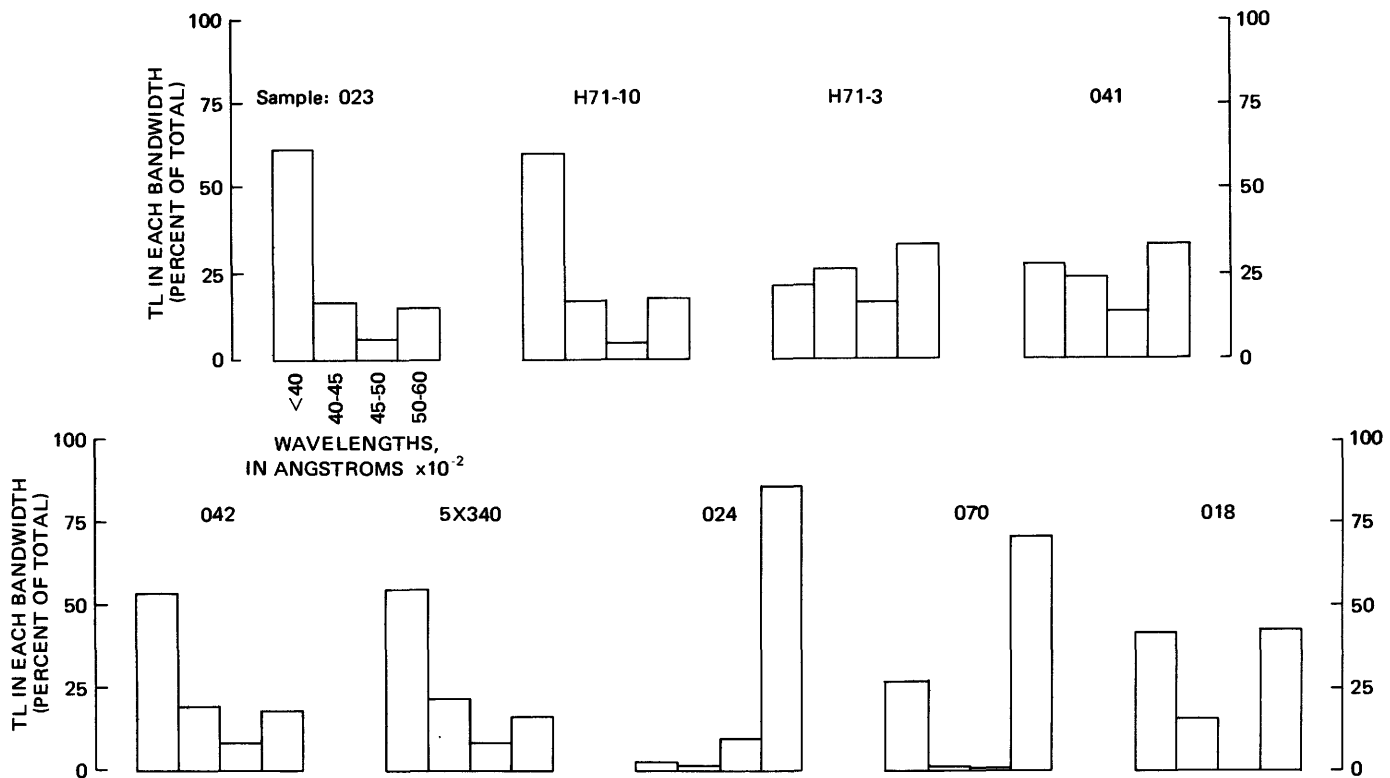


FIGURE 9.—Spectral composition of the 300°C artificial TL emission from selected alkalic and tholeiitic basalt plagioclase separates. The spectra are normalized for filter attenuation and PM-tube bias; the wavelength increments are the same for all analyses. Alkalic basalts: 023, H71-10, H71-3, 041, 042, and 5X340. Tholeiitic basalts: 024, 070, and 018.

lar to spectra defined for the artificial TL because the same traps and recombination centers are responsible for both types of emission. The probable similarity of the natural and artificial TL spectra is discussed in more detail under "Artificial TL."

There are no consistent correlations between spectral characteristics and measured chemical components for either the alkalic or tholeiitic basalts. One of the most significant aspects of the data is the prominent component of TL below 4,000 Å that appears in the spectrum of all the alkalic basalts and two of the three tholeiitic basalts. Emission in this bandwidth has not heretofore been reported for plagioclase. The emission occurs between 1,700 Å, the approximate lower limit of detection of the PM tube, and 4,000 Å, the nominal cut-off limit of the shortest wavelength interference filter available. Since the peak has not been reported previously, the upper limit of significant emission must actually occur at less than 3,500 Å, the lower limit of detectability for the systems used by most other workers (for example, Sippel and Spencer, 1970; Geake and others, 1971, 1972, 1973). The magnitude of the short-wavelength component reported for each sample in figure 9 may be in error (too large) by as much as 10 percent owing to reflection at the lower glass-air interface of the interference filter. This re-

flection was not present in unfiltered measurements. The short-wavelength component does not appear to vary systematically with either increasing sample age or chemical composition among the alkalic basalt samples studied. It does appear to increase with age in the three tholeiitic basalts, but an explanation for this relation is not available at this time.

The overall spectral characteristics of the alkalic and tholeiitic basalts differ significantly. The only recognizable spectral trend common to both rock types is the poorly defined tendency for the proportional amplitude of the 4,500-Å peak, which can be approximated by summing the percentage values in the 4,000–4,500-Å and 4,500–5,000-Å bandwidths, to increase with age. The percentage values in this band for the alkalic basalts are listed in table 2. This trend, which could be a function of increase in the number of crystal defects with age, is shown more clearly for both the alkalic and tholeiitic basalts by the rate of increase in the amplitude of the 300°C artificial TL peak measured (with filter CS5-60) for these and the other samples studied. Within the alkalic basalt suite, the enhanced 4,500-Å emission from samples H71-3 and 041, both of which have relatively low whole-rock K<sub>2</sub>O contents, provides the basis for a circumstantial correlation whose validity and significance are unknown.

TABLE 2.—Percentage of total TL in the 4,000-Å to 5,000-Å bandwidth for the 300°C alkalic basalt plagioclase artificial TL peak

Sample No.	Sample age (years B.P. <sup>1</sup> )	Percent TL in the band 4,000 Å to 5,000 Å	Whole-rock K <sub>2</sub> O (weight percent)
023	4,500	21.8	2.02
H71-10	62,000	21.8	2.82
H71-3	150,000	44.2	1.81
041	181,000	38.2	1.61
042	184,000	28.6	2.34
5X340	3.3×10 <sup>6</sup>	29.8	1.23

<sup>1</sup> See sample location and age data at end of report.

One of the most significant differences in the spectra of the two rock types is the marked enhancement of the >5,000-Å component in the tholeiitic basalts relative to the alkalic basalts. The emission correlates with the 5,600-Å emission peak, and its prominence in the tholeiitic basalts may be the combined effect of a lower density of defects and higher manganese contents in the plagioclase from these rocks. This relation agrees in general with the findings of Sippel and Spencer (1970) that the green peak is relatively low in plagioclase near the albite end of the plagioclase series, presumably in response to low concentrations of manganese.

For most of the samples analyzed, the broad composite TL peak between 150° and 250°C (fig. 7) was found to consist of a greater percentage of >5,000-Å (green peak) emission than that observed for the 300°C peak. For the alkalic basalts, the >5,000-Å component accounts for between 15 and 50 percent of the middle temperature peak TL emission. The origin and significance of this difference in emission spectra between the different temperature TL peaks is not understood at the present time.

The significant differences in the TL emission spectra of plagioclase of differing compositions do not necessarily present a serious problem for use of the data in dating work provided the natural and artificial TL spectra are closely similar. Differences in spectra, and consequent differences in TL peak amplitudes, are largely cancelled by the natural-to-artificial TL peak height ratio used in the final age determination.

#### SUMMARY

The results of this experiment indicate that there are large differences in the emission spectra of the plagioclase of the tholeiitic and alkalic basalts and significant variations among samples of each of the two rock types. These variations show no consistent correlation with identified chemical properties but, in the case of the 4,500-Å emission peak, do show a tentative correlation with sample age. Differences in emission spectra between samples do not influence age calcula-

tions if the natural and artificial spectra are closely similar. There is significant TL emission in the bandwidth 1,700 Å–4,000 Å that has not been reported before and whose origins were not identified during this study. The emission for the tholeiitic basalts in the bandwidth >5,000 Å is significantly enhanced relative to that for the alkalic basalts. The difference probably originates in a lower concentration of defects and higher manganese contents in the plagioclase from the tholeiitic basalts. The emission spectra from different temperature TL peaks from a given sample differ, that from the composite 150°–250°C peak having a larger percentage of >5,000-Å emission than the 300°C peak.

#### LINEARITY OF TL ACQUISITION, SATURATION EFFECTS, AND SENSITIZATION

A series of experiments was performed to evaluate: possible changes in the TL properties of plagioclase caused by progressively increasing exposures of X-radiation, the appearance of saturation effects from large radiation exposures, and changes in TL response resulting from repeated irradiation and heating. The experimental procedure used to study the first two effects consisted of exposing two aliquants of plagioclase from each of the alkalic and tholeiitic basalts selected for study to increasing doses of X-radiation, followed by measurement of the unfiltered TL; data for the third was obtained during the spectrum analysis experiment.

#### LINEARITY OF TL ACQUISITION AND SATURATION

During the linearity experiment, the 300°C peak was measured for all samples in which it was detectable. For the tholeiitic basalts, the 150°C peak was measured as well. The values reported are the averages for the two aliquants analyzed from each rock.

The radiation exposures used in this experiment ranged from 217 to 34,800 rads. This range of radiation exposures is relatively small compared to that used by other workers; the maximum exposure of approximately 35,000 rads was similar to the level used by many workers for normal dating studies. In previous studies of saturation effects, exposures exceeding one million rads have been reported (Hwang, 1972; Durrani and others, 1973).

The TL sensitivities of the plagioclase separates from the two rock types varied so widely that no one sample was exposed to the whole exposure range. The alkalic basalt response was studied with lower exposures, and that for the tholeiitic basalts was studied with exposures which started higher and progressed to the upper limit.

The TL intensities produced in the plagioclase from both rock types by progressively increasing exposures of X-radiation increased at a slightly lower than linear rate, as shown in figure 10. The data are presented in terms of peak heights plotted against the activating X-ray exposures. For comparison and convenience, the data for the 150°C peak for alkalic basalt sample 023 are plotted with that for the tholeiitic basalts.

The artificial radiation exposures used to study TL production in the alkalic basalt plagioclase ranged from 217 to 6,960 rads. The plagioclase had such a high TL efficiency, however, that for several samples, including H71-10 and Mol 1e, an exposure of only 1,740 rads produced saturation of the photon counter. Values reflecting equipment saturation are not shown in the accumulation plots (fig. 10), since actual TL saturation of the 300°C peak was not observed in any of the samples studied.

The tholeiitic basalt samples had a lower TL sensitivity to radiation than the alkalic basalts. As a result, radiation exposures were started at 1,740 rads and increased to an arbitrary maximum of 34,800 rads. The lower sensitivity for the tholeiitic basalt is shown by the markedly lower  $X$ -intercept values obtained by extending the TL accumulation lines for both rock types to the abscissa. These values provide a relative assessment of the overall TL sensitivity of the samples, a complex quantity composed of chemical and crystal defect influences on TL storage and emission. The  $X$ -intercept values could be used to quantify TL response for age calculation purposes and might provide an increase in accuracy over estimates of trap density obtained at a single radiation exposure.

The rate of increase in TL from greater exposures of X-radiation can be approximated by an exponential equation of the form.

$$y = (1 - e^{-x})$$

where  $y$  is peak height in units of centimeters per milligram and  $x$  a representation of the radiation dose in rads. The lines drawn through the data points in the plot are described by this equation, which has also been shown to define the artificial TL acquisition rate for fluorite and reportedly for other materials as well (Kaufhold and Herr, 1968).

The results of this study are not applicable to an assessment of either the accumulation rate or maximum storage capacity for natural TL, because the dose rates and exposure times for natural and artificial radiation differ radically and this difference, in particular the duration of exposure, produces large differences in the effects of thermal and nonthermal drainage on the stored-electron populations.

The parallel arrangement of the empirically derived

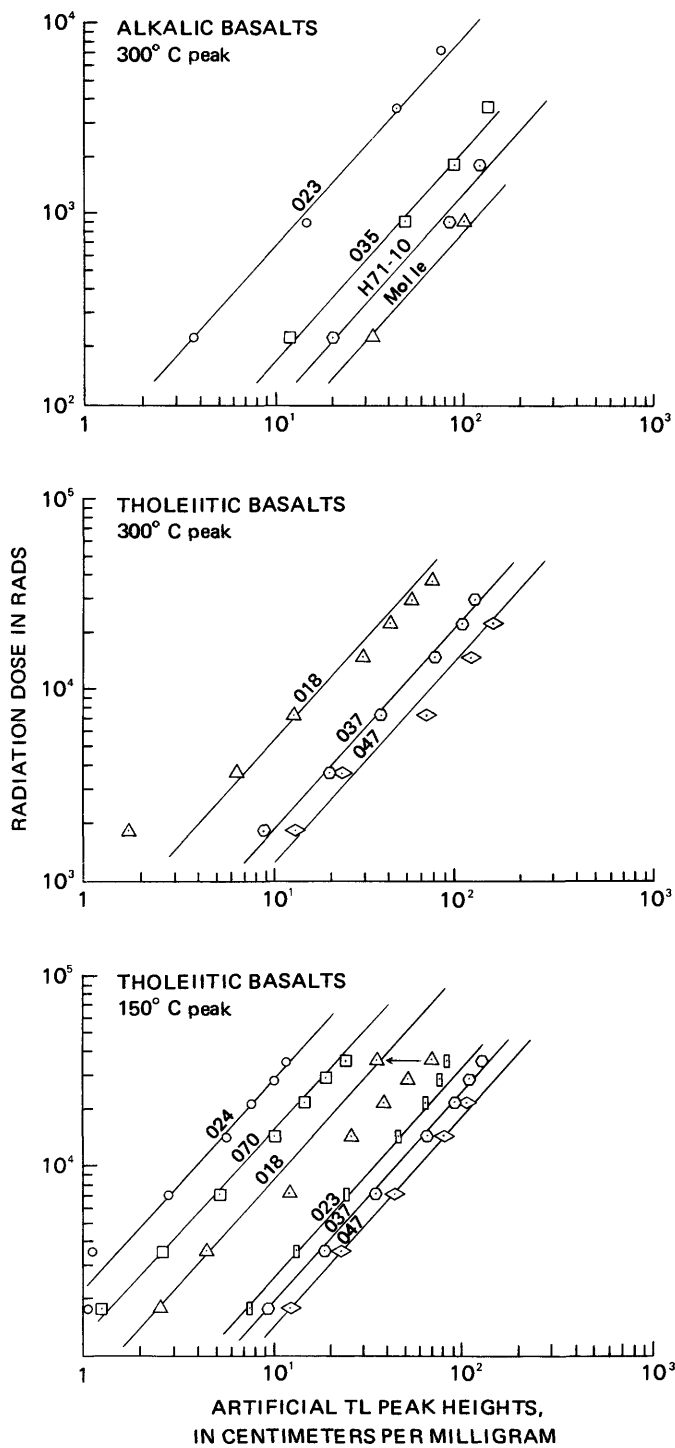


FIGURE 10.—Rate of TL accumulation with increasing radiation exposure in both the alkalic and tholeiitic basalts.

best-fit lines through the data for each sample of both the alkalic and tholeiitic basalts is significant, as it indicates the existence of a uniform process governing the rate of TL acquisition with increasing radiation dose that is independent of mineral composition. In

the case of the tholeiitic basalts, the similarity of the TL growth rates for both the 150° and 300°C peaks indicates that the trapping parameters and partitioning of untrapped electrons among the recombination centers during TL measurement remain constant with increasing radiation dose.

The progressive deflection of some of the plotted points for the 150°C peak of sample 018 to the right of the TL acquisition line for that sample reflects an increase in TL sensitivity produced by some aspect of the repeated irradiation and heating cycles. The extent of sensitization can be quantified, and compensated, with the aid of low-dose calibration irradiations interspersed through the irradiation series. Comparison of the calibration peak heights with the peak from an initial equivalent radiation exposure provides a means for calculating a sensitivity correction factor. An example of such a correction is shown for the 150°C peak from 34,800 rads for sample 018. The direction and magnitude of the correction is indicated by the arrow between the points.

With the exception of samples 037 and 074, for which both the 150°C and 300°C peaks were affected by equipment saturation at high exposures (values not shown in fig. 10), the only apparent sample saturation effects are those shown by the deflection of some of the 150°C peak values for sample 023 to the left of the TL acquisition line. The general absence of saturation effects is in agreement with the work of most investigators, who report that the short-term shortage capacity of many minerals is not exceeded for exposure levels of less than many tens of kilorads of artificial radiation.

#### SENSITIZATION EFFECTS

The heating of some materials during TL measurement and annealing experiments has been found to produce systematic changes in TL sensitivity (Foranca-Rinaldi, 1968; Hwang, 1972), which may be either increased or decreased, with increases being more commonly observed. The effect is commonly variable among samples of the same material. In some materials, the tendency for TL to increase is exacerbated by exposure to a large radiation exposure prior to heating.

Data on sensitivity changes in feldspar are limited but generally indicate either no change or slight enhancement in TL response; no significant decrease in TL sensitivity with heating has been reported. Experimental studies include an annealing experiment by Hoyt and others (1970) in which samples of lunar fines that contain plagioclase were heated to 800°C. Lattice defects should be mobile at this temperature, but no change in TL response was detected. A similar

experiment by Garlick and others (1971) in which samples of lunar fines were annealed in an atmosphere of pure argon at 600°C also produced no detectable change in TL response. More recently, Durrani and others (1973) found that heating lunar fines to 550°C during TL measurement enhanced the response of the heated material to a subsequent 800-kilorad dose of gamma radiation by 40 percent in the 300°–500°C range but that after the initial heating there was no further change. In another experiment, Durrani and others (1973) exposed a sample of lunar fines to a gamma-ray dose of 1.4 megarads, then annealed the sample at 450°C for 1 hour. The sensitivity of the sample to a subsequent radiation exposure was increased by 50 percent. Geake and others (1971) heated feldspar to 1,050°C for 30 minutes and found no change in the position of the spectral emission peaks.

#### PROCEDURE AND RESULTS

Most of the data used in this study to evaluate changes in TL sensitivity were obtained during the spectrum analysis experiment. The data show that for the two heating cycles and one irradiation required for age determination, there is a negligible change in the TL sensitivity of plagioclase from the alkalic and tholeiitic basalts within the limits of experimental error. This result may be a function of the relatively short (<25 s) heating times and low radiation exposures used in this investigation; it is significant because it indicates that the artificial TL peaks provide an accurate relative measure of TL sensitivity.

The effect of the first heating (for natural TL measurement) on TL sensitivity was tested for the six alkalic basalt samples selected for spectrum analysis. The samples were exposed to 870 rads of X-radiation prior to the first heating. The artificial TL peak heights obtained were compared with those from equivalent samples that had been thermally drained. The peak amplitudes were identical to within less than the normal 5 percent experimental error. A comparable analysis of four tholeiitic basalts gave similar results.

The exposure of aliquants of both alkalic and tholeiitic basalt plagioclase to more than four to six irradiations and heatings produced a definite but somewhat erratic increase in sensitivity in most samples. The effect was more pronounced in the tholeiitic than in the alkalic basalt separates. In the 8 to 10 cycles required during analysis of the spectral composition of plagioclase from the alkalic basalts, increases in the sensitivity of the 300°C peak were found to range from 0 to 15 percent and to average about 4 percent. For plagioclase from the tholeiitic basalts, calculations of sensitivity were based on the 150°C peak

because in unfiltered runs involving young samples the 300°C peak was not well enough defined for measurement. The percentage increases in sensitivity calculated for the 150°C peak are probably comparable to the sensitivity changes in the 300°C peak in most cases. Sensitivity increases for the plagioclase from the tholeiitic basalts averaged about 20 percent in 10 cycles and increased to an average of about 25 percent in 15 cycles although behavior was very erratic. Sensitivity increased by as much as 50 percent or more in 15 runs in a few cases. There was no discernible correlation of sensitivity changes with measured plagioclase composition for either rock type.

#### SUMMARY

The results of the linearity study show that the rate of TL accumulation with increasing radiation dose follows a precise pattern that is independent of both dose level (within limits) and mineral composition. The only difference in the data between samples is the X-intercept dependency of each TL accumulation line on trap density and TL emission properties. The uniformity of TL acquisition over a wide range of radiation exposures provides justification for the use of low exposures to determine relative differences in TL sensitivity between samples. No evidence of TL saturation was observed in the 300°C peaks of any of the samples studied; sensitization problems were significant only for the 150°C peak of sample 018.

The results of the sensitization analysis indicate that although plagioclase is sensitized by repeated heatings and irradiations, there is no perceptible change in response during the two cycles necessary for dating. For other experiments requiring repeated irradiation and heating, the calibration irradiations discussed for sample 018 can provide a means of compensating for the enhanced response.

#### FADING OF ARTIFICIALLY INDUCED TL

An experiment was performed to assess the extent of peak interference caused by the tail of the 225°C peak overlapping the peak maximum of the 300°C peak (fig. 7). The experiment involved storing irradiated samples in the dark at room temperature for varying lengths of time to produce a greater degree of decay of the 110°, 150°, and 225°C peaks than of the 300°C peak, owing to the greater probability for the spontaneous untrapping of electrons in shallower traps.

The experiment provided an opportunity to study the rate and extent to which TL fade (drainage) occurs in plagioclase. Spontaneous fading has already

been shown to be a complex process involving both thermally dependent and nonthermal decay processes (see sections on "Stability of Trapped Electrons" and "Nonthermal Drainage"). It poses a potentially serious problem for "absolute" TL dating methods that require the cumulative storage of all electrons trapped over geologic time.

#### PROCEDURE AND RESULTS

The experimental procedure consisted of exposing at least 8, and in a few cases 12, of the aliquants from each of the rocks selected for study to 1,740 rads of X-radiation. The aliquants were those that had been used previously for TL-dating studies. The reirradiation of these aliquants permitted the use of previous measurements of the unfiltered 300°C peak artificial TL in the calculation of the amount of peak decay that had occurred during each storage interval. Two aliquants were measured 7 minutes after exposure, and the peak amplitudes were compared with those obtained previously for the same samples to provide a check on possible changes in sensitivity resulting from storage of the drained aliquants between the initial irradiation experiment and this study. These measured changes listed in table 3 show a tendency for the sensitivity of the samples to decrease slightly during storage. The changes were considered to be generally small enough not to require comprehensive sensitivity correction for all samples.

The remaining samples were stored in the dark at room temperature after irradiation. Three, and where the number available permitted four, aliquants from each rock were removed and run at intervals of 10, 20, and, for samples for which enough material was available, 40 days. The reported decay values given in table 3 are the averages of the three to four aliquants measured at each decay interval.

TABLE 3.—*Percentage of TL remaining in the 300°C peak of both the alkalic and tholeiitic basalts at the end of each decay interval*

[The decay percentages were calculated by comparing the peak heights obtained at each decay interval with the initial peak from the same radiation dose measured 7 minutes after irradiation, both without filters CS6-60. +, increase; -, decrease, in sensitivity relative to the initial radiation series; n.d., values not determined]

Sample No.	Sensitivity change (percent)	Percent TL left		
		10 days	20 days	40 days
023-----	n.d.	33.6	26.7	n.d.
H71-10-----	+ 4.4	37.2	34.6	25.9
035-----	- 9.9	21.7	18.3	n.d.
H71-3-----	- 2.0	23.6	21.8	21.4
036-----	- 4.6	29.7	25.3	n.d.
041-----	- 2.2	22.5	21.0	20.7
042-----	- .4	27.1	26.4	26.3
033-----	- .1	31.9	29.2	26.1
Mol le-----	- 2.1	28.0	25.5	22.1
Kipa 10a-----	+ 8.8	35.0	25.0	23.7
5X340-----	+ 1.2	30.5	27.9	24.0
P71-13-----	- 9.0	14.7	10.3	7.4
P71-4-----	-14.6	34.6	38.3	20.6
P71-3-----	- 4.2	39.0	31.9	30.6
P71-5-----	+ 3.0	35.6	30.4	22.0

The extent of TL decay during each storage interval was determined by comparing the peak amplitudes measured for each aliquant after one of the three storage intervals with those produced by the same radiation exposure and measured 7 minutes after irradiation. This technique worked well for the tholeiitic basalts, for which the TL measured 7 minutes after irradiation did not produce equipment saturation. It was not satisfactory for the alkalic basalts, however, because for several of them a 1,740-rad dose did produce saturation of the TL equipment. This problem was circumvented by using the peak data for the 217- and 870-rad exposures and the TL-accumulation-rate-with-increasing-radiation-dose relation described in the section on "Linearity of TL Acquisition and Saturation" to calculate an approximate TL peak amplitude at the 1,740-rad dose level for those alkalic basalts that produced saturation. The projected values are accurate to within an estimated  $\pm 10$  percent.

The results of the decay experiment were generally as expected in terms of the relative amounts of decay observed for the different temperature peaks. The delayed TL measurements provide a much improved resolution of the 300°C peak in cases of peak overlap. Reproductions of the TL glow curves for alkalic basalts numbers 033, H71-10, and Mol 1e (fig. 11) show the amount of decay of the various temperature peaks. The more rapid decay of the low-temperature peaks relative to the 300°C peak is indicative of a largely thermally controlled decay process similar to that described by the Randall-Wilkins equation. Unfortunately, the data do not facilitate determination of the extent to which nonthermal drainage contributes to the decay process.

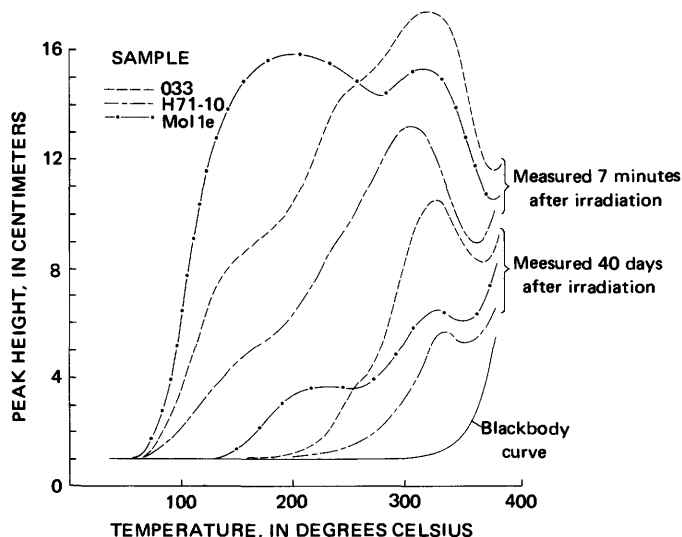


FIGURE 11.—Artificial TL decay during 40-day storage of irradiated samples.

Averages for the percentage of 300°C peak TL remaining at the end of each decay interval for both alkalic and tholeiitic basalts, table 3 and figure 12, clearly show that the largest proportion of the total decay recorded over the 40-day duration of the experiment occurred during the first 10 days. All samples lost at least 60 percent of the trapped electron population responsible for the 300°C peak during this initial period, many nearly 70 percent. The decay rate decreased sharply following this initial period. Except for four samples, less than 10 percent additional decay occurred during storage up to the maximum 40-day limit.

The decay rate shown by the curves (fig. 12) appears to be exponential, but careful examination of similar data by Garlick (1973) has shown the decay process to be more accurately represented by a summation of a number of exponential decays. The individual exponential functions define untrapping rates for the range of trap depths that contribute to individual TL peaks.

## DISCUSSION

The similar TL decay rates for plagioclase from the alkalic and tholeiitic basalts is significant because the rates appear to be approximately independent of both trap density and mineral composition. The relatively uniform reduction of the trapped electron population to approximately 20 percent of the intitial level in 40 days shows that many more electrons are trapped during laboratory irradiation than can be stored stably and suggests that the number trapped initially is proportional to the number of stable traps available. This observation has not been reported previously. The phenomenon may be produced by a metastable clustering of a limited number of electrons around traps capable of the stable retention of only one electron, or

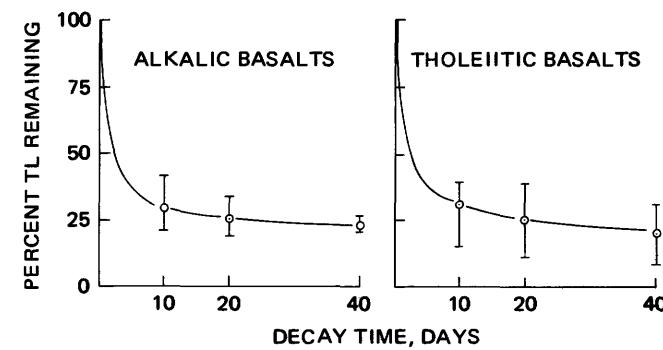


FIGURE 12.—Average percentage of 300°C peak TL remaining in the alkalic and tholeiitic basalt samples after each decay interval. Vertical bars indicate the range of values observed in each interval.

by some other process that produces an equivalent result.

The variation in decay rates observed for the 300°C peak in individual samples, particularly within the alkalic basalt suite, shows a rough correlation with the proportional amplitude of the adjacent 225°C peak in the 10- and 20-day intervals of the decay experiment. The samples with the least amount of overlap interference from the tail of the 225°C peak tend to show the greatest amount of TL remaining during the two initial decay intervals. Those with more extensive interference, such as samples 035 and 041, tend to have the lowest percentage of TL remaining. An analysis of the effect based on measurements at the 10-day interval showed that overlap interference from the tail of the 225°C peak may contribute a maximum of about 10 percent to the amplitude of the 300°C peak; the average is considerably less.

The TL decay patterns identified in this investigation are in qualitative agreement with observations of a similar nature made by Dalrymple and Doell (1970 a, b) and Hwang (1973) on lunar fines. Wintle (1973) investigated TL fading in a number of minerals and found a wide variation in decay rates. Her study included several feldspar samples whose TL faded by less than 5 percent in 4 weeks. Causes for this variation in TL retention properties have not been proposed.

It is not certain how the data developed on the basis of high-intensity doses of artificial radiation in this investigation apply to comparable retention properties for natural TL except that it is clear that long-term natural TL storage capacity is only a fraction of the apparent capacity identified on the basis of short-term storage of artificial TL. The extent of this difference is demonstrated by the fact that the natural TL peak amplitudes for the alkalic basalts vary from a low of 0.67 percent of the artificial TL amplitude from 870 rads of X-radiation for sample 023 to a high of 6.43 percent for sample 033. The natural TL peak heights were produced by adjusted natural radiation doses that were approximately equal to or greater than the artificial dose for sample 023 and more than 50 times greater for sample 033. Some of the difference is due to enhanced artificial TL peaks caused by the metastable short-term storage of laboratory-excited electrons, some probably due to spontaneous drainage of natural TL-producing electrons over geologic time.

Using decay-diminished peak amplitudes to provide a measure of trap density for use in TL age calculations was not investigated in this experiment, principally because the measurements were made with unfiltered TL. It is uncertain what effect differences in the extent of decay at, say, the 20-day interval

would have on using these peaks to quantify the relative magnitudes of trap densities. Possibly the extent of decay is indicative of the natural TL storage properties of individual samples, in which case the decay amplitudes would be valuable, but this hypothesis is untested.

## SUMMARY

Spontaneous decay of artificial TL reduces the 300°C peak amplitudes of both the alkalic and tholeiitic basalts to about 20 percent of their initial value in 40 days. This rapid and extensive decay provides a measure of the metastability with which most of the electrons trapped during relatively high intensity laboratory irradiations are stored.

The artificial TL decay produced by storage of irradiated samples for 10 to 40 days is faster and more complete for the low-temperature peaks than the 300°C peak and yields a much-improved resolution of the high-temperature peak in cases of peak overlap. Interference from the 225°C peak contributes a maximum of 10 percent to the measured amplitude of the 300°C peak in the samples studied. The use of TL peaks measured after storage of irradiated samples to quantify TL response characteristics for dating applications was not investigated in this study but could conceivably provide reliable data. The decay rates suggest that the use of artificial TL measured a short time after irradiation to define natural TL storage capacity is invalid. The same data indicate that the short-term artificial TL peaks are suitable for defining relative differences in trap density.

## RADIOACTIVE ELEMENT CONTENTS OF THE ALKALIC AND THOLEIITIC BASALTS AND DOSE-RATE CALCULATIONS

### RADIOACTIVE ELEMENT CONTENTS OF THE BASALTS

The production of natural TL and probably secondary defects in basaltic plagioclase, as well as in other geologic materials, is dependent on the interaction of decay particles and recoil nuclei from radioactive elements and cosmic rays with the lattice atoms of the dosimeter crystals. The most important radioactive nuclides in igneous rocks are  $^{238}\text{U}$ ,  $^{235}\text{U}$ ,  $^{232}\text{Th}$ , and  $^{40}\text{K}$  and the intermediate daughter products of the uranium and thorium decay series. For the purpose of energy calculations in this investigation, the decay chains were considered to be in secular equilibrium. For rocks less than one million years old, this assumption is only approximately correct owing to probable disequilibrium in the uranium and thorium decay chains, but in the absence of detailed isotopic analy-

ses, it represents the most reasonable basis for dose-rate calculation. The actual extent of disequilibrium in the  $^{238}\text{U}$  series for several historic and prehistoric tholeiitic and alkalic Hawaiian basalts has been determined by Somayajulu and others (1966), who found that although  $^{238}\text{U}$  and  $^{234}\text{U}$  were in secular equilibrium,  $^{230}\text{Th}$  exceeded the amount necessary for equilibrium by 10 to 50 percent in all the samples studied; the excess averaged about 25 percent.  $^{210}\text{Pb}$  was found to be depleted in most samples, possibly as a consequence of radon loss, by an average of about 25 percent of the quantity required for equilibrium.

The effect that this disequilibrium has on dose rates calculated on the basis of assumed secular equilibrium can be determined if it is assumed that the depletion of  $^{210}\text{Pb}$  is indeed due to radon loss. Approximately 60 percent of the decay energy in the  $^{238}\text{U}$  series originates from the portion of the chain including and beyond radon. If the average amount of radon loss and  $^{230}\text{Th}$  excess for the Hawaiian rocks is used as the basis for computation, the disequilibrium dose rates for the  $^{238}\text{U}$  series are about 80 percent of those calculated on the assumption of secular equilibrium. Variations in the extent of disequilibrium result in a range of approximately  $\pm 10$  percent around the average value. The extent of disequilibrium in the decay chains of  $^{235}\text{U}$  and  $^{232}\text{Th}$  were not determined for the Hawaiian rocks, but if the extent of disequilibrium is comparable to that for the  $^{238}\text{U}$  series, then the average total dose rate for the Hawaiian basalts may be as much as 20 percent lower than that calculated on the basis of secular equilibrium. This apparent discrepancy between the probable actual average annual dose rates and those calculated on the basis of secular equilibrium would not adversely affect relative TL-dating studies if the difference was consistent between samples. The apparent range in actual dose rates caused by variations in the extent of disequilibrium between samples is potentially more critical, but since available data suggest that this does not exceed a maximum of about  $\pm 10$  percent, and the average is probably less, it does not appear that this variation will be a significant source of error in the final TL ratio.

#### PROCEDURE AND RESULTS

Radioactive element contents were measured on whole-rock material because the plagioclase dosimeter crystals, in addition to being exposed to the decay products from radioactive elements incorporated in the crystals themselves, can intercept decay particles from nuclides located in the matrix. Radiation from the matrix is important because geochemical partitioning of atoms among the coexisting minerals in a

crystallizing basalt melt results in the incorporation of most of the uranium and thorium in minerals other than plagioclase or in the residual glassy groundmass.

Uranium and thorium were measured by delayed neutron activation (DNA);  $\text{K}_2\text{O}$  was measured by flame photometry. The precision of the  $\text{K}_2\text{O}$  measurements is uniformly equal to or less than 1 percent. The errors in the uranium and thorium measurements are considerably greater because the contents of these elements in the Hawaiian basalts are near or below the lower detection limit of the DNA method (1 ppm for uranium, 10 ppm for thorium) for reasonable precision and accuracy. The DNA method was used in this investigation to test the feasibility of this relatively accessible and rapid means of analysis. More sensitive, and expensive, methods such as isotope dilution exist and could be used to achieve better measurement precision and accuracy if necessary.

The uranium, thorium, and  $\text{K}_2\text{O}$  contents of the alkalic basalts are given in table 4. The  $\text{K}_2\text{O}$  values represent the total content of that element, consisting of all the naturally occurring isotopes; the  $^{40}\text{K}$  content can be calculated by multiplying the total  $\text{K}_2\text{O}$  content by 0.8301 to convert to weight percent K and the potassium content by the natural abundance of  $^{40}\text{K}$ ,  $1.9 \times 10^{-4}$  mol/mol, to obtain the amount of that isotope. In practice, the proportionality constants are expressed so that the dose rate from  $^{40}\text{K}$  can be calculated directly from weight percent natural K.

Each of the uranium and thorium measurements is accompanied by an estimate of measurement precision expressed as a coefficient of variation ( $cv$ ). The magnitude of the errors for the alkalic basalts are generally acceptable relative to the other errors in the TL measurements, as they constitute less than about 25 percent of the total error in the TL ratio. The data show that for samples with radioactive element contents equivalent to, or greater than, the alkalic basalts, delayed neutron activation is an acceptable method of analysis.

TABLE 4.—*Radioactive element contents of the alkalic basalts*

[Uranium and thorium measured by Hugh Millard;  $\text{K}_2\text{O}$  measured by Lois Schlocker.  
 $cv$ , coefficient of variation]

Sample No.	Ppm U	$\pm cv$ (percent)	Ppm Th	$\pm cv$ (percent)	Weight percent $\text{K}_2\text{O}$
023	1.07	5.5	3.65	13.6	2.016
H71-10	2.57	4.8	7.07	13.5	2.82
035	1.62	4.8	5.27	11.7	2.92
H71-3	1.39	5.7	3.96	15.7	1.807
036	1.27	6.7	7.67	10.0	2.137
041	1.00	6.6	2.79	19.3	1.613
042	1.79	5.7	4.69	17.4	2.34
033	1.38	4.9	2.98	17.7	2.178
Mol le	1.06	6.6	2.23	24.6	1.293
Kipa 10a	.22	23.1	1.46	31.1	.293
5X340	.67	8.7	2.85	17.7	1.228

The uranium, thorium, and  $K_2O$  contents of the tholeiitic basalts are given with the errors in the measurements in table 5. Coefficients of variation greater than 30 percent mean that the accompanying parts per million values are not reliable. The poor precision of the measurements, particularly for thorium, indicates that the DNA method is not very well suited to rocks with radioactive element contents equivalent to or lower than those for the ocean island tholeiites. An attempt to measure the uranium concentrations in the tholeiitic basalts by fission-track spark counting (FTSC) gave values that were in good agreement with the DNA values for about half of the samples (Hugh Millard, written commun., 1975). The data are preliminary, but the reproducibility of the two measurements reported for each sample appears to be comparable to that for the DNA method. As estimates of analytical precision were not included with the analyses, it is difficult to tell whether the method provides a substantial increase in accuracy over the DNA method for low-uranium rocks. The FTSC values were not used for dose-rate calculations.

#### DISCUSSION

The tholeiitic basalts show an apparently greater range in uranium and thorium contents than the alkalic basalts, although some of this variation may be attributable to the larger experimental error in the measurements. The amounts of the elements, lower than those for the alkalic basalts by a factor of three to five or more, result in calculated annual dose rates for the two rock types that differ by approximately a factor of six. This large difference in dose rates, perhaps coupled with the significant difference in average feldspar composition, has a marked effect on TL properties. Differences in dose rate within each of the two suites are smaller and have a lesser effect, which

TABLE 5.—Radioactive element contents of the tholeiitic basalts

[Uranium and thorium measured by Hugh Millard;  $K_2O$  measured by Lois Schlocker;  $cv$ 's (coefficient of variation) are uniformly equal to or less than 1.0 percent; n.d., not detectable]

Sample No.	Ppm U	$\pm cv$ (percent)	Ppm Th	$\pm cv$ (percent)	Weight percent $K_2O$
012	0.38	10.7	0.88	42.7	0.587
015	.35	12.3	1.201	32.8	.680
026	.20	21.6	.35	120.7	.379
030	.21	20.7	.61	66.4	.455
050	.27	15.0	1.32	28.3	.609
051	.18	21.9	.98	40.4	.423
032	.13	26.6	.25	127.9	.410
024	.16	20.3	n.d.	—	.454
070	.17	19.7	.31	99.7	.504
074	.12	28.4	.25	121.5	.341
018	.15	23.8	.69	50.6	.344
019	.34	16.7	.92	54.1	.369
P71-13	.08	73.7	.69	84.6	.091
037	.49	8.8	.94	40.2	.868
P71-4	.11	44.6	.78	55.5	.120
P71-3	.20	25.2	.62	69.4	.329
P71-5	.11	51.2	.63	83.6	.143

in most cases can be normalized by dividing the peak-height averages by annual dose rates calculated from the radioactive element contents.

#### CALCULATION OF RADIOACTIVE DECAY ENERGIES

The most direct method of quantifying the TL-producing effectiveness of natural radiation consists of calculating the amount of energy evolved during the successive disintegrations in the decay chains of each of the primary nuclides. Decay energies represent the maximum possible effective energy because only part of the total energy emitted during a decay is likely to be absorbed in the plagioclase crystals and only a small part of that absorbed energy will result in ionization and stably trapped electrons. If, however, the distribution of radioactive elements in the host rock is reasonably homogeneous relative to the dosimeter grains (a reasonable assumption for most rocks), the plagioclase crystals should intercept a representative proportion of the total radiation emitted. Dose rates based on decay energies should then provide a reasonably accurate relative measure of the level of internal radiation to which the dosimeter grains have been exposed and a reliable measure of differences in dose rate between samples. This relative dose rate is adequate for use in age calculations in this investigation.

Natural radiation dose rates calculated from decay energies are expressed in rads, the standard unit of absorbed dose in radiation dosimetry. One rad is equal to 100 ergs of energy absorbed per gram of any absorber ( $10^{-2} \text{ J kg}^{-1}$ ). The representation of energy emitted during radioactive decay in terms of absorption units is an approximation, especially in view of the implicit assumption that the absorption will produce mainly ionization, but is accepted practice.

The end members of the decay series, the number of each of the principal particles emitted during a complete decay, and the approximate energies evolved are given in table 6. Beta particles were assigned an effective energy equal to one-third the maximum beta energy (Mladsenović, 1973) except where the energy of the dominant emission for a particular isotope was

TABLE 6.—Abbreviated radioactive decay series and decay energies for the radioactive isotopes of uranium, thorium, and potassium

[Weast (1974); Lederer and others (1967). Ec, electron capture]

Isotope	End members of the series	Principal decay particles	Particle energies (MeV)			
			$\alpha$	$\beta^-$	$\gamma$	Total
$^{238}\text{U}$	$^{238}\text{U}$ $^{206}\text{Pb}$	$8\alpha, 6\beta^-$ , $\gamma$	42.97	1.45	1.91	46.33
$^{235}\text{U}$	$^{235}\text{U}$ $^{207}\text{Pb}$	$7\alpha, 4\beta^-$ , $\gamma$	41.40	1.02	1.17	43.59
$^{232}\text{Th}$	$^{232}\text{Th}$ $^{208}\text{Pb}$	$6\alpha, 4\beta^-$ , $\gamma$	36.80	1.41	.689	39.80
$^{40}\text{K}$	$^{40}\text{K}$ – $^{40}\text{Ca}$ (0.89)	$\beta^-$	—	.60	—	—
$^{40}\bar{\text{K}}$	$^{40}\text{K}$ – $^{40}\text{Ar}$ (0.11)	Ec	—	—	1.46	.69

<sup>1</sup>Total average emission energy adjusted for the proportions of the two decay modes.

specified in the literature. For  $^{40}\text{K}$ , the maximum beta energy is 0.60 MeV (Pertsov, 1964). Gamma-ray energies were calculated by weighing the dominant emissions by their relative proportions.

### DOSE-RATE CALCULATIONS

### PROCEDURE AND RESULTS

The calculation of dose rates from measured quantities of the radioactive elements requires conversion of particle energies into energy constants in terms of rad per parts per million per year. The energy constants are adjusted for natural abundances of the isotopes to facilitate calculation of dose rates directly from the reported amounts of the natural elements. With the isotopic abundances, half-lives, and decay constants for uranium, thorium, and potassium given in table 7, energy constants ( $E_c$ ) can be calculated from decay energies with the equation

$$E_c = A Q \alpha_1 \alpha_2 \alpha_3$$

where  $A$ , the specific activity of each isotope, is defined by the equation

$$A = \frac{\lambda}{m} N_A \alpha_1$$

where  $\lambda$  and  $m$  are the decay constant and gram atomic weight for each isotope, respectively,  $N_A$  Avogadro's number, and  $\alpha_1$  a constant,  $3.1536 \times 10^7$  s/yr. In the equation for energy constants,  $Q$  is the decay energy for each particle in the complete disintegration of each primary isotope (1 MeV =  $1.6021 \times 10^{-6}$  erg); the values for the constants  $\alpha_2$  and  $\alpha_3$  are  $10^{-2}$  rad/erg, and  $10^6$  g/ppm.

Energy constants in rads per parts per million per year adjusted for the natural abundances of the isotopes are listed for alpha and beta plus gamma radiation in table 8.

Dose rates reflecting the estimated TL-producing effectiveness of natural radiation were obtained by adding one-tenth of the calculated alpha-particle dose to the sum of the beta and gamma doses. The alpha-radiation coefficient reflects the reduced efficiency of

TABLE 7.—Natural abundances and half-lives ( $t$ ) of the isotopes

[Data from Lederer and others (1967)]

Isotope	Natural abundance percent	$t^{1/2}$ (years)	Decay constant ( $\lambda$ )
$^{238}\text{U}$	99.276	$4.51 \times 10^9$	$1.54 \times 10^{-10}$ yr $^{-1}$
$^{235}\text{U}$	.7196	$7.13 \times 10^8$	$9.72 \times 10^{-10}$ yr $^{-1}$
$^{232}\text{Th}$	100	$1.41 \times 10^{10}$	$4.92 \times 10^{-10}$ yr $^{-1}$
$^{40}\text{K}$	.0119	$1.28 \times 10^9$	$5.42 \times 10^{-10}$ yr $^{-1}$

TABLE 8.—Energy constants in rads per parts per million per year adjusted for natural isotope abundances

Isotope	$\alpha$ energy	$\beta + \gamma$ energy	Total effective energy
$^{238}\text{U} + ^{235}\text{U}$	0.0278	0.0215	$^{10.0493}$
$^{232}\text{Th}$	.0075	.0043	$^{1.0118}$
$^{40}\text{K}$	—	.108	$^{2.108}$

<sup>1</sup>Alpha-particle energies in the energy total are adjusted to 0.1 of the nominal calculated energy; see text for explanation.

<sup>2</sup>Dose rate is in terms of rads per weight percent natural K-yr.

alpha particles in producing ionization. It was derived from experiments with lithium fluoride (Morehead and Daniels, 1957) and other materials (Aitken, 1968) in which the trap-filling efficiency of alpha particles per rad of radiation was compared with that of beta and gamma radiation. This coefficient has been used by other workers and found to be approximately correct. The annual dose rates and errors in the dose rates for both the alkalic and tholeiitic basalts are given in table 9.

### DISCUSSION

The cumulative errors in the annual dose rates of table 9 were calculated with a standard propagation-of-errors equation using only the analytical errors in the isotopic measurements. The cumulative errors do not include compensation for probable variations in the degree of disequilibrium in individual samples or

TABLE 9.—Annual dose rates for the alkalic and tholeiitic basalts

Sample No.	$\text{U}^1$ (rad/yr)	$\text{Th}^1$ (rad/yr)	$\text{K}$ (rad/yr)	Total (rad/yr $\pm \sigma^2$ )
Alkalic basalts				
023	0.053	0.043	0.181	$0.277 \pm 0.007$
H71-10	.127	.083	.253	$.463 \pm .013$
035	.080	.062	.262	$.404 \pm .009$
H71-3	.069	.048	.162	$.278 \pm .009$
036	.062	.091	.192	$.345 \pm .010$
041	.050	.033	.145	$.228 \pm .007$
042	.088	.055	.210	$.353 \pm .010$
033	.068	.039	.193	$.300 \pm .008$
Mo1 le	.052	.026	.116	$.194 \pm .007$
Kipa 10a	.011	.017	.026	$.054 \pm .006$
5X340	.033	.034	.110	$.177 \pm .007$
Tholeiitic basalts				
012	0.018	0.011	0.052	$0.081 \pm 0.005$
015	.017	.016	.060	$.093 \pm .006$
026	.010	.005	.034	$.049 \pm .006$
030	.010	.008	.040	$.058 \pm .006$
050	.013	.017	.054	$.084 \pm .005$
051	.009	.013	.038	$.060 \pm .006$
032	.006	.003	.036	$.045 \pm .002$
024	.008	—	.040	$.048 \pm .002$
070	.008	.004	.045	$.057 \pm .004$
074	.006	.003	.030	$.039 \pm .004$
018	.008	.009	.031	$.048 \pm .005$
019	.017	.012	.033	$.062 \pm .007$
P71-13	.004	.009	.008	$.021 \pm .008$
037	.024	.012	.077	$.113 \pm .005$
P71-4	.006	.010	.011	$.027 \pm .006$
P71-3	.010	.008	.035	$.053 \pm .006$
P71-5	.005	.008	.013	$.026 \pm .007$

<sup>1</sup>Alpha particles assigned an energy efficiency of 0.1.

<sup>2</sup>The cumulative error in the total energy dose was calculated with the equation  $\sigma_{\text{cum}} = (\sigma_{\text{U}}^2 + \sigma_{\text{Th}}^2 + \sigma_{\text{K}}^2)^{1/2}$ .

<sup>3</sup>Dose rate for sample 024 does not include radiation from thorium.

for small errors in the energy-conversion coefficients.

The magnitude of the analytical errors in the thorium measurements for the tholeiitic basalts indicates that the isotopic concentrations, and therefore the dose rates calculated from these concentrations, are not very reliable. This limits the usefulness of the dose-rate data, but since the dose rate from thorium constitutes less than 20 percent of total dose rate (the average is in the range of 10 to 15 percent), it does not completely abrogate the usefulness of the cumulative dose-rate figure for normalizing differences in TL caused by variations in the natural radiation environment.

The annual dose rates in table 9 do not include energy from cosmic radiation. The mean cosmic-ray dose at sea level has been calculated by Herbst (1964) to be about 0.033 rad/yr, by Spiers and others (1964) to be about 0.037 rad/yr, and by Schilling (1964) to range from about 0.035 rad/yr at the equator to about 0.050 rad/yr at lat 50°. The increase in intensity of cosmic radiation with altitude has been estimated by Pertsov (1964) to be approximately a factor of three in 3 km from sea level.

The annual cosmic-ray dose rate has been estimated by Aitken (1968) to be attenuated to about 0.015 rad/yr at a depth of about 1.5 m below the surface in soil. An annual cosmic-ray dose rate of 0.014 to 0.016 rad/yr is used routinely by several investigators in work with archeologic materials (Tite, 1968; Aitken, 1968, 1970; Fleming and others, 1970).

In this investigation, energy from cosmic radiation was not included in the dose rate, because the absolute magnitude of the dose for individual samples could not be accurately determined. The omission of the cosmic-ray dose infers that the dose rate is constant. The probable error introduced by this assumption can be evaluated by determining the proportional influence of the probable maximum cosmic-ray dose rate of 0.015 rad/yr on the internal radiation dose rate for the alkalic and tholeiitic basalts. Since it represents only 4.5 percent of the average radiogenic dose rate for the alkalic basalts from the Hawi Volcanic Series, the error added to the internal radiation dose rates by variations in the cosmic-ray component between samples should be negligible. The cosmic-ray dose of 0.015 rad/yr is equivalent to about 25 percent of the average annual radiogenic dose rate for the tholeiitic basalts, and it is likely that the assumption of uniformity of the cosmic-ray dose introduces an error of perhaps several percent in the calculated radiogenic dose rates for samples collected within less than about 1 meter of the surface.

The average annual dose rate for alkalic basalt samples 023 to 033 in table 9 is 0.335 rad/yr. This average

is approximately 20 percent lower than a typical dose rate for pottery of 0.410 rad/yr as recalculated from data tabulated by Aitken (1970), using an  $\alpha$ -radiation efficiency of 0.1 and excluding energy from cosmic radiation. The average dose rate for the alkalic basalts is similar to an annual dose rate of approximately 0.336 rad/yr recalculated from data for a lava sample from the volcano Thera by Aitken (Aitken and Fleming, 1971), again excluding cosmic radiation and using an alpha-particle efficiency of 0.1.

The average annual dose rate for the historic and carbon-14-dated tholeiitic basalts (samples 012 through 019 in table 9) is 0.055 rad/yr. This is significantly lower than the dose rates for most of the materials for which TL dating has been attempted.

The radioactive element contents of the ocean-island basalts studied in this investigation are in general lower than those for rocks of comparable bulk composition but continental origin. This should make continental rocks, particularly those of basalt composition, better suited for TL dating than their ocean-island equivalents.

#### SUMMARY

The uranium, thorium, and potassium contents of the basalts were measured on crushed whole-rock material, uranium and thorium by delayed neutron activation, and  $K_2O$  by flame photometry. The amounts of the elements and the energy emitted during a complete decay of each of the primary nuclides were used to calculate an annual dose rate for each rock. The dose rates represent the maximum possible TL and defect-producing radiogenic energy; the actual effective dose rates are lower since energy is dissipated in modes other than TL production in plagioclase.

The average radiogenic dose rate for the alkalic basalts, 0.335 rad/yr, is higher than that for the tholeiitic basalts (0.055 rad/yr) by a factor of six. These dose rates do not include cosmic-radiation energy, which for samples buried more than a meter or so below the surface has a maximum intensity of 0.015 rad/yr (Aitken, 1968). The dose rates for the alkalic basalts are approximately 40 percent lower than the typical dose rate for pottery and lower than the dose rate for rocks of comparable bulk composition but continental in origin.

#### NATURAL TL

The amplitude of the high-temperature natural TL peak with a maximum intensity between 325° and 350°C was used to quantify TL response in this investigation. Natural TL glow curves were reproduced from actual TL graphs for four alkalic basalts and four

tholeiitic basalts, as shown in figure 13A and figure 13B. Corresponding artificial TL glow curves are shown for comparison.

#### ALKALIC BASALT NATURAL TL

#### PROCEDURE AND RESULTS

Seven natural TL peak-height measurements, normalized for adjusted sample weight, were averaged for each crushing stage for individual samples to yield the values given in table 10 (in centimeters per milligram). The natural TL values for both crushing stages were then averaged and plotted against the independently determined ages of the samples, as shown in figure 14. The line through the data is a least-squares fit calculated by weighting the data to reflect the estimated degree of deviation from the mean trend pro-

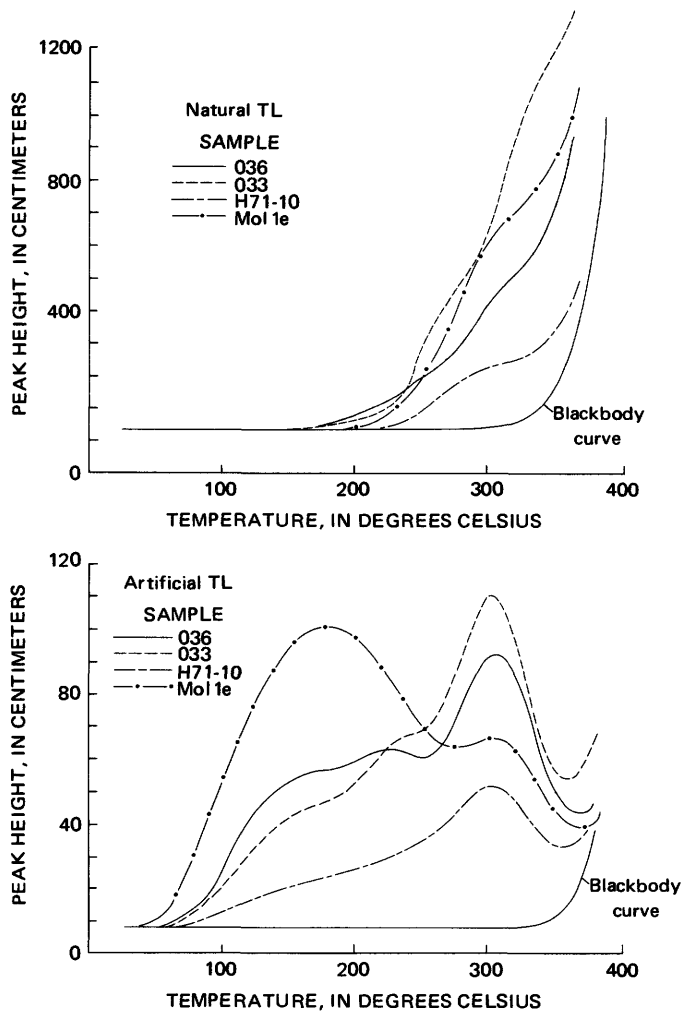
duced in individual samples by variations in spectral composition and trap density. Sample 023 has a disproportionately large influence on the best-fit line by virtue of its distal position relative to most of the other samples. Its TL value appears to be approximately correct for its age in comparison with values for both the older alkalic basalts and the tholeiitic basalts of young age; it was weighted more heavily in recognition of its apparent reliability.

#### DISCUSSION

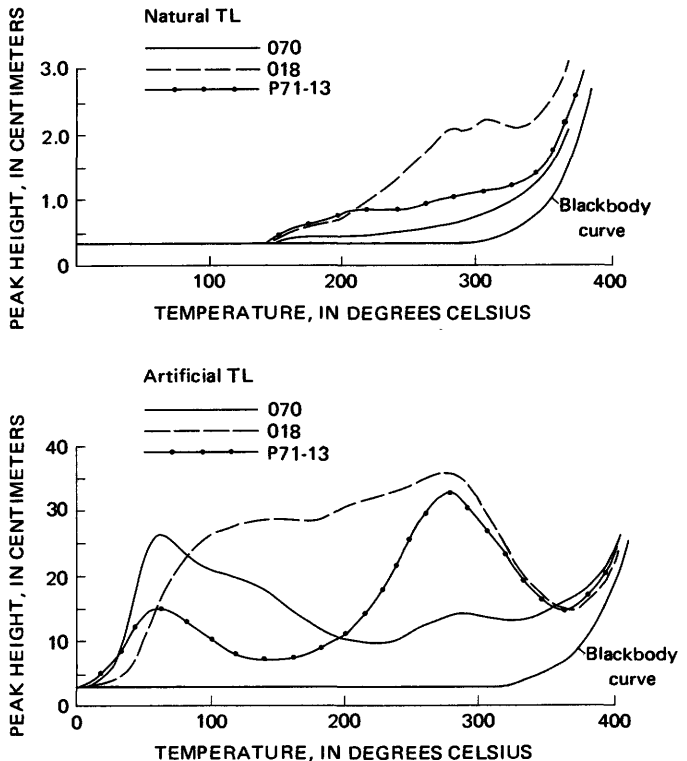
The best-fit line on the plot of TL relative to age, figure 14, in effect defines the average rate of natural TL increase in basaltic plagioclase. The TL values show a moderate degree of scatter with respect to this best-fit line, but they have not been normalized for differences in trap density or spectral composition, both of which strongly influence measured natural TL amplitudes. The equation for the best-fit line in figure 14 is of the form

$$y = ae^{bx}.$$

The reasonably close approximation of the data to a predictable curve is critical because it is the first demonstration that the increase in natural TL over ex-



**A**



**B**

FIGURE 13.—Natural (solid lines) and artificial (dashed lines) TL glow curves for selected alkalic basalts (A) and tholeiite basalts (B). Both natural and artificial TL were measured with filter CS5-60; curves were measured 7 minutes after irradiation. The artificial TL (A) is from a standard 870-rad exposure and (B) from a standard 1,740-rad exposure of X-radiation.

TABLE 10.—Alkalic basalt natural TL peak-height averages for crushing stages 1 and 2

Sample No.	Sample age (years B.P.)	Type of age determination	Natural TL cr. st. 1 <sup>1</sup> (cm/mg)	Natural TL cr. st. 2 <sup>1</sup> (cm/mg)	Average TL cr. st. 1 and 2 <sup>2</sup>
023	4,500	<sup>14</sup> C	0.15 ± 0.03	0.13 ± 0.04	0.14 ± 0.03
H71-10	62,000	K-Ar	3.44 ± .16	3.70 ± .21	3.57 ± .13
035	140,000	do.	4.84 ± .27	4.48 ± .15	4.66 ± .15
H71-3	150,000	do.	20.71 ± .60	20.91 ± .67	20.81 ± .44
036	153,000	do.	10.46 ± .85	10.69 ± .49	10.57 ± .49
041	181,000	do.	7.57 ± .86	9.28 ± .97	8.42 ± .65
042	184,000	do.	22.23 ± 2.04	19.00 ± 2.37	20.61 ± 1.61
033	196,000	do.	21.97 ± 2.04	20.42 ± 1.08	21.19 ± 1.14
Mol 1e	~1.35×10 <sup>6</sup>	Est.	14.45 ± .84	14.52 ± .64	14.48 ± .52
Klpa 10a	~1.5×10 <sup>6</sup>	do.	4.55 ± .18	4.67 ± 1.23	4.59 ± .61
5X340	3.3×10 <sup>6</sup>	K-Ar	25.14 ± 1.18	22.36 ± 1.01	23.75 ± .78

<sup>1</sup>Errors are 1 standard deviation.

<sup>2</sup>The cumulative error in the peak-height average for crushing stages 1 and 2 was calculated with the error equation  $cv_{cum} = \sqrt{2}((cv_1^2 + cv_2^2)^{1/2})$ .

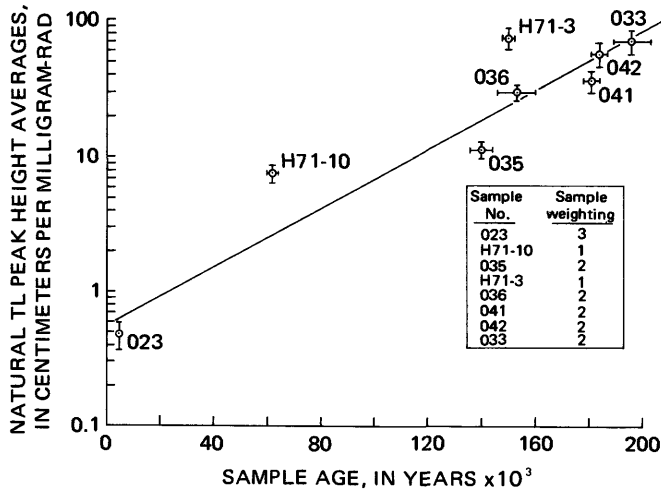


FIGURE 14.—Alkalic basalt natural TL, 350°C peak, relative to sample age. The plotted points are the peak-height averages for crushing stages one and two, normalized for both sample weight and individual natural radiation dose rates. The horizontal error bars represent the uncertainty in the independently measured ages, where large enough to be shown; the vertical error bars represent the cumulative error in the normalized peak-height averages (table 11).

tended periods of time is monotonic and because it suggests that the rate of increase is approximately exponential. In most previous studies covering shorter periods of time, which have used quartz as the principal TL dosimeter, the increase in TL with age has been assumed to be linear (see for example Aitken, 1970). This conclusion may be correct for the quartz from pottery, which is likely to be geologically old and to have a relatively high defect density, but it does not appear from the data available in this study to be applicable to geologically young basaltic plagioclase.

The errors in the TL measurements and the dose rates and the cumulative sum of these errors calculated for each sample with a standard error propagation equation, given in table 11, are for most samples less than 10 percent.

TABLE 11.—Individual and cumulative errors in the energy-normalized peak-height average for the alkalic basalts

Sample No.	[Cr. st., crushing stage; cv, coefficient of variation]					
	Cr. st. 1 ± cv (percent)	Cr. st. 2 ± cv (percent)	cv <sub>cum</sub> (percent)	Annual dose rate cv (percent)	Sample weight ± cv (percent)	Cumulative error (percent <sup>1</sup> )
023	20.1	31.3	18.6	2.45	4.0	19.2
H71-10	4.7	5.6	3.7	2.81	4.0	6.1
035	5.5	3.4	3.2	2.13	4.0	5.5
H71-3	2.9	3.2	2.2	3.11	4.0	5.5
036	8.1	4.5	4.6	2.95	4.0	5.5
041	11.4	10.4	7.7	3.21	4.0	9.3
042	9.2	12.5	7.8	2.72	4.0	9.2
033	9.3	5.3	5.4	2.63	4.0	7.2
Mol 1e	5.8	4.4	3.6	3.79	4.0	6.6
Klpa 10a	3.9	26.4	13.3	10.88	4.0	17.6
5X340	4.7	4.5	3.3	6.14	4.0	8.0

<sup>1</sup>The cumulative error in the energy-normalized natural TL peak-height averages was calculated with the error equation  $cv_{cum} = (cv_{TL\ cum}^2 + [cv_{dose\ rate}]^2 + [cv_{wt}]^2)^{1/2}$ .

The TL data for samples Mol 1e, Klpa 10a, and 5X340 are not shown on the plot in figure 14, because they are much older than the rocks from the Hawi Volcanic Series and because their natural TL peak-height values are lower than the age of the samples and the TL-accumulation rate defined in figure 14 for alkalic basalts would predict. The dose rates for these older samples are lower than those for the younger basalts, but it is not certain that the lower TL amplitudes are entirely a function of the differences in dose rates between the two sample groups. It is probable that the older samples are affected to some extent by TL saturation, which probably begins to diminish the rate of increase in stored natural TL at an age of not much more than 200,000–300,000 years. The TL averages for both crushing stages of each sample are essentially identical, differing in most cases by less than the statistical error in either set of measurements. This similarity demonstrates that the stage 2 crushing does not measurably alter the trapped-electron population of the samples relative to crushing stage 1. It does not prove that there is no modification of TL during the initial crushing, but the fact that the natural TL peak heights for both crushing stages of each sample differ in the same direction for many samples by approximately the same percentage amount as the corresponding artificial TL (table 14A) strongly suggests that any changes are small. The proportionality of the natural and artificial TL would require that any significant drainage of electrons during crushing to be accompanied by an equivalent destruction of traps, and this is unlikely.

#### THOLEIITIC BASALT NATURAL TL

##### PROCEDURE AND RESULTS

Natural TL peak heights for the tholeiitic basalts given in table 12 for those samples for which TL was

TABLE 12.—Tholeiitic basalt natural TL peak-height averages for crushing stages (cr. st.) 1 and 2

[n.d., not detectable]

Sample No.	Sample age (years B.P.)	Type of age determination	Natural TL <sup>1</sup> cr. st. 1 (cm/mg)	Natural TL <sup>1</sup> cr. st. 2 (cm/mg)	TL average cr. st. 1 and 2 <sup>2</sup>
012	16	Historic	n.d.	n.d.	
015	21	do.	n.d.	n.d.	
026	69	do.	n.d.	n.d.	
030	114	do.	n.d.	n.d.	
050	≈225	do.	n.d.	n.d.	
051	≈500	do.	n.d.	n.d.	
032	2,500	<sup>14</sup> C	0.33±0.02	n.d.	
			.26±.20	n.d.	
024	3,740	<sup>14</sup> C	.26±.03	0.12±0.09	0.19±0.07
			.20±.04	.07±.05	.13±.05
070	10,140	<sup>14</sup> C	.20±.03	.09±.04	.14±.03
			.28±.09	.21±.12	.24±.08
074	>10,140	n.d.	.46±.05	.38±.05	.42±.04
			.47±.02	.32±.02	.39±.02
018	17,360	<sup>14</sup> C	.69±.06	.31±.17	.50±.14
			.36±.09	.28±.09	.32±.06
019	>17,360	n.d.	.80±.08	.64±.02	.72±.06
P71-13	327,000	K-Ar	.17±.03	.17±.03	.17±.02
037	400,000	do.	2.52±.12	2.90±.03	2.71±.13
P71-4	403,000	do.	3.20±.11	2.06±.07	2.63±.07
P71-3	414,000	do.	10.43±.71	12.32±1.34	11.37±.73
P71-5	447,000	do.	2.06±.04	2.53±.11	2.29±.05

<sup>1</sup>Errors are 1 standard deviation.

<sup>2</sup>The cumulative error in the peak-height average for crushing stages 1 and 2 was calculated with the same error equation used for the alkalic basalt (table 10).

Note: Samples 074 and 019 were collected below samples 070 and 018, respectively.

measureable show that at least 2,500 years is required for TL to accumulate to a level that is reliably distinguishable from ambient background and that reasonable statistical precision is not attained for rocks much younger than 10,000 years of age. The low TL signal is principally a function of the much lower internal radiation dose rocks for these rocks. What produces the poor precision in the measurements is not clear. Some of the TL variation within crushing stages may originate in the proportionately large influence of normal experimental errors on the small natural TL signal, but the variation appears to be too large to be entirely attributable to experimental errors. The variation in the TL properties of the aliquants does not appear to be related to sample size.

The peak-height data for samples 032 through 019 display a consistent pattern of lower TL amplitudes for crushing stage 2 than for crushing stage 1. This may be an indication of TL drainage produced by the second stage relative to the first; it could be responsible for some of the TL variability observed within crushing stages. Why TL drainage should occur in the tholeiitic basalts, if it does, but not noticeably affect the alkalic basalts is not clear.

The significant increase in TL amplitudes from the second crushing stage relative to the first for several of the older tholeiitic basalts from the Pololu Volcanic Series (P71-13 through P71-5) cannot be explained at this time. It is almost certainly not the result of enhancement of the inherent natural TL signal; it could result from the release of a larger proportion of grain boundary material from the enclosing matrix during

the second crushing. The boundaries of the plagioclase crystals probably have higher natural TL intensities in these older samples because of a greater production rate for both TL and trap density in the near-surface regions of the crystals by short-range alpha particles from uranium and thorium atoms located in the matrix.

Where two TL values are listed in table 12 for each crushing stage of a particular sample, they represent separate determinative series starting with fresh pieces of basalt. These duplicate analyses were performed to evaluate the reproducibility of the TL measurements from these generally low TL tholeiitic basalts. For young samples, the reproducibility is generally poor, although the averages for crushing stage 1, in particular, do not vary in many cases by more than the standard deviation error of the individual sets of measurements.

Peak-height averages for crushing stages 1 and 2 were plotted for the four prehistoric carbon-14-dated basalts in figure 15. The two points for each of the

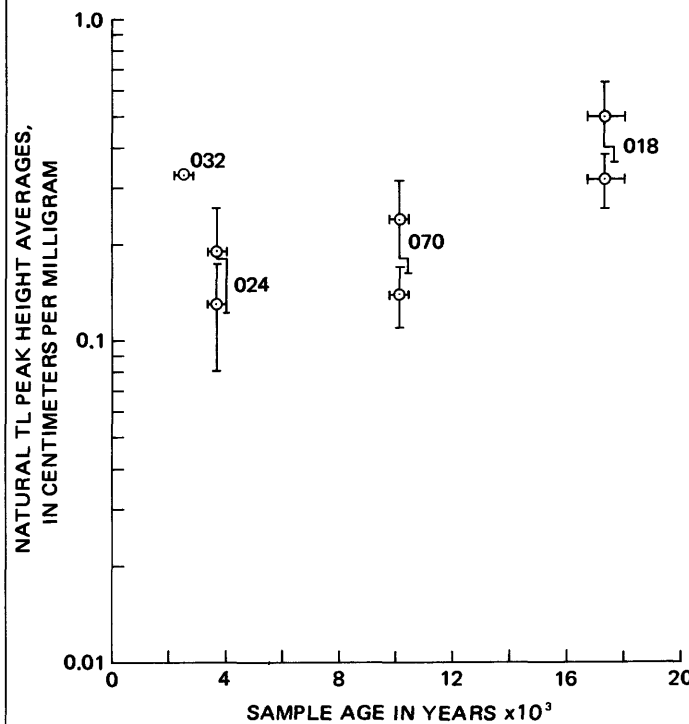


FIGURE 15.—Tholeiitic basalt natural TL, 350°C peak, relative to sample age. The TL data have been normalized for variations in dose rate and sample weight. Except for sample 032, the points are the peak-height averages for crushing stages 1 and 2. Only the stage 1 crushing data is shown for sample 032. The two points for three out of the four samples are for separate determinative series. Vertical error bars represent the cumulative error in the dose rate and TL measurements (table 13). Horizontal error bars represent the uncertainty in the carbon-14 ages.

three out of four samples shown represent the crushing stage averages for the two separate determinative series for each sample. The error in the energy-normalized natural TL data, listed in table 13, exceeds 20 percent in many cases.

#### DISCUSSION

The limited data on tholeiitic basalt shown in figure 15 suggests that the rate of increase in TL with age in the tholeiitic basalts is exponential and similar to that identified for the alkalic basalts in figure 14. The rate of increase is lower than that for the alkalic basalts, however, possibly owing to the difference in dose rates.

The natural TL values for samples 074 and 019 are not shown in figure 15 because the samples have not been dated by independent means. The data for the older tholeiitic basalts (samples P71-13 through P71-5 in table 12) are not shown because their natural TL values are significantly lower than would be expected from their ages, dose rates, and the TL-accumulation rate for the carbon-14-dated basalts. These older samples are probably affected to some extent by TL and trap-density saturation. The time of appearance of saturation effects cannot be ascertained from the data available.

#### SUMMARY

The natural TL peak heights for both crushing stages for the alkalic basalts are closely similar, indicating minimal drainage of TL by crushing during sample preparation. The TL for these samples in-

creases at an exponential rate to at least 200,000 years B.P. The data for the tholeiitic basalts show that at least 2,500 years is required for measurable natural TL to accumulate and that reasonable measurement precision is not attained for samples much younger than 10,000 years of age. The rate of increase in TL for the tholeiitic basalts appears to be exponential but is slower than that for the alkalic basalts possibly because of the difference in dose rates.

#### ARTIFICIAL TL

Four distinct but variably overlapping TL peaks with maxima in the temperature ranges 90°–110°C, 150°–175°C, 200°–225°C, and 300°–325°C occur in plagioclase that has been exposed to laboratory radiation at room temperature and heated for TL measurement a short time after irradiation. The 300°C peak could be clearly distinguished in every sample studied, but not all of the three lower temperature peaks could be resolved in every sample, probably owing to masking by more intense adjacent peaks. Only the 300°C peak was used to quantify differences in trap density between samples in this investigation.

Artificial TL glow curves for plagioclase from four alkalic and four tholeiitic basalts are shown in figures 13A and 13B. The only feldspar TL peak observed by other workers but not detected in this investigation is the one at approximately 450°C (Hoyt and others, 1970; Brito and others, 1973; Durrani and others, 1973), which is beyond the blackbody-saturation limit of the detection system used in this study.

#### ALKALIC BASALT ARTIFICIAL TL

##### PROCEDURE AND RESULTS

The 300°C artificial TL peak heights were measured both with and without filter CS5-60 for both crushing stages with the results given in table 14. The unfiltered TL data were not used for age calculation but are included for comparison. Attenuation factors given represent the ratio of unfiltered to filtered TL. Attenuation factors for samples H71-3 and 041 are artificially low because the unfiltered TL peaks for these samples were diminished by saturation of the TL detection equipment.

The artificial TL peak-height averages for samples 023 through 033 in table 14A, normalized only for sample weight, were plotted against the age of the samples in figure 16. The line through the data is a computer-derived least-squares fit based on the same sample-weighting factors used for the natural TL (fig. 14). The relatively close approximation of the data to a predictable curve indicates an apparently exponen-

TABLE 13.—Individual and cumulative errors in the energy-normalized peak-height average for the tholeiitic basalts

[Cr. st., crushing stage; cv, coefficient of variation]

Sample No.	Cr. st. 1 ± cv (percent)	Cr. st. 2 ± cv (percent)	cv <sub>cum</sub> (percent)	Annual dose rate cv (percent)	Sample weight ± cv (percent)	Cumulative error (percent) <sup>1</sup>
012	—	—	—	6.30	4.0	—
015	—	—	—	6.11	4.0	—
026	—	—	—	13.10	4.0	—
030	—	—	—	9.85	4.0	—
050	—	—	—	6.21	4.0	—
051	—	—	—	9.37	4.0	—
032	5.2	—	—	4.72	4.0	—
	76.6	—	—	—	—	—
024	9.7	71.1	35.9	3.44	4.0	36.1
	20.9	67.5	35.3	—	—	36.1
070	12.8	40.8	21.4	7.59	4.0	22.7
	31.3	56.3	32.2	—	—	33.1
074	9.9	14.0	8.6	10.35	4.0	13.5
	3.5	7.5	4.1	—	—	11.1
018	8.9	55.2	27.9	10.30	4.0	29.7
	24.4	32.4	20.3	—	—	22.8
019	10.0	14.4	8.8	11.44	4.0	14.4
P71-13	20.2	14.8	12.5	38.89	4.0	40.8
037	4.8	8.2	4.7	4.71	4.0	6.6
P71-4	3.3	3.6	2.4	22.82	4.0	22.9
P71-3	6.8	10.9	6.4	11.53	4.0	13.2
P71-5	2.0	4.2	2.3	27.55	4.0	27.6

<sup>1</sup>The cumulative error in the energy normalized natural TL peak-height averages was calculated with the same error equation listed for the alkalic basalts in table 11.

TABLE 14.—Alkalic basalt 300°C artificial TL peak-height averages for crushing stages (cr. st.) 1 and 2 measured with and without filter CS5-60

A. Averages with filter CS5-60

Sample No.	Sample age (years)	Artificial TL cr. st. 1 <sup>1</sup> (cm/mg)	Artificial TL cr. st. 2 <sup>1</sup> (cm/mg)	Average artificial TL cr. st. 1 and 2 <sup>2</sup>
023	4,500	22.7 ± 0.9	18.2 ± 2.6	20.4 ± 1.5
H71-10	62,000	129.3 ± 3.0	134.1 ± 8.3	131.7 ± 4.3
035	140,000	89.0 ± 3.4	80.8 ± 12.6	84.9 ± 6.8
H71-3	150,000	515.0 ± 35.1	632.2 ± 17.1	623.6 ± 17.5
036	153,000	221.5 ± 19.3	227.6 ± 11.2	224.5 ± 11.2
041	181,000	473.4 ± 34.1	507.9 ± 19.3	490.6 ± 20.1
042	184,000	306.6 ± 11.0	300.4 ± 14.7	303.5 ± 9.4
033	196,000	350.0 ± 16.4	306.0 ± 18.7	328.0 ± 12.5
Mol 1e	1.35 × 10 <sup>6</sup>	186.3 ± 7.1	197.8 ± 5.9	192.0 ± 4.6
Klpa 10a	1.5 × 10 <sup>6</sup>	20.5 ± 1.5		
5X340	3.3 × 10 <sup>6</sup>	227.8 ± 13.6		

<sup>1</sup>Errors are 1 standard deviation.

<sup>2</sup>The cumulative error in the peak-height average for crushing stages 1 and 2 was calculated with the error equation listed in table 10.

B. Averages without filter CS5-60

[n.d., not determined]

Sample No.	Artificial TL cr. st. 1 <sup>1</sup> (cm/mg)	Artificial TL cr. st. 2 <sup>1</sup> (cm/mg)	Average artificial TL cr. st. 1 and 2 <sup>2</sup>	Attenuation factors <sup>3</sup>
023	n.d.	82.3 ± 3.6		4.52
H71-10	n.d.	632.3 ± 26.6		4.72
035	n.d.	369.6 ± 17.4		4.57
H71-3	1,273.6 ± 39.5	1,212.8 ± 25.4	1,242.7 ± 23.6	2.07
036	n.d.	828.9 ± 34.8		3.64
041	1,193.0 ± 69.2	1,222.7 ± 33.0	1,208.5 ± 38.7	2.52
042	1,006.5 ± 43.4	1,001.3 ± 39.0	1,003.9 ± 29.1	3.28
033	n.d.	1,088.7 ± 65.3		3.56
Mol 1e	738.0 ± 28.8	741.4 ± 34.8	739.7 ± 22.9	3.96
Klpa 10a	96.1 ± 5.7	87.3 ± 5.0	91.7 ± 3.8	4.68
5X340	816.0 ± 71.0	813.9 ± 34.2	814.9 ± 39.1	3.53

<sup>1</sup>Errors are 1 standard deviation.

<sup>2</sup>The cumulative error in the peak-height average for crushing stages 1 and 2 was calculated with the error equation listed in table 10.

<sup>3</sup>Attenuation factors are the ratio of the unfiltered to filtered artificial TL.

tial rate of increase in the storage capacity of progressively older samples for the electrons that produce TL in the 3,500-A to 5,000-A bandwith. A possible explanation for the increase in trap density is that although natural radiation produces defects at an approximately constant rate, as the number of defects increases, interlocking reduces the probability for spontaneous annihilation. The net result would be a faster-than-linear increase in the aggregate defect population.

### DISCUSSION

There is a close correlation between the proportional amplitudes of the natural and artificial TL peak heights (fig. 14 and 16) for all the alkalic basalts studied except one (sample 041). This relation suggests that in each case the level of natural TL storage was near the maximum storage capacity for a sample of that age; further significant increases in TL would require an increase in trap density. If this is correct, it could explain the observed exponential rate of increase in natural TL.

For sample 041, the artificial TL peak height is anomalously high relative to the natural TL peak

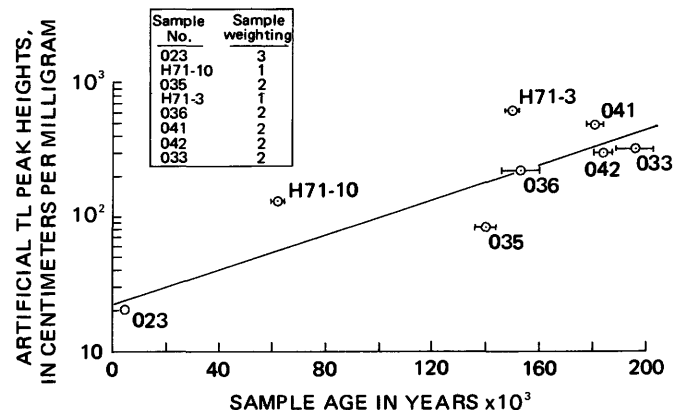


FIGURE 16.—Alkalic basalt 300°C peak artificial TL relative to age. Plotted points are the peak-height averages for crushing stages 1 and 2, normalized only for sample weight. Horizontal error bars represent the uncertainty in the sample ages where large enough to be shown.

height for a sample of its age and dose rate. The reasons for this anomaly are not clear. It could be produced by a slight shift in the emission for the artificial TL relative to the natural TL; 041 has the largest percentage of 4,500-A artificial TL peak emission of all the samples analyzed.

The data for samples Mol 1e, Klpa 10a, and 5X340 were excluded for the same reason they were omitted from the natural TL data (fig. 14); the TL values were lower than expected, in this case possibly because of trap-density saturation.

The attenuation factors in table 14B tend to decrease with increasing age among the samples studied because the proportional amplitude of the 4,500-A emission peak increases progressively with age. The trend confirms the change in the 4,500-A peak with age that was initially described during the spectrum analysis experiment.

### THOLEIITIC BASALT ARTIFICIAL TL

#### PROCEDURE AND RESULTS

The 300°C artificial TL peak-height averages were measured both with and without filter CS5-60 with the results given in table 15. The precision of the artificial TL measurements is no better in most cases than that for the corresponding natural TL, even though the artificial TL for these samples is considerably more intense, which should reduce the influence of measurement errors. This suggests that much of the observed variability is produced by inhomogeneity in the TL properties of the plagioclase composing each aliquant. Attenuation factors for tholeiitic basalts (table 15B) are similar to those described for the alkalic basalts.

TABLE 15. Tholeiitic basalt 300°C artificial TL peak-height averages for crushing stages (cr. st.) 1 and 2 measured with and without filter CS5-60

A. Averages with filter CS5-60

Sample No.	Sample age (years)	Artificial TL cr. st. 1 <sup>1</sup> (cm/mg)	Artificial TL cr. st. 2 <sup>1</sup> (cm/mg)	Average artificial TL cr. st. 1 and 2 <sup>2</sup>
012	13	60.0 ± 2.5	74.6 ± 7.2	68.3 ± 3.6
015	15	15.0 ± 0.7	16.4 ± 0.9	15.7 ± 0.5
026	66	14.5 ± 1.1	11.8 ± 0.4	13.1 ± 0.6
030	114	1.0 ± 0.1	.8 ± 0.2	.9 ± 0.1
050	≈ 225	4.8 ± 0.2	2.9 ± 0.3	3.8 ± 0.2
051	≈ 500	.5 ± 0.1	.4 ± 0.1	.4 ± 0.0
032	2,500	.3 ± 0.1	.5 ± 0.0	.4 ± 0.0
			.3 ± 0.1	.2 ± 0.0
024	3,740	.2 ± 0.0	.2 ± 0.0	.2 ± 0.0
070	10,140	.9 ± 0.1	.9 ± 0.3	.9 ± 0.2
074	>10,140	9.3 ± 1.2	6.8 ± 0.3	8.0 ± 0.5
		10.3 ± 0.7	10.3 ± 0.6	10.3 ± 0.4
018	17,360	2.7 ± 0.8		
		3.5 ± 0.3	2.4 ± 0.3	2.9 ± 0.2
019	>17,360	13.7 ± 2.0	14.3 ± 1.4	14.0 ± 1.2
P71-13	327,000	3.2 ± 0.4	2.6 ± 0.1	2.9 ± 0.2
037	400,000	8.1 ± 1.7	9.2 ± 0.4	8.6 ± 0.9
P71-4	403,000	5.6 ± 0.3	3.9 ± 0.1	4.7 ± 0.1
P71-3	414,000	11.3 ± 0.8	12.8 ± 1.6	12.0 ± 0.8
P71-5	447,000	7.1 ± 0.3	9.3 ± 0.4	8.2 ± 0.3

<sup>1</sup>Errors are 1 standard deviation.

<sup>2</sup>The cumulative error in the peak-height averages calculated with the error equation listed in table 10.

B. Averages without filter CS5-60

[n.d., not detected]

Sample No.	Artificial TL cr. st. 1 <sup>1</sup> (cm/mg)	Artificial TL cr. st. 2 <sup>1</sup> (cm/mg)	Average artificial TL cr. st. 1 and 2 <sup>2</sup>	Attenuation factors <sup>3</sup>
012	137.2 ± 6.7	155.0 ± 12.7	146.1 ± 7.0	2.14
015	72.6 ± 5.2	76.2 ± 5.3	74.4 ± 3.6	4.74
026	67.3 ± 5.6	50.4 ± 2.5	58.8 ± 2.8	4.48
030	n.d.	n.d.		
050	29.1 ± 7.4	25.3 (one measurement)		
	30.0 ± 3.9	28.9 ± 4.2	29.4 ± 2.6	7.61
051	n.d.	n.d.		
031	n.d.	n.d.		
024	n.d.	n.d.		
070	4.8 ± 0.5	3.6 ± 0.7	4.2 ± 0.4	4.32
074	51.7 ± 0.5			
	67.1 ± 4.4	62.2 ± 3.0	64.6 ± 2.6	6.47
018	10.6 ± 2.1	12.1 ± 2.4	11.3 ± 1.6	
	17.4 ± 0.9	12.9 ± 2.1	15.1 ± 1.3	5.12
019	103.2 ± 12.9	92.7 ± 7.9	97.9 ± 7.4	7.00
P71-13	13.8 ± 0.8	13.5 ± 0.8	13.6 ± 0.6	4.77
037	32.6 ± 2.9	33.2 ± 4.5	32.9 ± 2.7	3.79
P71-4	25.5 ± 1.6	17.5 ± 2.1	21.5 ± 1.5	4.51
P71-3	28.7 ± 1.3	35.8 ± 3.2	33.2 ± 1.6	2.68
P71-5	28.8 ± 2.4	37.0 ± 2.1	32.9 ± 1.7	3.99

<sup>1</sup>Errors are 1 standard deviation.

<sup>2</sup>The cumulative error in the peak-height averages was calculated with the error equation listed in table 10.

<sup>3</sup>Attenuation factors are the ratio of the unfiltered to filtered TL.

Artificial TL amplitudes were plotted relative to age (fig. 17) for the four prehistoric carbon-14-dated tholeiitic samples whose natural TL peak heights were plotted in figure 15. Four samples is too limited a data base for broad conclusions, but the rate of increase in peak amplitude with age appears to be approximately exponential.

The slope of a best-fit line through the artificial TL data in figure 17 (not shown) would be steeper than that through the natural TL data (fig. 15), possibly because of differences in the effect of short-term electron storage (artificial TL) relative to long-term stor-

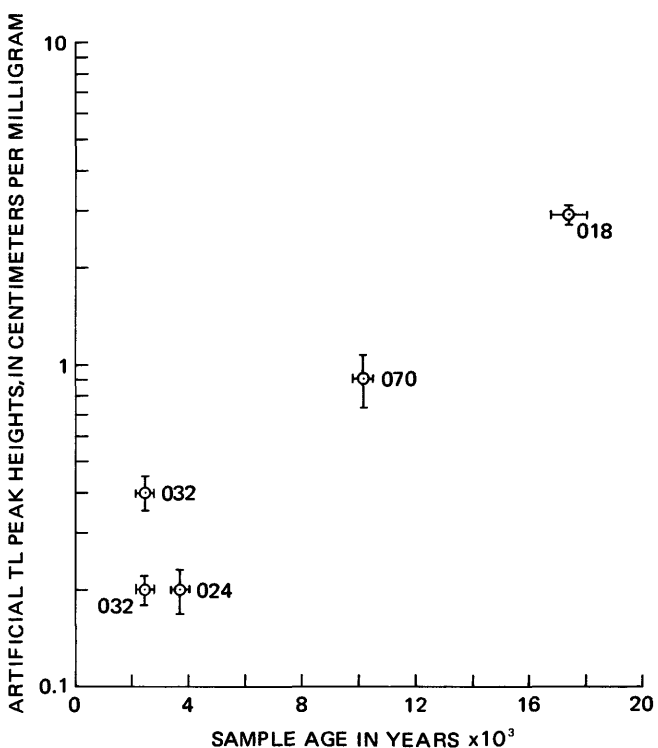


FIGURE 17.—Tholeiitic basalt 300°C peak artificial TL relative to age. Plotted points are the peak-height averages for crushing stages 1 and 2, normalized only for variations in sample weight. The two values for sample 032 represent data for the two separate determinative series. Vertical error bars represent the error in the peak-height averages and the horizontal error bars the reported uncertainty in the carbon-14 ages.

age (natural TL) on TL emission. It is unlikely that it means that trap density actually increases more rapidly than stored TL, since per decay event there is a greater probability for ionization than for defect production. The relation is therefore likely an artifact of the experimental procedure.

Although the historic tholeiitic basalts did not emit measurable natural TL, most of the samples did emit artificial TL after excitation with X-radiation. The artificial TL peak-height relations reveal significant information concerning the structural reorganization that apparently occurs in plagioclase crystals during the first few hundred years following eruption. Artificial TL data for samples 012 through 051 (table 15A), figure 18, show the peak heights to decrease progressively with age to a minimum somewhere in the neighborhood of 500 years after eruption. This decrease in TL denotes a gradual decrease by annealing of the large number of primary defects incorporated in the plagioclase during crystallization from the melt. Exposure to the low levels of internal natural radiation then probably causes a gradual increase in the defect population from the minimum with increasing age (fig. 17) until saturation is attained at an age of per-

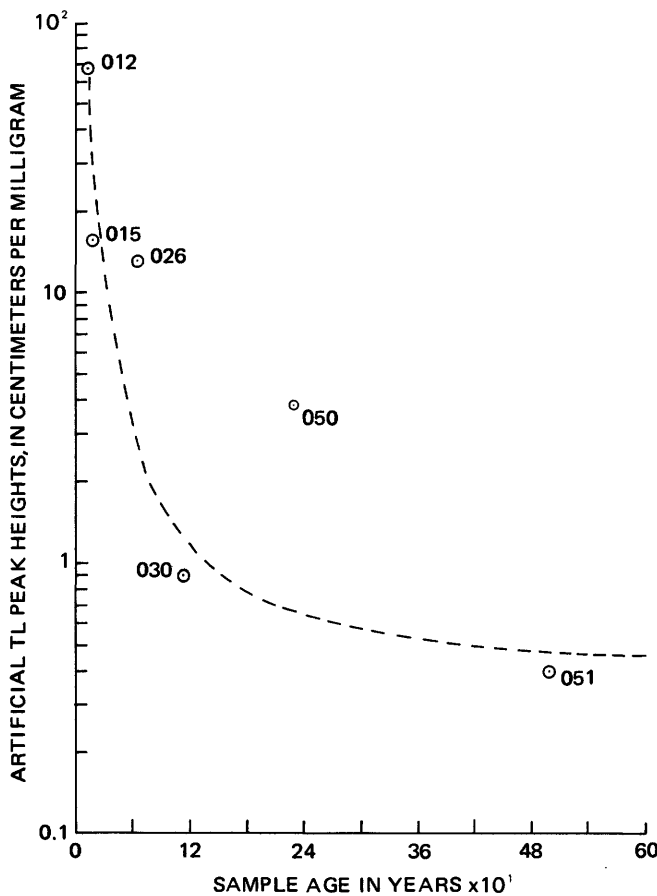


FIGURE 18.—300°C artificial TL peak-height averages for the historic tholeiitic basalts.

haps 200,000 to 300,000 years. Note that the defect density in tholeiitic basalt plagioclase to 500,000 years old is only a fraction of that which exists in newly formed crystals.

The poorly defined increase in the attenuation factors with age for the historic samples (012 through 050, table 15B) provides yet another indirect measure of the progressive decrease in defect density with age in the young samples. Since both the artificial TL peak heights and trap density decrease with age, it is likely that the increase in attenuation factors is largely produced by shifts in the spectral composition of the TL. The progressive decrease in the attenuation factors for the prehistoric samples (032 through P71-5) signifies a progressive increase in the trap density of the samples from natural radiation.

#### SUMMARY

The artificial TL peak heights for the alkalic basalts increase at an exponential rate with age, apparently indicating an exponential rate of increase in trap density with time. The artificial TL peaks are closely pro-

portional in relative magnitude to the corresponding natural TL peaks, which suggests that natural TL for each sample is near the maximum long-term stable storage capacity for the particular trap density; further significant increases in TL are dependent on increases in trap density.

The artificial TL for the tholeiitic basalts also appears to increase exponentially but at a lower rate than for the alkalic basalts. The data for the historic samples reveals a rapid annealing of primary defects to a minimum achieved within approximately 500 years after eruption. The defect density then increases slowly from the effects of natural radiation but even after 500,000 years does not equal the trap density that exists in newly formed crystals.

#### TL DATING AND ANALYSIS OF ERRORS

The formulation of a TL-dating method requires that differences in natural TL caused by variations in trap density, natural radiation dose rate, and TL spectral composition between samples be accurately compensated. The development of a normalizing procedure for natural TL will first be undertaken for the alkalic basalts because a more uniform distribution of material over an extended age range is available from these than for the tholeiitic basalts. Moreover, the lower measurement errors for the various quantities make the values for the alkalic basalts more reliable. The normalized natural TL will be used to define an equation that should be suitable for assigning ages to other samples of similar chemical composition but unknown age. The technique will then be applied to the tholeiitic basalts.

#### TL DATING OF ALKALIC BASALTS

The variables affecting measured natural TL amplitudes are age, dose rate, trap density, and TL spectral composition. In this experiment, sample ages are known, dose rates have been calculated, and trap density is represented on a relative basis by artificial TL. The only variable not directly measured for all samples is TL spectral composition. Compensation for this variable is automatically accomplished during calculation of the TL ratio, however, the spectra for both natural and artificial TL emission, being produced by the same traps and recombination centers, should be closely similar. If they were not, the close proportionality of the natural and artificial TL peak heights (figs. 14 and 16) would not exist.

Differences in the variables for the alkalic basalts were treated linearly because the differences were relatively small and no consistent departure from linear-

ity could be detected. This approach would probably not be applicable for a group of samples with a significantly wider range in chemical and TL properties such as would be encountered in the development of a single TL equation for both the alkalic and tholeiitic basalts.

#### PROCEDURE AND RESULTS

The normalized natural TL ratio ( $r$ ) used in this investigation for TL dating is a dimensionless number defined by the equation

$$r = k (NE_a/AE_n)$$

where  $N$  is the average natural TL peak height (crushing stages 1 and 2),  $E_n$  the annual dose rate, and  $A$ , the average 300°C artificial TL peak height (crushing stages 1 and 2) normalized to a standard X-radiation exposure base ( $E_a$ ). The constant  $k$  is  $10^{-2}$  years. This numerical value  $10^{-2}$  is required to shift the decimal point in the TL ratio so that the  $\log_e r$  is a positive number; the unit years is required to cancel the unit years in the TL ratio that results from  $E_n$  being in units of rads per year while  $E_a$  is in rads. The ratio represents natural TL normalized for all pertinent intrinsic variables.

The TL ratio is not original in general form to this investigation; the basic concepts embodied in an  $N/A$  ratio were probably first advanced during early attempts to apply TL dating to archeologic artifacts at Oxford University (Aitken and others, 1964). The ratio has been used widely (Aitken, 1970; Fleming, 1970; Hwang, 1972; Goksu and others, 1974), but as employed by these workers for "absolute" TL dating, the context in which the expression is used, and the meaning of the constituent parameters, differs significantly from that defined in this investigation.

The TL ratios calculated for alkalic basalt samples 023 through 033 are given in table 16. The error listed for each ratio was calculated with the equation

$$\sigma_r' = (\sigma_N^2 + \sigma_A^2 + \sigma_{E_n}^2 + \sigma_{E_a}^2)^{1/2}$$

where  $\sigma_r'$  is the fractional error in the TL ratio when the errors in the other quantities are expressed as fractional errors. The equation is derived in the section on derivation of equations at the end of this report.

In the plot of TL ratios relative to sample age, figure 19, samples Mol 1e, Klpa 10a, and 5X340 were not included, because they are probably affected by saturation, as discussed. The uniform increase in the amplitudes of the ratios when plotted in terms of increasing age in figure 19 is a compelling indication of both the systematic nature of the TL process and the

inherent reliability of the TL ratio. The equation for the best-fit line through the data set, excluding sample 041, was calculated with the double-regression York II least-squares cubic fit analysis (York, 1969). The equation for the line is

$$r = ae^{bt}$$

where  $r$  is the TL ratio,  $t$  sample age,  $b$  the slope, and  $a$  the y-intercept. The slope is  $1.0056 \times 10^{-5} \pm 0.0422 \times 10^{-5}$ , the y-intercept  $2.146 \pm 0.129$ . Both errors are one standard deviation. The final TL age equation is

$$r = 2.146^{1.0056 \times 10^{-5} t}$$

or, expressed in a more convenient form for age calculation.

$$t = 9,947 (\log_e r - 0.7637).$$

TABLE 16.—Alkalic basalt TL ratios, TL ages, and calculated errors

Sample No.	Sample age (years, B.P.)	TL ratio ( $r^1$ )	TL age (years $^2$ )
023	$4,500 \pm 110$	$2.41 \pm 0.60$	$-12,000 \pm 23,500$
H71-10	$62,000 \pm 2,000$	$5.77 \pm 1.88$	$70,000 \pm 14,350$
035	$140,000 \pm 4,000$	$13.45 \pm 2.07$	$150,000 \pm 14,500$
H71-3	$150,000 \pm 2,000$	$11.92 \pm 2.04$	$139,000 \pm 16,000$
036	$153,000 \pm 7,000$	$13.37 \pm 1.86$	$150,000 \pm 13,000$
041	$181,000 \pm 3,000$	$7.46 \pm 1.66$	$95,000 \pm 21,000$
042	$184,000 \pm 3,000$	$18.97 \pm 3.83$	$183,000 \pm 19,000$
033	$196,000 \pm 7,000$	$21.53 \pm 4.21$	$195,000 \pm 18,500$

<sup>1</sup>Error calculated with the error equation derived in the section at end of report on derivation of equations.

<sup>2</sup> $t = 99,447 (\log_e r - 0.7637)$ , where  $t$  is sample age.

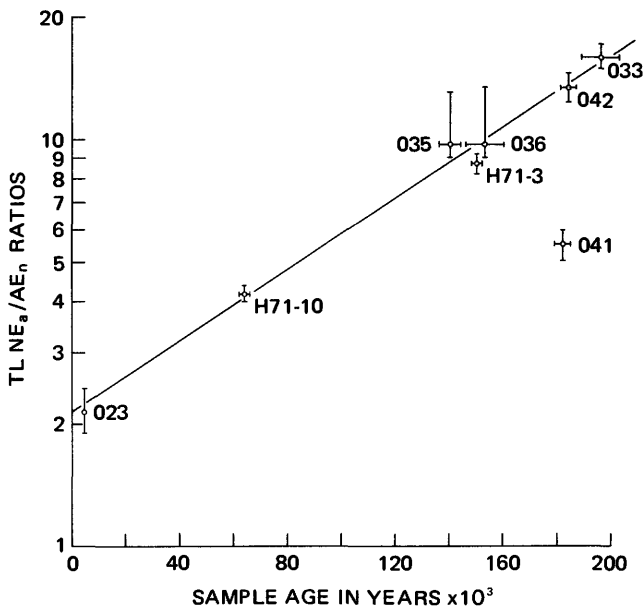


FIGURE 19.—Alkalic basalt TL ratios plotted in relation to sample age. The equation for the best-fit line through the data represents the TL age equation. Horizontal error bars represent the uncertainty in the independently determined sample ages where large enough to be shown; the vertical error bars represent the error in the TL ratios.

The generalized form of the equation defines the basic properties of the TL ratio for alkalic basalt plagioclase. The specific form is applicable only to TL ratios determined in the same analytical fashion with the same equipment as that used for the measurements employed in the derivation of the equation. Changes in either equipment or experimental technique will almost certainly result in a modification of the slope and intercept values for the equation. The precision of TL ages calculated with the age equation can be estimated with the preliminary error equation.

$$\sigma_{t'} = \left( \frac{\sigma_r^2}{b^2 t^2} \right)^{1/2}$$

where  $\sigma_{t'}$  is the fractional error in the TL age. The error equation is derived in the section on derivation of equations at the end of this report. The equation does not include the statistical error in the best-fit line itself, because at this preliminary stage in the development of the method only the errors in the TL data are being considered. The error in the best-fit line itself, which includes the error in the potassium-argon ages as well as those in the TL ratios, is more properly in the realm of accuracy, as distinct from precision. A more comprehensive error analysis designed to include errors in the best-fit line will eventually have to be made, however, before routine assignment of TL ages to rocks can begin.

The TL ages calculated with the age equation for the individual samples used in its derivation differ by less than  $\pm 10$  percent from the respective potassium-argon ages, with the exception of samples 023 and 041. The TL ages, though not strictly independent because each of the ratios was used in the derivation of the equation, provide a preliminary indication of the probable degree of concordance of TL and potassium-argon ages. The statistical errors in the TL ages determined on the basis of the errors in the TL ratio can be seen from table 16 to average approximately  $\pm 10$  percent for rocks older than about 50,000 years of age. Reduction of this error is feasible, but 5 percent is likely to be the minimum error attainable in routine TL age determinations; errors closer to  $\pm 10$  percent will probably prove more common.

#### DISCUSSION

The exponential rate of increase in the TL ratio ( $r$ ) with age is a critical finding. The positive slope of the best-fit line indicates that the increase in trap density with age results in an even faster increase in natural TL storage capacity, possibly by an increased initial trapping probability for conduction band electrons. The uniform rate of increase in the TL ratios with age,

when compared with the scatter in both the natural and artificial TL data alone, demonstrates the effectiveness of the TL-normalizing procedure for canceling differences in natural TL due to differences in trap density between samples. It also indicates that small differences in plagioclase composition, at least within the range from sodic oligoclase to andesine (fig. 4), do not have a detectable systematic effect on the ratio.

The close proportionality of the natural and artificial TL peak amplitudes for individual samples strengthens the hypothesis that natural TL storage is near maximum capacity. Since the artificial TL is significantly more intense than the corresponding natural TL, the process of short-term electron trapping and storage can at least for the sake of discussion be conceptualized as a metastable clustering of a number of electrons around trapping centers capable of the stable retention of probably only one electron.

Sample 041 was not included in the age-curve calculation, because the large difference between the natural and artificial TL amplitudes for the sample results in a TL ratio with a magnitude of about half the value appropriate for a sample of its age. The natural TL amplitude for sample 041 is approximately correct (fig. 14), whereas the artificial TL appears anomalously high (fig. 16). The reason for the difference is not clear; the possibility of its being due to a slight shift in emission spectra has been proposed here. Whatever the cause, the disparity of the two TL values and the anomalously low ratio were deemed adequate grounds for omitting the sample from the age-curve derivation. Comparable TL differences in samples of unknown age could be used as a basis for rejection of such samples as unsuitable for TL dating. The simple existence of a large difference in values is not sufficient grounds for rejection, however, since the difference in the natural and artificial TL values could possibly occur in a sample 100,000 years old, the approximate age obtained for sample 041 with the TL ratio. At this preliminary stage in the development of the method, some geologic control would be required for a reliable assessment of validity.

#### TL SATURATION AND THE AGE LIMITS OF THE METHOD

Samples Mol 1e and 5X340, 1.5 and 3.3 m.y. old, respectively, have TL ratios that are significantly lower than expected; the ages obtained for these two samples with the TL age equation are 225,000 and 300,000 years, respectively. Although both samples have annual dose rates that are lower than the average for the younger basalts, it is almost certain that the low dose rates are not entirely responsible for the erroneous

ages. The samples appear to be affected by both TL and trap-density saturation. Sample Klpa 10a was not included in the age analysis, because it is a transitional alkalic basalt with chemical and TL properties closer to the tholeiitic basalt group.

Saturation is probably initially manifest in a decrease in the rate of accumulation of defects. The specific cause of this approach to a limiting defect density has not been identified but is probably related to spontaneous annealing. The amount and rate of annealing defined by the artificial TL data for historic basalts (fig. 18) indicates a greater defect mobility than has been generally thought to occur in minerals at ambient surface temperatures. It suggests that spontaneous annealing probably occurs continuously, degrading a small percentage of the radiogenically produced defect population. Theoretically, at a high defect density, a small percentage annealing rate could produce a number of annihilations equal to the rate of defect production; the equivalence of the two rates would define saturation. Attenuation of the defect accumulation rate is expected to cause a proportionate decrease in the TL accumulation rate, and TL saturation should follow defect saturation fairly closely.

The defect density at which saturation occurs should be largely dependent on the natural dose rate. There is probably also a specific relation between dose rate and the length of time required for the saturation effects to appear, but whether an increase in dose rate is accompanied by an increase or a decrease in the elapsed time to saturation is not clear.

The age at which saturation effects begin to appear in the alkalic basalts cannot be determined from the data available. The TL ratios for samples Mol 1e and 5X340 are clearly attenuated, but the ratio for the oldest of the young alkalic basalts, sample 033, is not. The TL ages for samples Mol 1e and 5X340 suggest that the upper age limit for the TL method may be as young as 250,000 to 275,000 for rocks of their approximate composition and dose rate.

Estimates of an upper limit for TL dating by other workers are few and inconclusive. They include an estimate by Sabels (1963) that TL would prove useful for dating lavas to several tens of thousands of years of age. Goksu and others (1974) anticipated the extension of their preliminary TL method for pyrolyzed chert to more than 100,000 years.

A lower limit for the TL method is specified by the age at which natural TL first becomes measurable with acceptable precision. For the ocean island alkalic basalts, this would probably be at an age of about 2,000 years. For continental rocks with higher dose rates, the lower limit may be as young as 1,000 years.

#### TL DATING OF THE THOLEIITIC BASALTS

An attempt to use the limited data available for the tholeiitic basalts to establish a unique relation between TL and sample age similar to that developed for the alkalic basalts was not successful, as the age distribution of dated material available is limited and the statistical precision for both the TL measurements and the supporting data was generally poor. A systematic relation between natural TL and sample age exists, however, and future work involving samples of known age in the 10,000- to 200,000-year range should produce a reliable TL-dating method for these rocks.

#### PROCEDURE AND RESULTS

Natural TL peak-height averages for samples 024, 070, and 018, shown in figure 20, indicate a uniform rate of increase in natural TL with age that appears to be more rapid than that for the alkalic basalts. The natural TL data for samples 074 and 019 are included in figure 20 at positions on the estimated best-fit line specified by their natural TL peak heights. Neither 074 or 019 has been independently dated, but both were collected from flows in known stratigraphic relation to dated flows. The apparent

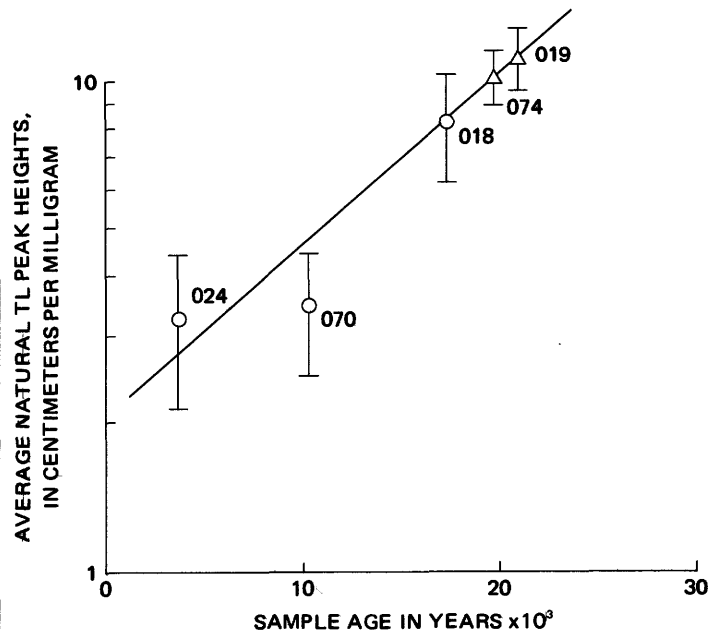


FIGURE 20.—Tholeiitic basalt natural TL peak-height averages for the carbon-14-dated prehistoric basalts. The data are the average of the peak-height values for the two separate TL series, where available, normalized for sample weight and annual dose rates. The estimated best-fit line is based on the data for samples 024, 070, and 018; the data for undated samples 074 and 019 are included in the graph at positions specified by their natural TL peak-height averages.

TL age of approximately 20,000 years for sample 074, collected from the lava flow stratigraphically below the flow from which sample 070 was obtained and separated from it by about 1 meter of volcanic ash from the widespread Pahala Ash (Stearns and Macdonald, 1946) is geologically reasonable. Sample 074 occupies approximately the same stratigraphic position relative to the ash as sample 018. The two flows could be of similar age if the ash is coeval at the two sampling locations. The apparent TL age of approximately 21,000 years for sample 019, collected either one or two flows (field relations were obscure) below the flow from which sample 018 was obtained, is also reasonable. The accuracy of the apparent TL ages for these two samples cannot be evaluated at this time; the plot of peak-height averages for tholeiitic prehistoric carbon-14-dated basalt (fig. 20) was prepared primarily to demonstrate that natural TL for the basalts appears to increase rather uniformly with age. Unnormalized natural TL is too dependent on variations in the other TL parameters to be of significant value alone for reliable age determination, although accuracy to within a factor of two, which the natural TL data may be capable of providing with some reliability, could be valuable for some applications.

To determine the trend of  $NE_a/AE_n$  ratios for the tholeiitic basalts with age, these ratios were plotted relative to sample age in figure 21. Samples 074 and 019 are included in the figure at sample ages specified by their natural TL peak amplitudes (fig. 20). The ratios for the older tholeiitic basalts from the Pololu Volcanic Series, included in the figure even though they are probably affected by saturation, serve to illustrate in general the increasing trend that should be

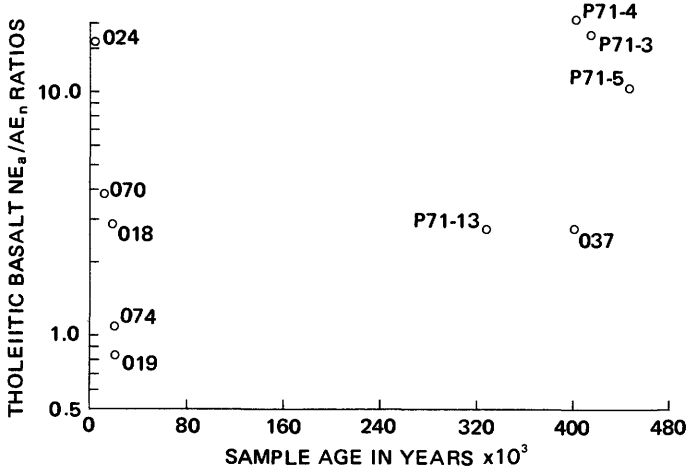


FIGURE 21.—Tholeiitic basalt  $NE_a/AE_n$  ratios plotted relative to sample age. Samples 074 and 019 are included at the tentative sample ages indicated by their natural TL peak heights (fig. 20).

followed by the ratios for younger rocks as they increase in age.

#### DISCUSSION

The progressive decrease in the  $NE_a/AE_n$  ratios for the tholeiitic basalts to an age of greater than 20,000 years is an unexpected result. This trend is produced by an apparently more rapid rate of increase in artificial TL (trap density) than natural TL and as discussed earlier, may possibly be an artificial relation caused by the experimental procedure. A study of the TL properties of several of these same prehistoric carbon-14-dated flows using unfiltered TL by Berry (1973) led to the identification of a progressive increase in the TL ratios with age. In any case, the trend of decreasing ratios appears to reverse itself at around 20,000 years. The ratios for samples older than approximately 20,000 years should increase with age, as suggested by the magnitude of the ratios for the older samples from the Pololu Volcanic Series.

The predictable increase in both the natural and artificial TL for the tholeiitic basalts suggests that a reliable TL-dating method for these rocks is probably feasible but would require considerable further research incorporating a wider age distribution of dated material. These rocks cannot be directly dated with the age equation for the alkalic basalts because the difference in dose rates and feldspar composition between the two rock types produces a significant non-linear difference in the rate of TL and trap-density accumulation.

#### SUMMARY OF THE TL-DATING PROCEDURES AND PREDICTIONS FOR FUTURE APPLICATIONS

The preliminary TL-dating method defined in this investigation for Hawaiian alkalic basalts is capable of age resolution over the age range from 2,500 to perhaps 250,000 years B.P. with a precision for rocks older than about 50,000 years of approximately  $\pm 10$  percent. The TL ages have a potential estimated accuracy of about  $\pm 10$  percent relative to potassium-argon ages.

The method was developed using plagioclase separates from rocks of independently determined age as the TL dosimeter. The separates range in average composition from oligoclase to andesine and have  $K_2O$  contents that range from 2.3 to 3.3 weight percent. The whole-rock uranium contents of the samples range from 1 to 2.6 ppm, thorium from 2.8 to 7.6 ppm. Annual radioactive dose rates calculated on the basis of assumed secular equilibrium and exclusive of the cosmic-ray energy dose, and with an assumed TL-producing efficiency for alpha particles of 0.1 of the tabulated total alpha-particle energy, range from 0.240 to

0.500 rad/yr and average 0.350 rad/yr.

The TL measurements were made using 4- to 7-mg aliquants of plagioclase of a 37- to 44- $\mu\text{m}$  size range sealed in a light-tight sample chamber in which the atmosphere was adjusted during TL measurement to exclude oxygen. Heating was at a rate of  $20^\circ\text{C s}^{-1}$  by infrared radiation focused on the bottoms of the sample planchets. TL was detected with an EMI 6255S "Q" photomultiplier tube coupled to an SSR model 1105/1120 photon-counting system. The TL was filtered with a Corning filter number CS5-60 to restrict the TL detected to that from the 4,500-Å plagioclase emission peak. This spectral peak is apparently caused by a specific but as yet unidentified structural defect rather than an impurity element in a substitutional or intersitial lattice position.

Thermoluminescence is basically a three-dimensional phenomenon that can be depicted spatially by three orthogonal axes representing light intensity, activation temperature, and spectral composition. Plagioclase natural TL consists of a signal peak at about  $350^\circ\text{C}$ ; the artificial TL from laboratory irradiations constituted four overlapping peaks with maxima about  $110^\circ$ ,  $150^\circ$ ,  $225^\circ$ , and  $300^\circ\text{C}$ . The light from each of these TL peaks has a characteristic spectral composition of three broad peaks with maxima at about 4,500 Å, 5,600 Å, and 7,200 Å. The relative intensities of the spectral peaks appear to vary between the different temperature peaks.

Both the  $350^\circ\text{C}$  natural TL peaks and  $300^\circ\text{C}$  artificial TL peaks appear to increase approximately exponentially in amplitude with increasing sample age. The increase in artificial TL is an indication of an increase in the aggregate number of crystal-defect-associated electron traps produced by internal radiation. The slightly faster rate of increase in natural TL is an indication of a rapid filling of these traps by excited electrons, and perhaps of an increased retention (re-trapping?) probability for electrons in samples with progressively larger trap populations. The natural to artificial TL ( $N/A$ ) ratios for the samples analyzed increase uniformly at an exponential rate with age; the equation for the best-fit line through the data represents a "relative" TL age equation that can be used to assign ages to other undated samples of similar chemical composition.

The TL method should be applicable to volcanic rocks similar in bulk composition to the alkalic basalts over the age range approximately 2,500 to at least 250,000 years. Volcanic rocks of continental origin should be particularly well suited to TL dating because they typically have higher radioactive-element contents than Hawaiian rocks of equivalent composition.

The TL method for the alkalic rocks cannot at this time be used to directly date the ocean island tholeiitic basalts, because the average dose rate for the tholeiitic basalts is lower than that for the alkalic basalts by a factor of two and produces natural TL intensities in the tholeiitic basalts that are lower than those in the alkalic basalts for samples of equivalent age by a nonlinear factor. An attempt to develop an independent method using tholeiitic basalts of known age and the same general technique developed for the alkalic basalts was not successful, primarily because of an inadequate age distribution of dated material and poor precision in the TL and dose-rate measurements. Both natural and artificial TL appear to increase rather uniformly with age at an approximately exponential rate, however, and a reliable TL-dating method for these rocks should eventually be feasible over the age range of approximately 10,000 years to at least 100,000 years.

#### REFERENCES CITED

- Aitken, M. J., 1968, Thermoluminescence dating in archaeology, introductory review, in McDougall, D. J., ed., Thermoluminescence of geological materials: New York, Academic Press, p. 369-378.
- 1970, Dating by archaeomagnetic and thermoluminescent methods: Royal Soc. London Philos. Trans., A, v. 269, p. 77-88.
- Aitken, M. J., and Fleming, S. J., 1971, Preliminary application of thermoluminescent dating to the eruptions of Thera: Internat. Sci. Cong. on the Volcano of Thera, 1st, Athens, Greece, p. 293-302.
- Aitken, M. J., Fleming, S. J., Doell, R. R., and Tanguy, J. C., 1968, Thermoluminescent study of lavas from Mt. Etna and other historic flows, Preliminary results, in McDougall, D. J., ed., Thermoluminescence of geological materials: New York, Academic Press, p. 359-366.
- Aitken, M. J., Fleming, S. J., Reid, J., and Tite, M. S., 1968, Elimination of spurious thermoluminescence, in McDougall, D. J., ed., Thermoluminescence of geological materials: New York, Academic Press, p. 133-142.
- Aitken, M. J., Tite, M. S., and Reid, J., 1964, Thermoluminescent dating of ancient ceramics: Nature, v. 202, p. 1032-1033.
- Aitken, M. J., Zimmerman, D. W., and Fleming, S. J., 1968, Thermoluminescent dating of ancient pottery: Nature, v. 219, p. 442-445.
- Armstrong, R. W., 1973, Atlas of Hawaii: Honolulu, Univ. Press of Hawaii, 222 p.
- Berry, A. L., 1973, Thermoluminescence of Hawaiian basalts: Jour. Geophys. Research, v. 78, p. 6863-6867.
- Blair, I. M., Edington, J. A., Chen, R., and John, R. A., 1972, Thermoluminescence of Apollo 14 lunar samples following irradiation at  $-196^\circ\text{C}$ : Geochim. et Cosmochim. Acta, Supp. 3, Proc. 3d Lunar Sci. Conf., v. 3, p. 2949-2953.
- Blanchard, F. N., 1966, Thermoluminescence age of fluorite and age of deposition: Am. Mineralogist, v. 51, p. 474-485.
- Bothner, M. H., and Johnson, N. M., 1969, Natural thermoluminescent dosimetry in Late Pleistocene pelagic sediments: Jour. Geophys. Research, v. 74, p. 5331-5338.

- Boyle, R., 1663, Experiments and considerations upon colours with observations on a diamond that shines in the dark: London, Henry Herringham, n. p.
- Braunlich, P., 1968, Thermoluminescence and thermally stimulated current-tools for the determination of trapping parameters, in McDougall, D. J., ed., Thermoluminescence of geological materials: New York, Academic Press, p. 61-68.
- Brito, Lalou, C., and Valladas, G., 1973, Thermoluminescence of lunar fines (Apollo 12, 14, and 15) and lunar rock (Apollo 15): *Geochim. et Cosmochim. Acta*, Supp. 3, Proc. 4th Lunar Sci. Conf., v. 3, p. 2453-2458.
- Christodoulides, C., and Ettinger, K. V., 1971, Some useful data from the Randall-Wilkins equation: *Modern Geology*, v. 2, p. 235-238.
- Crow, E. L., Davis, F. A., and Maxfield, M. W., 1960, Statistics Manual: New York, Dover, 288 p.
- Curie, D., 1963, Luminescence in crystals: New York, John Wiley, 332 p.
- Dalrymple, G. B., and Doell, R. R., 1970a, Thermoluminescence of lunar samples from Apollo 11: *Geochim. et Cosmochim. Acta*, Supp. 1, Proc. Apollo 11 Lunar Sci. Conf., v. 3, p. 2081-2092.
- 1970b, Thermoluminescence of lunar samples: *Science*, v. 167, p. 713-715.
- Daniels, F., Boyd, C. A., and Saunders, D. F., 1953, Thermoluminescence as a research tool: *Science*, v. 117, p. 343-349.
- Doell, R. R., and Dalrymple, G. B., 1973, Potassium-argon ages and paleomagnetism of the Waianae and Koolau Volcanic Series, Oahu, Hawaii: *Geol. Soc. America Bull.*, v. 84, p. 1217-1242.
- Drake, M. J., 1972, The distribution of major and trace elements between plagioclase feldspar and magmatic silicate liquid—An experimental study: Oregon Univ., Ph.D. thesis.
- Durrani, S. A., and Christodoulides, C., 1969, Allende meteorite—Age determination by thermoluminescence: *Nature*, v. 223, p. 1219-1221.
- Durrani, S. A., Christodoulides, C., and Ettinger, K. V., 1970, Thermoluminescence in tektites: *Jour. Geophys. Research*, v. 75, p. 983-995.
- Durrani, S. A., and Hwang, F. S. W., 1974, Thermoluminescence and thermal environment of some Apollo 17 fines: *Geochim. et Cosmochim. Acta*, Supp. 5, Proc. 5th Lunar Sci. Conf., v. 3, p. 2689-2702.
- Durrani, S. A., Prachyabrued, W., Hwang, F. S. W., Edington, J. A., and Blair, I. M., 1973, Thermoluminescence of some Apollo 14 and 16 fines and rock samples: *Geochim. et Cosmochim. Acta*, Supp. 4, Proc. 4th Lunar Sci. Conf., v. 3, p. 2465-2479.
- Fleming, S. J., 1970, Thermoluminescent dating—Refinement of the quartz inclusion method: *Archaeometry*, v. 12, p. 133-145.
- 1972, Thermoluminescent dating—Education in Chemistry, v. 19, p. 9-11.
- Fleming, S. J., Moss, H. M., and Joseph, A., 1970, Thermoluminescence authenticity testing of some "six dynasties" figures: *Archaeometry*, v. 12, p. 57-65.
- Fornaca-Rinaldi, G., 1968, Some effects of heating on the radiation sensitivity of natural crystals, in McDougall, D. J., ed., Thermoluminescence of geological materials: New York, Academic Press, p. 103-110.
- Garlick, G. F. J., 1973, Thermoluminescent dating: *Nature*, v. 245, p. 119-120.
- Garlick, G. F. J., and Gibson, A. F., 1948, The electron trap mechanism of luminescence in sulphide and silicate phosphors: Royal Soc. [London] Proc., v. 60, p. 574-590.
- Garlick, G. F. J., Lamb, W. E., Steigman, G. H., and Geake, J. E., 1971, Thermoluminescence of lunar samples and terrestrial plagioclases: *Geochim. et Cosmochim. Acta*, Supp. 2, Proc. 2nd Lunar Sci. Conf., v. 2, p. 2277-2283.
- Garlick, G. F. J., and Robinson, I., 1972, The thermoluminescence of lunar samples, in Urey, H. C., and Runcorn, S. K., eds., *The Moon: Internat. Astron. Union Symposium on the Moon*, 2d, Newcastle-upon-Tyne, 1971, Dordrecht, Reidel Pub., p. 324-329.
- Geake, J. E., and Walker, G., 1966, Luminescence spectra of meteorites: *Geochim. et Cosmochim. Acta*, v. 30, p. 927-937.
- Geake, J. E., Walker, G., Mills, A. H., and Garlick, G. F. J., 1971, Luminescence of Apollo lunar samples: *Geochim. et Cosmochim. Acta*, Supp. 2, Proc. 2nd Lunar Sci. Conf., v. 3, p. 2265-2275.
- 1972, Luminescence of lunar materials excited by electrons: *Geochim. et Cosmochim. Acta*, Supp. 2, Proc. 3d Lunar Sci. Conf., v. 3, p. 2971-2979.
- Geake, J. E., Walker, G., Telfer, D. J., Mills, A. H., and Garlick, G. F. J., 1973, Luminescence of lunar, terrestrial and synthesized plagioclase caused by Mn<sup>2+</sup> and Fe<sup>3+</sup>: *Geochim. et Cosmochim. Acta*, Supp. 4, Proc. 4th Lunar Sci. Conf., v. 3, p. 3181-3189.
- Goksu, H. Y., Fremlin, J. H., Irwin, H. T., and Fryxell, R., 1974, Age determination of burned flint by a thermoluminescent method: *Science*, v. 183, p. 651-654.
- Herbst, W., 1964, Investigations of environmental radiation and its variability, in Adams, J. A. S., and Lowder, W. M., eds., *The natural radiation environment*: Houston, Texas, Rice Univ., p. 781-796.
- Houtermans, F. G., and Liener, A., 1966, Thermoluminescence of meteorites: *Jour. Geophys. Research*, v. 71, p. 3387-3396.
- Hooy, H. P., Jr., Kardoes, J. L., Miyajima, M., Seitz, M. G., Sun, S. S., Walker, R. M., and Wittels, M. C., 1970, Thermoluminescence, X-ray and stored energy measurements of Apollo 11 samples: *Geochim. et Cosmochim. Acta*, Supp. 1, Proc. Apollo 11 Lunar Sci. Conf., v. 3, p. 2269-2287.
- Hooy, H. P., Jr., Walker, R. M., Zimmerman, D. W., and Zimmerman, J., 1972, Thermoluminescence of individual grains and bulk samples of lunar fines: *Geochim. et Cosmochim. Acta*, Supp. 3, Proc. 3d Lunar Sci. Conf., v. 3, p. 2997-3007.
- Hutchinson, C. S., 1968, The dating by thermoluminescence of tectonic and magmatic events in orogenesis, in McDougall, D. J., ed., Thermoluminescence of geological materials: New York, Academic Press, p. 341-358.
- Hwang, F. S. W., 1970, Thermoluminescence dating applied to volcanic lava: *Nature*, v. 227, p. 940-941.
- 1972, Evaluation of the thermoluminescence dating technique applied to smoky quartz: *Jour. Geophys. Research*, v. 77, p. 328-333.
- 1973, Fading of thermoluminescence induced in lunar fines: *Nature*, v. 245, p. 41-43.
- Hwang, F. S. W., and Goksu, H. Y., 1971, A further investigation on the thermoluminescence dating technique: *Modern Geology*, v. 2, 225-230.
- Isaacs, T. J., 1971, Fluorescence of alkaline-earth silicates activated with divalent Eu: *Electrochem. Soc. Jour.*, v. 118, p. 1009-1011.
- Johnson, N. M., 1963, Thermoluminescence in contact metamorphosed limestone: *Jour. Geology*, v. 71, p. 596-616.
- Johnson, N. M., and Blanchard, R. L., 1967, Radiation dosimetry from the natural thermoluminescence of fossil shells: *Am. Mineralogist*, v. 52, p. 1297-1310.
- Johnson, N. M., and Daniels, F., 1961, Luminescence during annealing and phase change in crystals: *Jour. Chem. Physics*, v. 34, p. 1434-1439.
- Kaufhold, J., and Herr, W., 1968, Factors influencing dating CaF<sub>2</sub> minerals by thermoluminescence, in McDougall, D. J., ed., Thermoluminescence of geological materials: New York, Academic Press, p. 324-329.

- demic Press, p. 153-168.
- Land, P. L., 1969a, Determining electron trap parameters from thermoluminescent or conductivity glow curves: *Jour. Physics and Chemistry Solids*, v. 30, p. 1681-1692.
- 1969b, Equations for thermoluminescence and thermally stimulated current as derived from simple models: *Jour. Physics and Chemistry Solids*, v. 30, p. 1693-1708.
- Laud, K. R., Gibbons, E. F., Tien, T. V., Stadler, H. L., 1971, Cathodoluminescence of  $\text{Ce}^{3+}$  and  $\text{Eu}^{2+}$ -activated alkaline-earth feldspars: *Electrochem. Soc. Jour.*, v. 118, p. 918-923.
- Lederer, C. M., Hollander, J. M., and Perlman, I., 1967, Table of isotopes, [6th ed.]: New York, John Wiley, 594 p.
- Leverenz, H. W., 1968, An introduction to luminescence of solids: New York, Dover, 569 p.
- Levy, P. W., 1968, A brief survey of radiation effects applicable to geology problems, in McDougall, D. J., ed., *Thermoluminescence of geological materials*: New York, Academic Press, p. 25-38.
- McDougall, Ian, 1964, Potassium-argon ages of lavas of the Hawaiian Islands: *Geol. Soc. America Bull.*, v. 75, p. 107-128.
- 1969, Potassium-argon ages of lavas of Kohala Volcano, Hawaii: *Geol. Soc. America Bull.*, v. 80, p. 2597-2600.
- McDougall, Ian, and Swanson, D. A., 1972, Potassium-argon ages of lavas from the Hawi and Pololu Volcanic Series, Kohala Volcano, Hawaii: *Geol. Soc. America Bull.*, v. 83, p. 3721-3738.
- Medlin, W. L., 1968, The nature of traps and emission centers in thermoluminescent rock materials, in McDougall, D. J., ed., *Thermoluminescence of geological materials*: New York, Academic Press, p. 193-223.
- Mladsenović, M., 1973, *Radioisotope and radiation physics*: New York, Academic Press, 242 p.
- Morehead, F. F., and Daniels, F., 1957, Thermoluminescence and coloration of lithium fluoride produced by  $\alpha$  particles, electrons,  $\gamma$  rays, and neutrons: *Jour. Chem. Physics*, v. 27, p. 1318-1324.
- Mott, N. F., and Gurney, R. W., 1964, *Electronic processes in ionic crystals* [2d ed.]: New York, Dover, 275 p.
- Nash, D. B., and Greer, R. T., 1970, Luminescence properties of Apollo 11 lunar samples and implications for solar-excited luminescence: *Geochim. et Cosmochim. Acta, Supp.*, Proc. Apollo 11 Lunar Sci. Conf., v. 3, p. 2341-2350.
- Panov, Ye. N., Sverdlov, Z. M., and Alekseyava, L. N., 1970, Thermoluminescence of quartz, plagioclase, and potash feldspar from granitoids of northeastern Transbaykalia: *Internat. Geology Rev.*, v. 12, p. 962-970.
- Pertsov, L. V., 1964, The natural radioactivity of the biosphere: Israel Program for Sci. Trans., Jerusalem (1967), 261 p.
- Porter, S. C., 1971, Holocene eruptions of Mauna Kea Volcano, Hawaii: *Science*, v. 172, p. 375-377.
- Randall, J. T., and Wilkins, M. H. F., 1945, Phosphorescence and electron traps. I, The study of trap distributions: *Royal Soc. [London] Proc. Ser. A*, v. 184, p. 366-389.
- Rubin, M., and Berthold, S. M., 1961, U.S. Geological Survey radiocarbon dates VI: *Radiocarbon*, v. 3, p. 86-98.
- Rubin, M., and Corrine, A., 1960, U.S. Geological Survey radiocarbon dates V: *Am. Jour. Sci. Radiocarbon Supp.*, v. 2, p. 129-185.
- Rubin, M., and Suess, H. E., 1956, U.S. Geological Survey radiocarbon dates, III: *Science*, v. 123, p. 442-448.
- Sabels, B. E., 1963, Age studies on basaltic lava using natural alpha activity and thermoluminescence, in *Radioactive Dating*: Vienna, Internat. Atomic Energy Agency, p. 87-104.
- Schilling, C. W., ed., 1964, *Atomic energy encyclopedia in the life sciences*: Philadelphia, Saunders, 474 p.
- Sippel, R. F., and Spencer, A. B., 1970, Luminescence petrography and properties of lunar crystalline rocks and breccias: *Geochim. et Cosmochim. Acta, Supp. 1*, Proc. Apollo 11 Lunar Sci. Conf., v. 3, p. 2413-2426.
- Smith, J. V., 1974, *Feldspar minerals*, v. 2: New York, Springer-Verlag, 690 p.
- Smith, J. V., and Stenstrom, R. C., 1965, Electron-excited luminescence as a petrologic tool: *Jour. Geology*, v. 73, p. 627-635.
- Somayajulu, B. L. K., Tatsumoto, M., Rosholt, J. N., and Knight, R. J., 1966, Disequilibrium of the  $^{238}\text{U}$  series in basalt: *Earth and Planetary Sci. Letters*, v. 1, p. 387-391.
- Spiers, F. W., McHugh, M. J., and Appleby, D. B., 1964, Environmental  $\gamma$ -ray dose to populations—Surveys with a portable meter, in Adams, J. A. S., and Lowder, W. M., eds., *The natural radiation environment*: Houston, Texas, Rice Univ., p. 885-906.
- Stearns, H. T., and Macdonald, G. A., 1946, Geology and groundwater resources of the island of Hawaii: Hawaii Div. Hydrography Bull., 9, 363 p.
- Sullivan, B. M., Spiker, E., and Rubin, M., 1970, U.S. Geological Survey radiocarbon dates XI: *Radiocarbon*, v. 12, p. 319-334.
- Telfer, D. J., and Walker, G., 1975, Optical detection of  $\text{Fe}^{3+}$  in lunar plagioclase: *Nature*, v. 258, p. 694-695.
- Tite, M. S., 1966, Thermoluminescent dating of ancient ceramics: A reassessment: *Archaeometry*, v. 9, p. 155-169.
- 1968, Some complicating factors in the thermoluminescent dating and their implications, in McDougall, D. J., ed., *Thermoluminescence of geological materials*: New York, Academic Press, p. 389-405.
- Van Doorn, C. Z., and Schipper, D. J., 1971, Luminescence of  $\text{O}^{2-}$ ,  $\text{Mn}^{2+}$ , and  $\text{Fe}^{3+}$  in sodalite: *Physics Letters*, v. 34A, p. 139-140.
- Vaz, J. E., and Senftle, F. E., 1971, Geologic age dating of zircon using thermoluminescence: *Modern Geology*, v. 2, p. 239-245.
- Walker, R. M., 1973, Solid state tract detectors—Achievements and current problems: Washington Univ., Laboratory for Space Physics SPP34, St. Louis, 19 p.
- Weast, R. C., ed., 1974, *Chemical Rubber Co. Handbook of Chemistry and Physics*: The Chemical Rubber Co.
- Winchell, A. N., and Winchell, H., 1951, *Elements of optical mineralogy, Part II, Descriptions of minerals*: New York, John Wiley, 551 p.
- Wintle, A. G., 1973, Anomalous fading of thermoluminescence in mineral samples: *Nature*, v. 245, p. 143-144.
- 1975, Thermal quenching of thermoluminescence in quartz: *Royal Astron. Soc. Geophys. Jour.*, v. 41, p. 107-113.
- York, D., 1969, Least squares fitting of a straight line with correlated errors: *Earth and Planetary Sci. Letters*, v. 5, p. 320-324.
- Zeller, E. J., 1968, Geologic age determinations by thermoluminescence, in McDougall, D. J., ed., *Thermoluminescence of geological materials*: New York, Academic Press, p. 311-325.
- Zeller, E. J., Wray, J., and Daniels, F., 1955, Thermoluminescence induced by pressure and by crystallization: *Jour. Chem. Physics*, v. 23, p. 2187.
- 1957, Factors in age determination of carbonate sediments by thermoluminescence: *Am. Assoc. Petroleum Geologists Bull.*, v. 41, p. 121-129.
- Zimmerman, D. W., 1971, Thermoluminescent dating using fine grains from pottery: *Archaeometry*, v. 13, p. 29-52.

**SUPPLEMENTAL INFORMATION****SAMPLE LOCATION AND AGE DATA****ALKALIC BASALTS**

[Listed in order of increasing age]

**Sample No.: 023****Source volcano:** Mauna Kea Volcano; Hale Pohaku flow.**Rock type:** Nominally an alkalic olivine basalt; precise petrologic type not determined.**Collected by:** R. May, 1972; recollection of a previously dated flow.**Location:**  $19^{\circ}43'54''N$ ,  $155^{\circ}26'50''W$ ; collected from flow surface outcrop near the unimproved road from Hwy. 20 to the Hale Pohaku Ranger Station, about 0.6 km SE. of Puu Hookomo; Puu 00  $7\frac{1}{2}'$  quadrangle (1956); elevation: 2.25 km.**Age information:**  $^{14}C$  age of  $4,000 \pm 110$  years B.P. on carbonaceous ash from the top of the Humuula palesol, beneath the Puu Kole flow, which has been determined to be essentially coeval with the Hale Pohaku flow on the basis of field relation (Porter, 1971).**Sample No.: H71-10****Source volcano:** Kohala Volcano; Hawi Volcanic Series.**Rock type:** Mugearite.**Collected by:** Ian McDougall and Don Swanson, 1971.**Location:**  $20^{\circ}07'10''N$ ,  $155^{\circ}34'45''W$ ; collected from a roadcut about 1 km west of Kukuihaele, Kukuihaele  $7\frac{1}{2}'$  quadrangle (1957); elevation: 300 m.**Age information:** Whole-rock K-Ar age of  $62,000 \pm 2,000$  years B.P. (McDougall and Swanson, 1972).**Sample No.: 035****Source volcano:** Kohala Volcano; Hawi Volcanic Series.**Rock type:** Trachyte.**Collected by:** R. May, 1972; recollection of a previously dated flow.**Location:**  $20^{\circ}04'30''N$ ,  $155^{\circ}45'50''W$ ; collected from a prominent roadcut about 11.5 km from the Kamauela Post Office on Hwy. 25, and about 1.1 km WSW. of Puu Loa, Kawaihae  $7\frac{1}{2}'$  quadrangle (1956); elevation: 1.04 km.**Age information:** Duplicates sample GA 1378, for which a whole-rock K-Ar age of  $140,000 \pm 4,000$  years was obtained (McDougall, 1969).**Sample No.: H71-3****Source volcano:** Kohala Volcano, Hawi Volcanic Series.**Rock type:** Mugearite.**Collected by:** Ian McDougall and Don Swanson, 1971.**Location:**  $20^{\circ}12'20''N$ ,  $155^{\circ}44'00''W$ ; collected from a flow partly filling Pololu Valley, Honokane  $7\frac{1}{2}'$  quadrangle (1957); elevation: 37 m.**Age information:** Whole-rock K-Ar age of  $150,000 \pm 2,000$  years B.P. (McDougall and Swanson, 1972).**Sample No.: 036****Source volcano:** Kohala Volcano; Hawi Volcanic Series.**Rock type:** Hawaiite.**Collected by:** R. May, 1972; recollection of a previously dated flow.**Location:**  $20^{\circ}04'45''N$ ,  $155^{\circ}46'00''W$ ; collected from a roadcut about 12.3 km from Kamauela Post Office on Hwy. 25, near**Keawewai Stream, Kawaihae  $7\frac{1}{2}'$  quadrangle (1956); elevation: 1.06 km.****Age information:** Duplicates sample GA 1377, for which a whole-rock K-Ar age of  $153,000 \pm 7,000$  years B.P. was obtained (McDougall, 1969).**Sample No.: 041****Source volcano:** Kohala Volcano; Hawi Volcanic Series.**Rock type:** Mugearite.**Collected by:** R. May, 1972; recollection of a previously dated flow.**Location:**  $20^{\circ}06'30''N$ ,  $155^{\circ}52'45''W$ ; collected from a roadcut 8.0 km south of Mahukona on the new section of Hwy. 26, Keawanui  $7\frac{1}{2}'$  quadrangle (1957); elevation approximately 61 m. NOTE: Location is approximate because the new road does not appear on the current topographic map.**Age information:** Supposed to duplicate sample HW-21, for which a whole-rock K-Ar age of  $181,000 \pm 3,000$  years B.P. was obtained (McDougall and Swanson, 1972).**Sample No.: 042****Source volcano:** Kohala Volcano; Hawi Volcanic Series.**Rock type:** Mugearite.**Collected by:** R. May, 1972; recollection of a previously dated flow.**Location:**  $20^{\circ}04'30''N$ ,  $155^{\circ}51'30''W$ ; collected from a roadcut about 1.45 km north of the North Kohala-South Kohala District Boundary, on the edge of Keawewai Stream, Kawaihae  $7\frac{1}{2}'$  quadrangle (1956); elevation: approximately 60 m. NOTE: The same location restrictions specified for sample 041 apply.**Age information:** Supposed to duplicate sample HW-22, for which a whole-rock K-Ar age of  $184,000 \pm 3,000$  years B.P. was obtained (McDougall and Swanson, 1972).**Sample No.: 033****Source volcano:** Kohala Volcano; Hawi Volcanic Series.**Rock type:** Hawaite.**Collected by:** R. May, 1972; recollection of a previously dated flow.**Location:**  $20^{\circ}02'00''N$ ,  $155^{\circ}42'25''W$ ; collected from a roadcut 9.6 km from the Kamauela Post Office on Hwy. 25, Kamauela  $7\frac{1}{2}'$  quadrangle (1956); elevation: 755 m.**Age information:** Duplicates sample GA 1376, for which a whole-rock K-Ar age of  $196,000 \pm 7,000$  years B.P. was obtained (McDougall, 1969).**Sample No.: Mol 1e****Source volcano:** Unknown.**Rock type:** Alkalic basalt.**Collected by:** M. Beeson, 1969.**Location:**  $21^{\circ}07'00''N$ ,  $156^{\circ}44'30''W$ ; Halawa  $7\frac{1}{2}'$  quadrangle (1952).**Age information:** Probable age of approximately 1.35 m.y. (M. Beeson, U.S.G.S., written commun.) based on K-Ar ages from associated basalts from East Molokai (McDougall, 1964).**Sample No.: Klpa 10a****Source volcano:** Unknown.**Rock type:** Transitional alkalic basalt.**Collected by:** M. Beeson, 1971.**Location:**  $21^{\circ}11'00''N$ ,  $157^{\circ}00'05''W$ ; Kaunakakai  $7\frac{1}{2}'$  quadrangle, island of Molokai (1952).**Age information:** Probable age of about 1.5 m.y. (M. Beeson,

U.S.G.S. written commun.) based on K-Ar ages ranging from 1.47 to 1.49 m.y. on associated basalts (McDougall, 1964).

*Sample No.: 5X340*

*Source volcano:* Waianae Volcano; Waianae Volcanic Series, upper member.

*Rock type:* Not precisely determined; either an alkalic basalt or a Hawaite.

*Collected by:* R. Doell and G. B. Dalrymple.

*Location:* 21°20'14" N., 158°05'33" W.; collected near Hwy. 90 near Kalealoa Road, Ewa 7½' quadrangle, island of Oahu (1962).

*Age information:* Material consisted of extra sections of drill cores 5X340 to 5X347 from site J, unit 56, collected originally for paleomagnetism and age-dating studies. The flow yielded a K-Ar age of  $3.30 \pm 0.10$  m.y. (Doell and Dalrymple, 1973).

### THOLEIITIC BASALTS

[Listed in order of increasing age]

*Sample No.: 012*

*Source volcano:* East rift of Kilauea Volcano; Puna Volcanic Series.

*Rock type:* Tholeiitic basalt.

*Collected by:* R. May, 1972.

*Location:* 29°30'38" N., 154°50'40" W.; collected from a roadcut on Hwy. 132, 0.6 km west of the intersection with Hwy. 137, Kapoho 7½' quadrangle (1965); elevation 36.5 m.

*Age information:* Historic flow, 1960.

*Sample No.: 015*

*Source volcano:* Kilauea Volcano, Puna Volcanic Series.

*Rock type:* Tholeiitic basalt.

*Collected by:* R. May, 1972.

*Location:* 19°26'20" N., 154°56'50" W.; collected in a roadcut on Hwy. 13 at the intersection with the road to Opihikau, Pahoa South 7½' quadrangle (1966); elevation: 305 m.

*Age information:* Historic flow, 1955.

*Sample No.: 026*

*Source volcano:* Mauna Loa Volcano; Kau Volcanic Series.

*Rock type:* Tholeiitic basalt.

*Collected by:* R. May, 1972.

*Location:* 19°05'40" N., 155°47'30" W.; collected in a roadcut on Hwy. 11, at the intersection with Ginger Blossom Lane, Pohue Bay 7½' quadrangle (1962); elevation: 587 m.

*Age information:* Historic flow, 1907.

*Sample No.: 030*

*Source volcano:* Mauna Loa; Kau Volcanic Series.

*Rock type:* Tholeiitic basalt.

*Collected by:* R. May, 1972.

*Location:* 19°49'45" N., 155°44'15" W.; collected in a roadcut on Hwy. 19, 2.8 km east of Puuanahulu, Puu Anahulu 7½' quadrangle (1959); elevation: 678 m.

*Age information:* Historic flow, 1859.

*Sample No.: 050*

*Source volcano:* East rift of Kilauea Volcano; Puna Volcanic Series.

*Rock type:* Tholeiitic basalt.

*Collected by:* R. May, 1972.

*Location:* 19°22'30" N., 154°58'00" W.; collected from a road metal pit adjacent to Hwy. 13 about 1.7 km north of the coast, Kalapana 7½' quadrangle (1966); elevation: 33 m.

*Age information:* Historic flow, age approximately 1,750 A.D.

*Sample No.: 051*

*Source volcano:* Kilauea Volcano; Puna Volcanic Series.

*Rock type:* Tholeiitic basalt.

*Collected by:* R. May, 1972.

*Location:* 19°19'25" N., 155°17'30" W.; collected from an outcrop adjacent to the road from Park Headquarters to Hilina Pali, near BM 2829, Kau Desert 7½' quadrangle (1963); elevation: 869 m.

*Age information:* Historic flow, age approximately 1,420 A.D. (Howard Powers, written commun.).

*Sample No.: 032*

*Source volcano:* Kilauea Volcano, Puna Volcanic Series.

*Rock type:* Tholeiitic basalt.

*Collected by:* R. May, 1972; recollection of a previously dated flow.

*Location:* 19°26'00" N., 155°15'20" W.; collected from a roadcut on Hwy. 11 at the entrance to Kilauea Volcano National Park, Kilauea Crater 7½' quadrangle (1963); elevation: 1.20 km.

*Age information:*  $^{14}\text{C}$  age of  $2,500 \pm 250$  years B.P. on charcoal from a fern mold in pumice overlying the flow (sample W-201) (Rubin and Suess, 1956).

*Sample No.: 024*

*Source volcano:* Mauna Loa; Kau Volcanic Series.

*Rock type:* Tholeiitic basalt.

*Collected by:* R. May, 1972; recollection of a previously dated flow.

*Location:* 19°04'20" N., 155°36'50" W., collected from a roadcut adjacent to the churchyard in central Waiohinu from which the dated sample was obtained, Naalehu 7½' quadrangle (1962); elevation: 323 m.

*Age information:*  $^{14}\text{C}$  age of  $3,740 \pm 150$  years B.P. on charcoal from beneath the flow exposed at the surface in the Waiohinu churchyard (sample W-856, Rubin and Corrine, 1960). A second age of  $3,620 \pm 250$  years B.P. was obtained for carbonaceous material from the same stratigraphic position collected from a different sampling site nearby (sample W2016, Sullivan and others, 1970).

*Sample No.: 070*

*Source volcano:* Mauna Loa; Kau Volcanic Series.

*Rock type:* Tholeiitic basalt.

*Collected by:* S. Grommé and Monte Marshall, 1972.

*Location:* 19°02'35" N., 155°33'30" W.; collected from the cliff section near the top of Maniania Pali about 1.2 km south-southwest of Kimo Point, near Naalehu 7½' quadrangle (1962); elevation: about 30 m.

*Age information:*  $^{14}\text{C}$  age of  $10,140 \pm 300$  years B.P. on carbonaceous ash baked by the flow sample (W-907, Rubin and Berthold, 1961).

*Sample No.: 074*

*Source volcano:* Mauna Loa; Kau Volcanic Series.

*Rock type:* Tholeiitic basalt.

*Collected by:* S. Grommé and Monte Marshall, 1972.

*Location:* 19°02'35" N., 155°33'30" W.; collected from the next basalt flow below the 10,140-year-old flow and separated from it by

2.5 m of volcanic ash from the Pahala Ash.  
*Age information:* Older than 10,140 on the basis of stratigraphic position.

*Sample No.: 018*

*Source volcano:* Kilauea Volcano; Puna Volcanic Series.

*Rock type:* Tholeiitic basalt.

*Collected by:* R. May, 1972; recollection of a previously dated flow.

*Location:* 19°16'20" N., 155°17'10" W.; collected near the top of the Kaone fault scarp, 200 m southwest of Puu Kaone, Kau Desert 7½' quadrangle (1963); elevation: 213 m (SE. of Hilina Pali).  
*Age information:*  $^{14}\text{C}$  age of 17,360  $\pm$  650 years of B.P. on carbonaceous ash beneath and baked by the flow (sample W-905, Rubin and Berthold, 1961).

*Sample No.: 019*

*Source volcano:* Kilauea Volcano (?).

*Rock type:* Tholeiitic basalt.

*Collected by:* R. May, 1972.

*Location:* 19°16'20" N., 155°17'10" W.; collected stratigraphically below the dated flow from which sample 018 was obtained and separated from it by 3 meters of volcanic ash from the complex series of ash units referred to collectively as the Pahala Ash. Poor exposure precluded a definitive assessment of whether this particular flow immediately underlies the ash or if there is another thin flow between the bottom of the ash and the flow from which sample 019 was obtained, but at most this flow could not be more than two flow units below the dated flow.

*Age information:* Older than 17,360 years on the basis of stratigraphic position.

*Sample No.: P71-13*

*Source volcano:* Kohala Volcano, Pololu Volcanic Series.

*Rock type:* Tholeiitic basalt.

*Collected by:* Ian McDougall and Dan Swanson, 1971.

*Location:* 20°0'7" N., 155°35'20" W.; collected from Waipio Valley, Kukuihaele 7½' quadrangle (1957); elevation: 170 m.

*Age information:* Whole-rock K-Ar age of 327,000  $\pm$  45,000 year B.P. (McDougall and Swanson, 1972).

*Sample No.: 037*

*Source volcano:* Kohala Volcano; Pololu Volcanic Series.

*Rock type:* Tholeiitic basalt.

*Collected by:* R. May, 1972; recollection of a previously dated flow.

*Location:* 20°11'10" N., 155°54'10" W.; collected from a roadcut in Mahukona, Mahukona 7½' quadrangle (1957); elevation: 10 m.

*Age information:* Supposed to duplicate sample HW-17, for which a whole-rock K-Ar age of 400,000  $\pm$  8,000 years B.P. was obtained (McDougall and Swanson, 1972).

*Sample No.: P71-4*

*Source volcano:* Kohala Volcano; Pololu Volcanic Series.

*Rock type:* Tholeiitic basalt.

*Collected by:* Ian McDougall and Don Swanson, 1971.

*Location:* 20°12'20" N., 155°44'00" W.; collected from Pololu Valley, about 110 m below the top of the exposed section of the Pololu Volcanic Series, Honokane 7½' quadrangle (1957).

*Age information:* Whole-rock K-Ar age of 403,000  $\pm$  141,000 years B.P. (McDougall and Swanson, 1972).

*Sample No.: P71-3*

*Source volcano:* Kohala Mountain; Pololu Volcanic Series.

*Rock type:* Tholeiitic basalt.

*Collected by:* I. McDougall and D. Swanson, 1971.

*Location:* 20°12'20" N., 155°44'00" W.; collected on the trail into Pololu Valley, about 40 m below the top of the exposed section of the Pololu Volcanic Series, Honokane 7½' quadrangle (1957).

*Age information:* Whole-rock K-Ar age of 414,000  $\pm$  18,000 years B.P. (McDougall and Swanson, 1972).

*Sample No.: P71-5*

*Source volcano:* Kohala Volcano; Pololu Volcanic Series.

*Rock type:* Tholeiitic basalt.

*Collected by:* I. McDougall and D. Swanson, 1971.

*Location:* 20°12'20" N., 155°44'00" W., collected on the trail into Pololu Valley about 90 m below the top of the exposed section of the Pololu Volcanic Series, Honokane 7½' quadrangle (1957).

*Age information:* Whole-rock K-Ar age of 447,000  $\pm$  27,000 years B.P. (McDougall and Swanson, 1972).

## DERIVATION OF EQUATIONS FOR THE ERROR IN THE TL RATIOS AND TL AGES

### ERROR EQUATION FOR THE TL AGE RATIO

The TL age ratio  $r$  is expressed as

$$r = k(NE_a/AE_n)$$

where  $k$  is a constant,  $N$  the natural TL peak-height average,  $A/E_a$  the average artificial TL peak-height average for the same samples from a standardized exposure of artificial radiation ( $E_a$ ) and  $E_n$  the natural annual radiation dose rate.

In the general case, if  $y = F(x_1, x_2, \dots, x_n)$  and the changes  $\Delta x_i$  in the  $x$ 's are small, then the differential  $\delta y$  approximates the change  $\Delta y$  in  $y$ ,

$$\Delta y \simeq dt = \frac{\partial F}{\partial x_1} \Delta x_1 + \frac{\partial F}{\partial x_2} \Delta x_2 + \dots + \frac{\partial F}{\partial x_n} \Delta x_n$$

and if the changes  $\Delta x$  in the  $x$ 's are independent, then the variance in  $\Delta y$  may be approximated by

$$\sigma_y^2 \simeq \left( \frac{\partial F}{\partial x_1} \right)^2 \sigma x_1^2 + \left( \frac{\partial F}{\partial x_2} \right)^2 \sigma x_2^2 + \dots + \left( \frac{\partial F}{\partial x_n} \right)^2 \sigma x_n^2$$

with the partial derivatives evaluated at nominal values of  $x_1, x_2, \dots, x_n$  (Crow and others, 1960, p. 69).

Given  $r = NE_a/AE_n$ , and the relation established above,

$$dr = \frac{\partial r}{\partial N} \Delta N + \frac{\partial r}{\partial A} \Delta A + \frac{\partial r}{\partial E_n} \Delta E_n + \frac{\partial r}{\partial E_a} \Delta E_a .$$

Taking partial derivatives and combining terms,

$$dr = \frac{1}{AE_n} E_a \Delta N + -\frac{NE_a}{A} \Delta A + -\frac{NE_a}{E_n} \Delta En + N \Delta E_a ;$$

if the changes  $\Delta N$ ,  $\Delta A$ ,  $\Delta E_n$ , and  $\Delta E_a$  are small, then  $\Delta N^2$  may be replaced by  $\sigma N^2$ , and so on, squaring each term in the previous equation and converting to variances

$$\sigma_r' = \left( \sigma_{N^2} + \sigma_A^2 + \sigma_{E_n^2} + \sigma_{E_a^2} \right)^{1/2}$$

Converting to fractional errors in the form of

$$\sigma r^2 = \sigma_r'^2 r^2$$

where  $\sigma r^2$  is the fractional error and combining terms and simplifying yields the final equation for the error in the TL ratio

$$\sigma_r^2 = \frac{1}{A^2 E_n^2} E_a \sigma N^2 + \frac{N^2 E_a^2}{A^2} \sigma A^2 + \frac{N^2 E_a^2}{E_n^2} \sigma E_n^2 + N^2 \sigma E_a^2 .$$

Note that  $E_n$ , the natural radiation dose rate, is actually a composite function incorporating errors in the measurement of the uranium, thorium, and potassium concentrations. Using an error equation similar to the one employed for the error in the TL ratio, the error in the quantity  $E_n$  is

$$\sigma E_n' = \left[ \left( \sigma_{E_U'} \right)^2 + \left( \sigma_{E_{Th}'} \right)^2 + \left( \sigma_{E_K'} \right)^2 \right]^{1/2}.$$

#### EQUATION FOR THE ERROR IN THE TL AGES

The TL age equation is of the form

$$t = \left[ \frac{1}{b} \ln r - \ln a \right]$$

where

$t$  is the sample age,

$r$  is the TL ratio,

$b$  is the slope of the best-fit line,

$a$  is the  $y$ -axis intercept.

Employing the same basic assumptions used in the preceding derivations regarding the size of the errors involved and permissible approximations in terms of substitutions of statistical quantities,

$$dt = \left[ \frac{\partial t}{\partial x} \frac{1}{b} (\ln r - \ln a) \right] \Delta y.$$

Taking partial derivatives, converting to fractional errors, and simplifying yields the equation for the fractional error in the TL ages:

$$\left( \sigma_t' = \frac{\sigma_r'^2}{b^2 t^2} \right)^{1/2}.$$

Note that the error in  $b$ , the slope of the age curve, is not included in the error equation. This is because the equation is designed to provide an estimate of the precision of the TL ages; errors in the slope of the line and in the  $y$  intercept are more properly in the realm of accuracy.